Hopf bifurcation for the hydrogen atom in a circularly polarized microwave field

Mercè Ollé[a], Juan R. Pacha[a],*

[a]*Department of Mathematics. Universitat Politècnica de Catalunya, Barcelona, Spain*

Abstract

We consider the CP problem, i.e., the Rydberg electron in a rotating electric field, whose dynamics is described by a Hamiltonian depending on one parameter, K>0. The corresponding Hamiltonian system of ODE has two equilibrium points L_1 (unstable for all K) and L_2 (a center for $K < K_{crit}$ and a complex saddle for $K > K_{crit}$). We study the Hamiltonian-Hopf bifurcation phenomena that take place for K close to K_{crit} around L_2. First, a local analysis based in the computation of the normal form (up to a finite order) is carried out and the steps for the computation of the resonant normal form are explained in a constructive manner. The results of the analysis enable us to use the dynamics of the (integrable) normal form to study the local behavior of the electron in a neighborhood of the equilibrium L_2 for the original non integrable Hamiltonian. Second, we compute numerically all the objects involved in such a bifurcation (periodic orbits, invariant 2D tori and the 2D manifolds of L_2) in order to have a local picture of the dynamics close to L_2. Finally a global description of the dynamics is carried out and the effect of the Hopf bifurcation as well as other objects that organize the dynamics are discussed.

Keywords: Hamiltonian dynamical systems, Hopf bifurcation, periodic orbits and tori, chaotic regions, invariant manifolds

1. Introduction

Within the classical mechanics context, we consider the hydrogen atom interaction with a circularly polarized electromagnetic field, which we will refer to, from now on, as the CP problem. In suitable rotating variables, the CP problem is modeled by a Hamiltonian system with two degrees of freedom (assuming planar motion for the electron) that depends only on a parameter $K > 0$. It is true that the CP problem has been studied by several authors (see [5], [9] and [16]) but it presents a variety of phenomena that remains to be well understood. Actually, we expect to have chaotic regions for this Hamiltonian since it is known that this system is non integrable (see [14]).

A remarkable property of the CP problem is that it can be regarded as a perturbed Kepler problem (the CP problem becomes the Kepler problem in rotating coordinates for $K = 0$) and, in fact, some features of the dynamics can be understood from the dynamics of the two body problem, when K is small.

Concerning the CP problem itself, it is well known (see [5]) that it has two equilibrium points for any value of K: L_1 which is of type center×saddle, for all $K > 0$, and L_2 which is a center×center for $K < K_{crit}$, being $K_{crit} = 3^{-4/3}/2 \approx 0.11556021$ a critical value, and a complex saddle for $K > K_{crit}$. As far as the authors know, all the papers are devoted to studies for small K and always $K < K_{crit}$. In such a case, different kinds of solutions appear in the CP problem: confined, periodic, homoclinic, chaotic, escaping/ionizing among others. For the latter, it is known that there are fast escaping orbits and slowly erratic escaping orbits, in the sense that they make several excursions reaching small and big distances from the nucleus in an apparent random way such that it is difficult to predict when the electron will actually ionize (see [5]). A recent study on trajectories ejecting/colliding with the nucleus can be found in [26].

Applying a *dynamical systems* theory approach, the authors in [5] were able to explain the mechanism for these kinds of orbits, based upon the invariant manifolds of some suitable periodic orbits. This was a main goal of that paper for $K < K_{crit}$ and the present paper is a natural continuation of it.

In this paper we study the dynamics of the CP problem also for the $K > K_{crit}$ case, and the remarkable fact that L_2 experiments the so called *s*upercritical Hopf bifurcation when K increases and crosses the critical value K_{crit}. Our purpose is to describe the dynamics, not only from a local point of view, but from a global one and the consequences that this Hopf bifurcation has on the behavior of the solutions. This will require, for numerical simulations, that we will have to compute periodic orbits, their 2d associated invariant manifolds as well as the 2D invariant manifolds associated with the complex saddle equilibrium point L_2. Also suitable Poincaré sections will become very useful to describe the dynamics as well as to find confinement regions where the electron remains trapped for ever in the middle of apparent chaotic regions.

So our contribution in this paper is threefold:

---

*corresponding author

Email addresses: merce.olle@upc.edu (Mercè Ollé), juan.ramon.pacha@upc.edu (Juan R. Pacha)

(i) To apply an analytical procedure to transform the *original* and *non-integrable* Hamiltonian to a four order Hamiltonian normal form (NF) plus a remainder. The explicit steps are given and an algorithm that might be implemented for any order is explained (see Remark 7, after Proposition 1). We point out that the papers dealing with the Hopf bifurcation typically consider an academic theoretical Hamiltonian, depending on generic parameters, with a *suitable* expression useful to carry out the normal form process, whereas here, we take the *given* Hamiltonian of the CP problem.

(ii) The analytical description of the dynamics of the *integrable* four order NF for K close to K_{crit}. Of course, this is a *local* approach due to the validity of the NF in a small neighborhood of the equilibrium point L_2. In particular, the two families of periodic orbits (and their stability) around the stable L_2, for $K < K_{crit}$, as well as their merging to become one bifurcated detached family, when L_2 becomes a complex saddle for $K > K_{crit}$ is explained. Also the parametrizations of the manifolds of the unstable L_2 are derived. The CP problem (the Rydberg electron in a rotating electric field) is also considered in [20] to illustrate the Hamiltonian Hopf bifurcation. However, the treatment found there is perturbative, in the sense that the authors consider the Hamiltonian system in a neighborhood of L_2 and check that this equilibrium point changes its stability from center to complex saddle when the polarization parameter crosses a critical threshold; they unfold the normalized quadratic part of the Hamiltonian with two different terms that yields to the supercritical and sub-critical bifurcation (see [7]), respectively. Here, we consider always the Hamiltonian of the CP problem, without any assumptions on the form of the higher order terms and carry out the computation of the normal form, in an explicit way, up to any given order. From the obtained four order NF, we determine the type –supercritical– of the bifurcation that *actually* takes place. Results are stated in Proposition 3.

(iii) So far the analytical part, next we focus on numerical simulations. On the one hand, we describe the Hopf bifurcation that takes places in the CP problem computing numerically all the invariant objects involved and showing the role they have in the dynamics. Although the analysis of the integrable NF is valid only for a tiny neighborhood of L_2 and a small interval containing K_{crit}, we take the original non-integrable Hamiltonian and make numerical simulations that allow big regions in the configuration plane (position coordinates for the electron) and any value of K. More precisely, for the energy level of L_2, we describe how the 2D invariant manifolds of the equilibrium point L_2, for $K > K_{crit}$, provide a mechanism to explain a rich variety of orbits, including homoclinic orbits, multi-bump ones (with several close passages to the L_2), chaotic ones and even low and fast ionization for the electron if K is big enough. Moreover, the elliptic bifurcated periodic orbits (of the Hopf bifurcation) determine a region of confinement in the middle of a chaotic area. On the other hand, for values of the energy close to that of L_2 and varying $K > 0$, we describe the dynamics, from a *global* point of view, for the original non integrable Hamiltonian. We explain how some periodic orbits, that exist regardless the Hopf bifurcation phenomena, the 2D invariant manifolds of the equilibrium point L_2, the 2D invariant manifolds of the Liapunov orbits around L_1, the bifurcated periodic orbits and 2D invariant tori organize the dynamics.

Remark 1. The CP problem is addressed here as classical Hamiltonian system. Quantum considerations are beyond the scope of this study. Nevertheless, it could be interesting to apply, somehow, quantization rules to the normal form. However, according to the observations in [20], though there exist methods to quantisize the Birkhoff-Gustavson normal form in the semi-classical approximation, the quantisation problem involving non semisimple resonances (as that taking in the Hopf bifurcation) is not yet completely understood. Even so, in the quoted paper, the authors manage to give, under some assumptions, the spectrum for the supercritical bifurcation. Readers interested in these aspects are referred to there.

The paper is organized as follows: Section 2 is devoted to give the equations of motion of the Rydberg electron in the CP hydrogen atom, seen as a Hamiltonian system written in a rotating reference frame; as well as some general features of the model. In Section 3 we describe the transformation from that initial Hamiltonian to a (resonant, integrable) normal form, plus a (non integrable) remainder. The reduction process is carried out "degree-by-degree", trying to remove, at every step –starting from the terms of degree 3– as many terms as possible. This removal is done through the successive application of symplectic changes whose generating functions are found solving their associated *homological* equations. For the current case of $1{:}-1$ resonance, we show explicitly these equations and study their solvability giving, in the resonant cases, the compatibility terms needed. Thus, it is shown how to compute effectively, up to any given degree, both the generating functions and the normal form terms. Particularly, for the Hamiltonian of the CP hydrogen atom model, the fourth order normal form is computed in the Examples 3, and 4. In Section 4 we use this normal form to discuss, for values of the polarization parameter K close to K_{crit}, the stability of the Rydberg electron in a neighborhood of the equilibrium point L_2. In Section 5 the dynamics of the normal form is explored, as a way to get an (approximate and local) description of the phase space in a neighborhood of the equilibrium point. Section 6 is devoted to explain the numerical tools used in Section 7, where we present a detailed description of the dynamics from a global point, when $K < K_{crit}$ and when $K > K_{crit}$, for values of the energy h close to the value at the equilibrium point $h(L_2)$, focusing our attention on the effects of the Hopf bifurcation. Conclusions are in section 8.

We remark that the numerical computations have been done with double precision and the integrations of the ODE carried out along the paper have used a Taylor method, through the software package provided by Jorba and Zou [19]. This is a robust method, both in speed and accuracy, and suitable for long time span integrations.

Finally, we notice that Section 3 is rather technical, so maybe we recommend for a first reading of the paper, once the reader is in this Section, to go directly to the results stated in Propositions 1 and 2, and go on. In that way the overview of the

paper is achieved. For a detailed analysis of Section 3, the reader can go deeper into it.

2. The CP problem

In this Section we present the equations of the problem and some basic properties related to equilibrium points, their stability, and some families of periodic orbits (PO) that play an important role in the dynamics of the problem.

Let us consider the relative motion of the electron in a hydrogen atom subjected to a circularly polarized (CP) microwave, where the pulse of the microwave field is taken with a *flat-top* shape, i.e., the field amplitude is ramped up in time until it achieves a final, constant amplitude. Here we ignore the ramping and only consider the dynamics after the flat-top has been reached (see [9] for a discussion of the implications of the initial ramp).

The Hamiltonian for the electron of the hydrogen atom (in the limit of an infinitely massive nucleus and in atomic units $m_e = \bar{h} = e = 1$) subjected to a CP microwave field, and assumed to move in the plane (x, y), is the following:

$$H = \frac{1}{2}(p_x^2 + p_y^2) - \frac{1}{r} + F(x \cos \tilde{\omega} t + y \sin \tilde{\omega} t), \tag{1}$$

where (x, y) and (p_x, p_y), with $p_x = x' - y$ and $p_y = y' + x$, are the canonical coordinates and their conjugate momenta; $r^2 = x^2 + y^2$; $\tilde{\omega}$ is the angular frequency of the microwave field and $F > 0$ is the field strength (see [9]).

Moving to a frame rotating with the CP field and by re-scaling time and distances the expression of the Hamiltonian (see [5] for details) is

$$H = \frac{1}{2}(p_x^2 + p_y^2) - xp_y + yp_x - \frac{1}{r} + Kx, \tag{2}$$

where $K = F/\tilde{\omega}^{4/3} > 0$ is the unique parameter and, for simplicity, we keep the same names for the position and momentum coordinates. Now the Hamiltonian becomes autonomous and the constant value of the Hamiltonian $H = h$ over each solution is called the energy.

The associated Hamiltonian equations of the motion are

$$\begin{aligned}
x' &= p_x + y, \\
y' &= p_y - x, \\
p_x' &= p_y - \frac{x}{r^3} - K, \\
p_y' &= -p_x - \frac{y}{r^3},
\end{aligned} \tag{3}$$

which satisfy the symmetry

$$(t, x, y, p_x, p_y) \quad \longrightarrow \quad (-t, x, -y, -p_x, p_y). \tag{4}$$

This implies that, for each solution of the equations of motion, there also exists another one which is symmetric with respect to $y = 0$ in configuration space (x, y). In particular, periodic symmetric solutions with respect to $y = 0$ intersect this axis perpendicularly twice. We use this property, in particular, to find families of periodic symmetric solutions.

The CP problem in rotating coordinates has two equilibrium points, denoted by L_1 and L_2 and located in the x-axis at $x(L_1) < 0$ and $x(L_2) > 0$ respectively ($x(L_i)$, $i = 1, 2$ varying with K). Regarding their linear stability, the first one is of type saddle $\times$ center for all values of K, whereas the second one is of type center $\times$ center for

$$K < K_{crit} = \frac{3^{-4/3}}{2} \approx 0.115560212391772 \tag{5}$$

and a complex saddle for $K > K_{crit}$.

It is worth noticing that, when the electron is not far away from the nucleus, the problem given by (2) may be regarded as a perturbed Kepler problem when the parameter K is small, which is the case considered in [5]. Actually, from the rotating two-body problem, $K = 0$, it is known that, for $h < -3/2$, there exists one family of retrograde periodic ones (denoted by o_r), family that persists when $K > 0$ and we denote it in the same way.

Also for $K > 0$ and small, since L_1 is of type saddle$\times$center, and L_2 of type center$\times$center (for $K < K_{crit}$), applying the Liapunov center theorem (see, for example [34], chap. 2, or [24], chap. 9), we obtain three families of periodic orbits (parametrized by the energy and known as Liapunov periodic orbits, LPO), one around L_1 (ol_1) and two around L_2 (one family existing for increasing values of the energy h, and the other family for decreasing values of h, both starting at $h(L_2)$).

One of the main goals of this paper is precisely to describe the Hopf bifurcation phenomenon that experiments the equilibrium point L_2 when K increases and crosses the critical value K_{crit}.

For this purpose, a very useful theoretical approach will be to consider a lower (four) order normal form associated with the Hamiltonian. This is done in the next Section.

3. Reduction to normal form around L_2

This section is devoted to the local study of the system around L_2 for values of the polarization parameter K close to the critical value K_{crit} in (5). As linearization shows, the stability type of this point changes from center to complex saddle as K moves from $K < K_{crit}$ to $K > K_{crit}$ passing through a double (degenerate) center at $K = K_{crit}$. For this value of K the characteristic exponents collide pairwise on the imaginary axis and the matrix of the linearized system has two pure imaginary eigenvalues, $\pm\, \mathrm{i}\, \varpi$, $\varpi > 0$; of algebraic multiplicity two, but geometric multiplicity one. This (parametric) resonance is known in the literature as 1:1 *non semisimple* resonance or, more briefly, as 1:-1 resonance and has drawn attention of many researchers (see [24], [33], [39], and references therein). The relevant features of the local dynamics can be gleaned from the resonant normal form around L_2 of the involved Hamiltonian (2). The normal form reduction process embraces the expansion of the Hamiltonian (subsection 3.2), linear reduction and complexification (subsection 3.3) –where the quadratic part of the Hamiltonian is put in a standard form (Williamson normal form) and complex coordinates are introduced–, and finally, the nonlinear reduction that, from a computational point of view, consists basically in setting and solving the so called *homological equations* (subsection 3.4). Before continuing, we need to state some additional notation. This is done right in subsection 3.1.

3.1. Notation and definitions

We shall denote by $\mathcal{M}_{n,m}(\mathbb{F})$ the vector space of matrices with n rows and m columns with coefficients in $\mathbb{F} = \mathbb{C}, \mathbb{R}, \mathbb{Z}$, or $\mathbb{N}_0 = \mathbb{N} \cup \{0\}$. For square $n \times n$ matrices, it is quite usual to write $\mathcal{M}_n(\mathbb{F})$ instead of $\mathcal{M}_{n,n}(\mathbb{F})$. Thus, if $A \in \mathcal{M}_{n,m}(\mathbb{F})$, $A^\top \in \mathcal{M}_{m,n}(\mathbb{F})$ will stand for its transpose. If $u = (u_1, \ldots, u_n)$, $v = (v_1, \ldots, v_n) \in \mathbb{F}^n$, then $w = (u, v) \in \mathbb{F}^n \times \mathbb{F}^n$. Furthermore, given $u = (u_1, \ldots, u_n) \in \mathbb{F}^n$,

$$|u|_1 = |u_1| + \cdots + |u_n|$$

indicates its vector 1-norm. $I_n = \mathrm{diag}[1, \ldots, 1] \in \mathcal{M}_n(\mathbb{F})$ is the unit matrix and J_n is the block matrix of the standard symplectic 2-form in $\mathbb{R}^{2n}$,

$$J_n = \begin{pmatrix} 0 & I_n \\ -I_n & 0 \end{pmatrix}.$$

For a set of m vectors $\eta_1, \eta_2, \ldots, \eta_m \in \mathbb{F}^n$,

$$M = (\eta_1 | \eta_2 | \cdots | \eta_m) \in \mathcal{M}_{n,m}(\mathbb{F})$$

is the matrix having these vectors as columns.

The upper bar will denote complex conjugation, i.e., if $z \in \mathbb{C}$, then $\bar{z} = \mathrm{Re}\, z - \mathrm{i}\, \mathrm{Im}\, z$, whereas for matrices and vectors this convention extends componentwise, so if $A = (a_{i,j}) \in \mathcal{M}_{n,m}(\mathbb{C})$, then $\bar{A} = (\bar{a}_{i,j}) \in \mathcal{M}_{n,m}(\mathbb{C})$, $i = 1, \ldots, n, j = 1, \ldots, m$; and we say that $\bar{A}$ is the *complex conjugate* (or simply, the *conjugate*) of A.

Given $R > 0$, $\mathscr{D}_R$ will denote the polydisk R, i.e.,

$$\mathscr{D}_R = \left\{ (\mu, \alpha, \beta) \in \mathbb{C} \times \mathbb{C}^2 \times \mathbb{C}^2 : |\mu| \leq R^2, |(\alpha, \beta)|_\infty \leq R \right\},$$

where $|\cdot|, |\cdot|_\infty$ denote the modulus of a complex number and the supremum norm, respectively.

In expansions, it is often used multi-index notation for the monomials involved so if $\nu \in \mathbb{C}$, $\alpha = (\alpha_1, \alpha_2)$, $\beta = (\beta_1, \beta_2) \in \mathbb{C}^2$; $f_{\ell\, r_1 r_2 s_1 s_2} \in \mathbb{C}$; $\ell \in \mathbb{N}_0$; $r, s \in \mathbb{N}_0^2$, we write

$$f_{\ell\, rs}\nu^\ell \alpha^r \beta^s = f_{\ell\, r_1 r_2 s_1 s_2}\nu^\ell \alpha_1^{r_1} \alpha_2^{r_2} \beta_1^{s_1} \beta_2^{s_2}. \tag{6}$$

Hence, let $\mathbb{C}[[\nu, \alpha, \beta]] := \mathbb{C}[[\nu, \alpha_1, \alpha_2, \beta_1, \beta_2]]$ be the ring of complex formal power series in $\nu \in \mathbb{C}$, $\alpha = (\alpha_1, \alpha_2) \in \mathbb{C}^2$, $\beta = (\beta_1, \beta_2) \in \mathbb{C}^2$. Therefore, $F \in \mathbb{C}[[\nu, \alpha, \beta]]$ if, and only if, it is a formal power series of type

$$F = \sum f_{\ell\, rs}\nu^\ell \alpha^r \beta^s,$$

where the summation is performed over $\ell \in \mathbb{N}_0$ and $r, s \in \mathbb{N}_0^2$.

For any two $F, G \in \mathbb{C}[[\nu, \alpha, \beta]]$,

$$\{F, G\} = \sum_{i=1,2} \left(\frac{\partial F}{\partial \alpha_i} \frac{\partial G}{\partial \beta_i} - \frac{\partial F}{\partial \beta_i} \frac{\partial G}{\partial \alpha_i} \right)$$

is their standard Poisson bracket with respect to (α, β). Now, given $G \in \mathbb{C}[[\nu, \alpha, \beta]]$ fixed, we define $L_G := \{\cdot, G\}$, so $L_G F = \{F, G\}$ for every $F \in \mathbb{C}[[\nu, \alpha, \beta]]$ and, recursively

$$L_G^0 F := F, \qquad L_G^k F := L_G \left(L_G^{k-1} F \right),$$

$k = 1, 2, 3, \ldots$ For the monomials (6), we define their *adapted* or *weighted* degree by

$$\deg\{\nu^l \alpha^r \beta^s\} := 2\ell + |r|_1 + |s|_1. \tag{7}$$

4

The reduction to normal form involves the following spaces of homogeneous polynomials: $\mathbb{E}_\sigma[\nu, \alpha, \beta]$ will stand for the space of the homogeneous polynomials of (adapted) degree $\sigma = 2, 3, \ldots$ made up of monomials of type (6). Furthermore, for $\ell, M, N \in \mathbb{N}_0$ fixed, $\mathbb{E}_{\ell MN}[\ell, \alpha, \beta]$ will denote the subspace of $\mathbb{E}_{2\ell+M+N}[\nu, \alpha, \beta]$ spanned also by monomials of type (6) with $M = r_1 + r_2$, $N = s_1 + s_2$. Clearly,

$$\mathbb{E}_\sigma[\nu, \alpha, \beta] = \bigoplus_{2\ell+M+N=\sigma} \mathbb{E}_{\ell MN}[\nu, \alpha, \beta].$$

Next, let $\mathcal{S} : \mathbb{C}[[\nu, \alpha, \beta]] \to \mathbb{C}[[\nu, \alpha, \beta]]$ be the linear operator defined by

$$F = \sum_{\ell,r,s} f_{\ell r_1 r_2 s_1 s_2} \nu^\ell \alpha_1^{r_1} \alpha_2^{r_2} \beta_1^{s_1} \beta_2^{s_2} \mapsto \mathcal{S}(F) := \sum_{\ell,r,s} (-1)^{r_1+s_2} \bar{f}_{\ell s_2 s_1 r_2 r_1} \nu^\ell \alpha_1^{r_1} \alpha_2^{r_2} \beta_1^{s_1} \beta_2^{s_2}. \tag{8}$$

We shall use the symbols $\mathbb{C}^{\mathcal{S}}[[\nu, \alpha, \beta]]$, $\mathbb{E}_\sigma^{\mathcal{S}}[\nu, \alpha, \beta]$, and $\mathbb{E}_{\ell MN}^{\mathcal{S}}[\nu, \alpha, \beta]$ to refer the subspaces of $\mathbb{C}[[\nu, \alpha, \beta]]$, $\mathbb{E}_\sigma[\nu, \alpha, \beta]$, and $\mathbb{E}_{\ell MN}[\nu, \alpha, \beta]$ respectively, that are invariant under $\mathcal{S}$, i. e., $F \in \mathbb{C}^{\mathcal{S}}[[\nu, \alpha, \beta]]$ ($F \in \mathbb{E}_\sigma^{\mathcal{S}}[\nu, \alpha, \beta]$, $F \in \mathbb{E}_{\ell MN}^{\mathcal{S}}[\nu, \alpha, \beta]$) if and only if $F \in \mathbb{C}[[\nu, \alpha, \beta]]$ ($F \in \mathbb{E}_\sigma[\nu, \alpha, \beta]$, $F \in \mathbb{E}_{\ell MN}[\nu, \alpha, \beta]$) and $\mathcal{S}(F) = F$. Then it is said that F satisfies the $\mathcal{S}$-invariance or the $\mathcal{S}$-symmetries. Finally, let $G(\nu, \alpha, \beta)$ be a real analytic function, we write $G \in \mathbb{C}[\nu, \alpha, \beta]$, and the associated Hamiltonian system,

$$\dot{\alpha}_j = \frac{\partial G}{\partial \beta_j}(\nu, \alpha, \beta), \qquad \dot{\beta}_j = -\frac{\partial G}{\partial \alpha_j}(\nu, \alpha, \beta), \tag{9}$$

$j = 1, 2$ (where ν is taken as a parameter), then

$$\alpha_j(t) = \varphi_j^G(t; \nu, \alpha^0, \beta^0), \qquad \beta_j(t) = \psi_j^G(t; \nu, \alpha^0, \beta^0) \tag{10}$$

will denote its solution with initial conditions $\alpha_j(0) = \alpha_j^0$, $\beta_j(0) = \beta_j^0$; $j = 1, 2$, and

$$\mathcal{T}_t^G\left(\nu, \alpha^0, \beta^0\right) = (\alpha(t), \beta(t)) = \left(\varphi^G(t; \nu, \alpha^0, \beta^0), \psi^G(t; \nu, \alpha^0, \beta^0)\right)$$

its flux at time t. More notation and definitions are introduced along the text as needed.

3.2. Expansion of the Hamiltonian

First we expand Hamiltonian (2) around the equilibrium point L_2, which is placed on the x axis in the configuration space. Let δ denote the distance from the origin to the equilibrium point L_2. Therefore from equations (3) we see on the one hand, that the position of L_2 –in the phase space coordinates of the Hamiltonian (2)– is given by $(x, y, p_x, p_y) = (\delta, 0, 0, \delta)$ and, on the other hand, that δ is the only positive solution of the equation

$$x^3 - Kx^2 - \text{sign}(x) = 0, \tag{11}$$

for $x > 0$. Notice that δ depends on K and let δ_0 denote the value of δ corresponding to the critical value of the parameter K, K_{crit}. An straightforward computation yields,

$$\delta_0 = \frac{3^{2/3}}{2}. \tag{12}$$

Moreover, we shall define the parameter μ as the difference:

$$\mu := \frac{1}{\delta_0} - \frac{1}{\delta}. \tag{13}$$

From (11) - (13) one can correlate K as a function of μ (see also equations (20)). Then it can be seen that K_{crit} corresponds to $\mu = 0$ and that K crosses the value K_{crit} from $K < K_{crit}$ to $K > K_{crit}$ as μ increases from $\mu < 0$ to $0 < \mu < 1/\delta_0$. Therefore, the equilibrium point L_2 changes from a center to a complex saddle as μ crosses the zero from negative to positive values.

Next, to translate the equilibrium point to the origin, we introduce the symplectic change of coordinates given by,

$$x = \delta(1 + x_1), \qquad y = \delta x_2, \qquad p_x = \frac{y_1}{\delta}, \qquad p_y = \delta + \frac{y_2}{\delta}. \tag{14}$$

As done in Celestial Mechanics, when one investigates the dynamics around a co-linear (L_1, L_2, L_3) or a triangular (L_4, L_5) equilibrium points of the Restricted Three Body Problem, it is usual to translate it to the origin and then expand the terms of the form $1/r$ as a sum of Legendre polynomials (see [13], [31], [32]). Applied to the case at hand, this approach leads to the sum

$$\frac{1}{r} = \frac{1}{\sqrt{x^2 + y^2}} = \frac{1/\delta}{\sqrt{1 + 2\frac{x-\delta}{\delta} + \left(\frac{x-\delta}{\delta}\right)^2 + \left(\frac{y}{\delta}\right)^2}} = \frac{1/\delta}{\sqrt{1 - 2\left(-\frac{x_1}{\rho}\right)\rho + \rho^2}} = \frac{1}{\delta}\sum_{\sigma=0}^\infty \rho^\sigma P_\sigma\left(-x_1/\rho\right),$$

5

where $\rho^2 := x_1^2 + x_2^2$ and $P_\sigma(t)$, $\sigma = 0, 1, 2, \ldots$ are the Legendre polynomials as generated by the recurrence relation

$$P_0(t) = 1, \quad P_1(t) = t,$$
$$P_{\sigma+1}(t) = 2tP_\sigma(t) - P_{\sigma-1}(t) - \frac{1}{\sigma+1}\left(tP_\sigma(t) - P_{\sigma-1}(t)\right), \tag{15}$$

with $\sigma = 0, 1, 2, \ldots$ (see, for example [1, Chap. 12]). If we define

$$R_\sigma(x_1, x_2) := \rho^\sigma P_\sigma(-x_1/\rho)$$

then, from (15), the recurrence relation for R_k,

$$R_0(x_1, x_2) = 1, \quad R_1(x_1, x_2) = -x_1,$$
$$R_{\sigma+1}(x_1, x_2) = -2x_1 R_\sigma(x_1, x_2) - \rho^2 R_{\sigma-1}(x_1, x_2)$$
$$+ \frac{1}{\sigma+1}\left(x_1 R_\sigma(x_1, x_2) + \rho^2 R_{\sigma-1}(x_1, x_2)\right), \quad \sigma = 1, 2, \ldots \tag{16}$$

follows at once. For example, for $\sigma = 1, 2, 3$,

$$R_2(x_1, x_2) = x_1^2 - \frac{x_2^2}{2}, \qquad\qquad R_3(x_1, x_2) = -x_1^3 + \frac{3}{2}x_1 x_2^2,$$
$$R_4(x_1, x_2) = x_1^4 - 3x_1^2 x_2^2 + \frac{3}{8}x_2^4, \qquad R_5(x_1, x_2) = -x_1^5 + 5x_1^3 x_2^2 - \frac{15}{8}x_1 x_2^4, \ldots$$

and induction shows at once that, for every $\sigma = 0, 1, 2, \ldots$ the corresponding R_σ is a homogeneous polynomial of degree σ in x_1 and x_2.

Now, if one substitutes the change (14) in the starting Hamiltonian (2), and replace $1/r$ by its expansion as the sum of the polynomials R_σ (times $1/\delta$) one obtains,

$$H\left(\delta(1+x_1), \delta x_2, \frac{y_1}{\delta}, \delta + \frac{y_2}{\delta}\right) = -\frac{\delta^2}{2} - \frac{1}{\delta} + K\delta - \frac{1}{\delta}\left(\delta^3 - K\delta^2 - 1\right)x_1 + \frac{1}{2\delta^2}\left(y_1^2 + y_2^2\right)$$
$$+ y_1 x_2 - y_2 x_1 - \frac{1}{\delta}\left(x_1^2 - \frac{x_2^2}{2}\right) - \frac{1}{\delta}\sum_{\sigma=3}^{\infty} R_\sigma(x_1, x_2).$$

Here, we recall that δ is a positive solution of equation (11) for $x > 0$, so

$$\delta^3 - K\delta^2 - 1 = 0. \tag{17}$$

Therefore,

$$H\left(\delta(1+x_1), \delta x_2, \frac{y_1}{\delta}, \delta + \frac{y_2}{\delta}\right) = H(\delta, 0, 0, \delta) + \frac{1}{2\delta^2}\left(y_1^2 + y_2^2\right)$$
$$+ y_1 x_2 - y_2 x_1 - \frac{1}{\delta}\left(x_1^2 - \frac{x_2^2}{2}\right) - \frac{1}{\delta}\sum_{\sigma=3}^{\infty} R_\sigma(x_1, x_2). \tag{18}$$

Besides, $H(\delta, 0, 0, \delta)$ (i.e., the energy at L_2) can be expanded in powers of μ, with coefficients given by functions of δ_0. Namely,

$$H(\delta, 0, 0, \delta) = -\frac{\delta^2}{2} - \frac{1}{\delta} + K\delta = \frac{\delta^2}{2} - \frac{2}{\delta} = \frac{\delta_0^2/2}{(1-\delta_0\mu)^2} - \frac{2}{\delta_0} + 2\mu$$
$$= H(\delta_0, 0, 0, \delta_0) + (2 + \delta_0^3)\mu + \sum_{\sigma=2}^{\infty} \frac{\sigma+1}{2}\delta_0^{\sigma+2}\mu^\sigma, \tag{19}$$

where we have used that in accordance, respectively, with property (17) and the equation (13) for the definition of μ,

$$K\delta = \delta^2 - \frac{1}{\delta}, \qquad \delta = \frac{\delta_0}{1-\delta_0\mu}; \tag{20}$$

so (19) follows at once after expanding in μ; moreover, one can substitute $1/\delta$ by $-\mu + 1/\delta_0$ in the right hand side of (18) and then define a new (transformed) Hamiltonian

$$\mathcal{H}(\mu, x, y) := H\left(\delta(1+x_1), \delta x_2, \frac{y_1}{\delta}, \delta + \frac{y_2}{\delta}\right) - H(\delta_0, 0, 0, \delta_0) \tag{21}$$

6

that can, in turn, be expanded as a sum of homogeneous polynomials of adapted degree (see (7))

$$\mathcal{H}(\mu, x, y) = \mathcal{H}_2(\mu, x, y) + \mathcal{H}_3(\mu, x, y) + \cdots + \mathcal{H}_\sigma(\mu, x, y) + \ldots, \tag{22}$$

with $\mathcal{H}_\sigma \in \mathbb{E}_\sigma[\nu, x, y]$ for $\sigma = 2, 3, \ldots$ Explicit computation shows,

$$\mathcal{H}_2(\mu, x, y) = (2 + \delta_0^3)\mu + \frac{1}{2\delta_0^2}(y_1^2 + y_2^2) + x_2 y_1 - x_1 y_2 - \frac{1}{\delta_0}\left(x_1^2 - \frac{x_2^2}{2}\right),$$

$$\mathcal{H}_3(\mu, x, y) = -\frac{1}{\delta_0} R_3(x),$$

$$\mathcal{H}_4(\mu, x, y) = \frac{3}{2}\delta_0^4 \mu^2 + \mu\left(x_1^2 - \frac{x_2^2}{2} - \frac{y_1^2}{\delta_0} - \frac{y_2^2}{\delta_0}\right) - \frac{1}{\delta_0} R_4(x), \tag{23}$$

$$\mathcal{H}_5(\mu, x, y) = \mu R_3(x) - \frac{1}{\delta_0} R_5(x),$$

$$\mathcal{H}_6(\mu, x, y) = 2\delta_0^5 \mu^3 + \frac{\mu^2}{2}(y_1^2 + y_2^2) + \mu R_4(x) - \frac{1}{\delta_0} R_6(x)$$

and, for $\sigma = 7, 8, \ldots$

$$\mathcal{H}_\sigma(\mu, x, y) = \frac{1 - (-1)^{\sigma+1}}{8}(\sigma + 2)\delta_0^{2+\sigma/2}\mu^{\sigma/2} + \mu R_{\sigma-2}(x) - \frac{1}{\delta_0} R_\sigma(x). \tag{24}$$

Remark 2. We point out that the parameter μ in Hamiltonian (21) can be thought of –rather than a parameter– as the action of a 3-degree of freedom Hamiltonian that does not depend explicitly on the conjugate angle, θ (which is then a cyclic coordinate). Hence, one can adapt the reduction in [28], that led to a suspension of the Sokol′skiĭ normal form around a $1:-1$ resonant periodic orbit (see [36], and also chap. 10 in [24] and references therein). That justifies the double weight of the "action" coordinate –the parameter μ in the problem at hand– in the definition of adapted degree (7).

3.3. Linear reduction

3.3.1. The (real) linear normal form. The study of the canonical reduction for linear Hamiltonian systems goes back to the three seminal papers of J. Williamson ([40], [41], [42]). A constructive approach to the subject, giving a method for finding canonical forms for both, Hamiltonian (infinitesimally symplectic) and symplectic matrices, can be found in [21] (see references therein for an account of other relevant contributions). Lemma 1 below gives an explicit canonical change to cast the quadratic part $\mathcal{H}_2$ of Hamiltonian (22) –see the first equation in (23)– to its Williamson normal form. This Lemma corresponds, for Hamiltonian matrices, to the result stated in Appendix D of [6] for the symplectic ones.

Lemma 1. *Let $A \in \mathrm{sp}(4, \mathbb{R})$ with*

$$\mathrm{Spec}(A) = \{\lambda_\pm = \pm \mathrm{i}\, \varpi\}, \qquad \dim \ker(A - \lambda_\pm I_4) = 1,$$

$\varpi \in \mathbb{R}, \varpi > 0$; $z_+, w_+ \in \mathbb{C}^4$ *be the geometric and the generalized eigenvectors respectively of $\lambda_+ = \mathrm{i}\,\varpi$, i.e.,*

$$A z = \lambda_+ z_+, \qquad (A - \lambda_+ I_4) w_+ = \lambda_+ z_+.$$

Let Δ, ϵ and α be the quantities defined by,

$$\Delta := z_+^\top J_2 \overline{w}_+, \qquad \epsilon := \mathrm{sign}(\Delta), \qquad \alpha := \frac{\mathrm{i}}{2\Delta} w_+^\top J_2 \overline{w}_+;$$

and $u_1, u_2, v_1, v_2 \in \mathbb{R}^4$ the vectors

$$u_1 = \sqrt{\frac{2}{|\Delta|}}\,\mathrm{Re}\, z_+, \qquad\qquad\qquad u_2 = \sqrt{\frac{2}{|\Delta|}}\,\mathrm{Im}\, z_+,$$

$$v_1 = \epsilon\sqrt{\frac{2}{|\Delta|}}(-\alpha\,\mathrm{Im}\, z_+ + \mathrm{Re}\, w_+), \qquad\qquad v_2 = \epsilon\sqrt{\frac{2}{|\Delta|}}(\alpha\,\mathrm{Re}\, z_+ + \mathrm{Im}\, w_+).$$

Then,

  (i) *$\Delta \in \mathbb{R}$, $\alpha \in \mathbb{R}$.*

  (ii) *u_1, u_2, v_1, v_2 form a symplectic basis, so $S = (u_1|u_2|v_1|v_2) \in \mathrm{Sp}(4, \mathbb{R})$.*

  (iii) *The linear symplectic change $z = \mathcal{U}(\zeta) := S\zeta$; $\zeta = (\xi, \eta)$, $z = (x, y)$ with $\xi, \eta, x, y \in \mathbb{R}^2$; transforms:*

(iii.1) The linear Hamiltonian system

$$\dot{z} = Az,$$

to its normal form

$$\dot{\zeta} = \Lambda\zeta$$

with

$$\Lambda = S^{-1}AS = \left(\begin{array}{c|c} \Omega & \epsilon I_2 \\ \hline 0 & \Omega \end{array}\right) \in \mathrm{sp}(4,\mathbb{R}), \quad \Omega = \begin{pmatrix} 0 & \omega \\ -\omega & 0 \end{pmatrix}.$$

(iii.2) The quadratic Hamiltonian,

$$\mathcal{H}_2(x,y) = -\frac{1}{2}z^\top J_2 Az;$$

to its normal form

$$K_2(\xi,\eta) = -\frac{1}{2}\zeta^\top J_2\Lambda\zeta = \frac{\epsilon}{2}\left(\eta_1^2 + \eta_2^2\right) + \varpi(\eta_1\xi_2 - \eta_2\xi_1). \tag{25}$$

PROOF. All the statements of the Lemma can be checked out straightforward from the very basic definitions of symplectic and Hamiltonian matrices and their properties.

3.3.2. Complexification of the Hamiltonian. To simplify the solution of the homological equations that give, both the successive reducing changes and the resonant terms, it is useful to introduce complex coordinates of type:

$$\xi_1 = \frac{q_1 - p_2}{\sqrt{2}}, \qquad \xi_2 = -\frac{q_1 + p_2}{\mathrm{i}\sqrt{2}}, \qquad \eta_1 = \frac{q_2 + p_1}{\sqrt{2}}, \qquad \eta_2 = -\frac{q_2 - p_1}{\mathrm{i}\sqrt{2}} \tag{26}$$

that define a linear symplectic change $\zeta = \mathcal{V}(w) := \mathcal{L}w$ with

$$w = (q,p), \qquad \zeta = (\xi,\eta), \qquad \mathcal{L} = \begin{pmatrix} 1/\sqrt{2} & 0 & 0 & -1/\sqrt{2} \\ \mathrm{i}/\sqrt{2} & 0 & 0 & \mathrm{i}/\sqrt{2} \\ 0 & 1/\sqrt{2} & 1/\sqrt{2} & 0 \\ 0 & \mathrm{i}/\sqrt{2} & -\mathrm{i}/\sqrt{2} & 0 \end{pmatrix}.$$

3.3.3. Effective linear reduction of $\mathcal{H}$. In the case at hand, explicit computations show that the composition of the linear change $\mathcal{U}$ and the complexification $\mathcal{V}$ in (26), defines the linear symplectic change $z = \Xi(w) := \mathcal{M}w$, being

$$w = (q,p), \qquad z = (x,y), \qquad \mathcal{M} = S\mathcal{L} = \begin{pmatrix} -\mathrm{i}\tilde{A}\sqrt{10} & -\tilde{A}\sqrt{2} & -\tilde{A}\sqrt{2} & -\mathrm{i}\tilde{A}\sqrt{10} \\ 5\tilde{A}\sqrt{2} & \mathrm{i}\tilde{A}\sqrt{10} & -\mathrm{i}\tilde{A}\sqrt{10} & -5\tilde{A}\sqrt{2} \\ -10\tilde{B}\sqrt{2} & -7\mathrm{i}\tilde{B}\sqrt{10} & 7\mathrm{i}\tilde{B}\sqrt{10} & 10\tilde{B}\sqrt{2} \\ 2\mathrm{i}\tilde{B}\sqrt{10} & 7\tilde{B}\sqrt{2} & 7\tilde{B}\sqrt{2} & 2\mathrm{i}\tilde{B}\sqrt{10} \end{pmatrix}, \tag{27}$$

$\tilde{A} = 3^{5/6}/15$, $\tilde{B} = 3^{1/6}/20$. Still, to take into account the dependence on μ of the Hamiltonian (22), we define the transformation $(\mu, z) = \chi(\mu, w) := (\mu, \Xi(w))$. Therefore $\mathcal{H} := \mathcal{H} \circ \chi$ is the complexified Hamiltonian. Then, the expansion (22) now casts

$$\mathcal{H}(\mu,q,p) = \mathcal{H}_2(\mu,q,p) + \mathcal{H}_3(\mu,q,p) + \cdots + \mathcal{H}_\sigma(\mu,q,p) + \ldots \tag{28}$$

with $\mathcal{H}_\sigma \in \mathbb{E}_\sigma[\mu,q,p]$; particularly,

$$\mathcal{H}_2(\mu,q,p) := \tilde{\alpha}\mu + \mathrm{i}\varpi(q_1p_1 + q_2p_2) + q_2p_1. \tag{29}$$

Remark 3. Here we stress that,

(i) $\eta_1^2 + \eta_2^2 = 2q_2p_1$ and $\eta_1\xi_2 - \eta_2\xi_1 = \mathrm{i}(q_1p_1 + q_2p_2)$ and, when the change (27) is applied to the particular Hamiltonian (22) then, $\tilde{\alpha} = 25/8$, $\varpi = \sqrt{5}/3$, and $\epsilon = 1$.

(ii) Substitution of (27) in the recurrence relations (16) gives the expansion (28). Thus, if $\mathcal{R}_\sigma := R_\sigma \circ \chi$; then

$$\mathcal{R}_0(q,p) = 1,$$

$$\mathcal{R}_1(q,p) = \mathrm{i}\frac{3^{5/6}}{15}\sqrt{10}\,q_1 + \frac{3^{5/6}}{15}\sqrt{2}\,q_2 + \frac{3^{5/6}}{15}\sqrt{2}\,p_1 + \mathrm{i}\frac{3^{5/6}}{15}\sqrt{10}\,p_2,$$

$$\mathcal{R}_{\sigma+1}(q,p) = 2\mathcal{R}_1(q,p)\,\mathcal{R}_\sigma(q,p) - \varrho^2(q,p)\,\mathcal{R}_{\sigma-1}(q,p) + \frac{1}{\sigma+1}\left(-\mathcal{R}_1(q,p)\,\mathcal{R}_\sigma(q,p) + \varrho^2(q,p)\,\mathcal{R}_{\sigma-1}(q,p)\right),$$

8

$\sigma = 1, 2, \ldots$; with $\varrho = \rho \circ \Xi$, that is

$$\varrho(q,p) = \frac{8}{15} 3^{2/3} q_1^2 + \frac{8}{25} i\, 3^{2/3} \sqrt{5}\, p_1 p_2 - \frac{16}{75} i\, 3^{2/3} \sqrt{5}\, q_2 p_2 - \frac{8}{5} 3^{2/3} q_1 p_2 - \frac{16}{75} i\, 3^{2/3} \sqrt{5}\, q_1 p_1$$

$$- \frac{8}{75} 3^{2/3} q_2^2 + \frac{8}{25} 3^{2/3} q_2 p_1 + \frac{8}{25} i\, 3^{2/3} \sqrt{5}\, q_1 q_2 - \frac{8}{75} 3^{2/3} p_1^2 + \frac{8}{15} 3^{2/3} p_2^2.$$

(iii) As pointed out, if the power series $K(\mu, z) \in \mathbb{C}[[\mu, x, y]]$ has real coefficients, its complexification $F(\mu, w) = K \circ \chi(\nu, w) = K(\mu, \Xi(w))$ satisfies the reality condition, i.e., $F(\mu, w) \in \mathbb{C}^{\mathcal{S}}[[\mu, q, p]]$. Conversely, if $F \in \mathbb{C}^{\mathcal{S}}[[\mu, q, p]]$, then $F(\mu, \Xi^{-1}(z)) \in \mathbb{C}[[\mu, x, y]]$ is a power series with real coefficients. Notably we remark that Poisson bracket preserves the $\mathcal{S}$-invariance. More precisely, if $F, G \in \mathbb{C}^{\mathcal{S}}[[\mu, q, p]]$, then $\{F, G\} \in \mathbb{C}^{\mathcal{S}}[[\mu, q, p]]$. (See for example [13], [28], Remark 3.4 or [35]).

3.4. Nonlinear reduction. Homological equations

Here we describe the process of reducing the Hamiltonian (2) to its normal form at the $1{:}{-}1$ resonant equilibrium L_2. We show how effective computations can be performed up to any arbitrary order $s \geq 3$.

So, starting from Hamiltonian (28) and naming $(q^{(0)}, p^{(0)}) = (q, p)$ to the original (complex) coordinates, the normalization is carried out degreewise by successive composition of the symplectic changes $(q^{(\sigma-3)}, p^{(\sigma-3)}) = \mathcal{T}_{t=1}^{G_\sigma}(\mu, q^{(\sigma-2)}, p^{(\sigma-2)})$, for $\sigma = 3, 4, \ldots$, where $\mathcal{T}_G^{t=1}$ is the flux of G at time $t = 1$ (see notation in section 3.1).

Thus, the first step consists in finding a pair $G_3, Z_3 \in \mathbb{E}_3[\mu, q^{(1)}, p^{(1)}]$ that fulfills the equation,

$$L_{Z_2} G_3 + Z_3 = \mathscr{H}_3^{(0)}, \tag{30}$$

with $Z_2 = \mathscr{H}_2$, $\mathscr{H}_3^{(0)} = \mathscr{H}_3$; then, the change generated by G_3, $(q^{(0)}, p^{(0)}) = \mathcal{T}_{t=1}^{G_3}(q^{(1)}, p^{(1)})$, transforms the Hamiltonian (28) to its 3rd order (degree) reduced form, which reads

$$\mathscr{H}^{(1)}(\mu, q^{(1)}, p^{(1)}) = \mathscr{H}^{(0)}(\mu, \mathcal{T}_{t=1}^{G_3}(\mu, q^{(1)}, p^{(1)})) = Z_2(\mu, q^{(1)}, p^{(1)}) + Z_3(\mu, q^{(1)}, p^{(1)}) + \mathscr{H}_4^{(1)}(\mu, q^{(1)}, p^{(1)}) + \ldots$$
$$\cdots + \mathscr{H}_\sigma^{(1)}(\mu, q^{(1)}, p^{(1)}) + \ldots$$

Thus, proceeding inductively, for $\sigma = 4, 5, \ldots$, up to $\sigma = s$,

$$\mathscr{H}^{(\sigma-2)}(\mu, q^{(\sigma-2)}, p^{(\sigma-2)}) = \mathscr{H}^{(\sigma-3)}(\mu, \mathcal{T}_{t=1}^{G_\sigma}(\mu, q^{(\sigma-2)}, p^{(\sigma-2)})) = Z_2(\mu, q^{(\sigma-2)}, p^{(\sigma-2)}) + Z_3(\mu, q^{(\sigma-2)}, p^{(\sigma-2)}) + \ldots$$
$$\cdots + Z_\sigma(\mu, q^{(\sigma-2)}, p^{(\sigma-2)}) + \mathscr{H}_{\sigma+1}^{(\sigma-2)}(\mu, q^{(\sigma-2)}, p^{(\sigma-2)}) + \mathscr{H}_{\sigma+2}^{(\sigma-2)}(\mu, q^{(\sigma-2)}, p^{(\sigma-2)}) + \ldots \tag{31}$$

provided $G_\sigma, Z_\sigma \in \mathbb{E}_\sigma[\mu, q^{(\sigma-2)}, p^{(\sigma-2)}]$ satisfy

$$L_{Z_2} G_\sigma + Z_\sigma = \mathscr{H}_\sigma^{(\sigma-3)}. \tag{32}$$

Equations (30) and (32) are the *homological* equations corresponding to the order (degree) 3 and $\sigma = 4, \ldots, s$, respectively; hence, at each fixed (adapted) degree $\sigma = 3, 4, \ldots, s$, to solve (32) one tries to find a generating function, G_σ, such that $L_{Z_2} G_\sigma = \mathscr{H}_\sigma^{(\sigma-3)}$. If this can be done, then on can set $Z_\sigma = 0$; otherwise it must be added a complementary (or resonant) term Z_σ to make the equation be valid.

Thus, assume that at the $(\sigma - 2)^{\text{th}}$ step, the corresponding G_σ and Z_σ have been determined from (32). To go on with the next iteration, one needs to transform the current Hamiltonian, $\mathscr{H}^{(\sigma-3)}$, by the time-1 flow of the Hamiltonian G_σ. This transformation is carried out through the successive application of Poisson brackets,

$$\mathscr{H}^{(\sigma-2)} = \mathscr{H}^{(\sigma-3)} + \frac{1}{1!} L_{G_\sigma} \mathscr{H}^{(\sigma-3)} + \cdots + \frac{1}{k!} L_{G_\sigma}^k \mathscr{H}^{(\sigma-3)} + \ldots$$

Remark 4. Therefore, since the Poisson parentheses preserve the $\mathcal{S}$-symmetries, it follows that all of the successive transformed Hamiltonians will also be $\mathcal{S}$-invariants, as long as each of the generating functions G_σ is, $\sigma = 3, 4, \ldots$

In practice, there are several useful algorithms to perform this computation in an effective way. For example, once the homological equations (32) are solved and G_σ is found, one can use Algorithm 1 above (see [17] for the corresponding software implementation) to compute the terms of the transformed Hamiltonian, $\mathscr{H}^{(\sigma-2)}$, from the current (adapted) degree σ, up to the given degree s to which the normal form is computed; more precisely, it outputs,

$$\mathscr{H}_\sigma^{(\sigma-2)} = Z_\sigma, \mathscr{H}_{\sigma+1}^{(\sigma-2)}, \ldots, \mathscr{H}_s^{(\sigma-2)}. \tag{33}$$

We note that, as the successive changes applied are near-identity transformations (see Remark 5 below), the first $\sigma - 2$ terms, $Z_2, Z_3, \ldots, Z_{\sigma-1}$ of $\mathscr{H}^{(\sigma-3)}$, remain the same in $\mathscr{H}^{(\sigma-2)}$ (as can be noted in (31)).

Algorithm 1: Computation of $\mathscr{H}_\sigma^{(\sigma-2)} = Z_\sigma, \mathscr{H}_{\sigma+1}^{(\sigma-2)}, \ldots, \mathscr{H}_s^{(\sigma-2)}$ (in [17]).

1: **for** $i \leftarrow s, \sigma, -1$ **do**   ▷ i from s to σ by -1
2:      $k \leftarrow 0$
3:      $l \leftarrow 1$
4:      $U \leftarrow H(i - \sigma + 2)$
5:      **for** $j \leftarrow i, s, \sigma - 2$ **do**   ▷ j from i to s by $\sigma - 2$
6:          $k \leftarrow k + 1$
7:          $l \leftarrow l * k$
8:          $U \leftarrow \{U, G(\sigma)\}$
9:          $H(j) \leftarrow H(j) + U/l$
10:      **end for**
11: **end for**

Remark 5. The transformation generated by G_3 are given by,

$$q_i^{(0)} = q_i^{(1)} + \left\{ q_i^{(1)}, G_3 \right\} + \frac{1}{2!} \left\{ \left\{ q_i^{(1)}, G_3 \right\}, G_3 \right\} + \frac{1}{3!} \left\{ \left\{ \left\{ q_i^{(1)}, G_3 \right\}, G_3 \right\}, G_3 \right\} + \ldots,$$

$$p_i^{(0)} = p_i^{(1)} + \left\{ p_i^{(1)}, G_3 \right\} + \frac{1}{2!} \left\{ \left\{ p_i^{(1)}, G_3 \right\}, G_3 \right\} + \frac{1}{3!} \left\{ \left\{ \left\{ p_i^{(1)}, G_3 \right\}, G_3 \right\}, G_3 \right\} + \ldots,$$

$i = 1, 2$; where $\left(q^{(0)}, p^{(0)} \right)$ are the original coordinates and $\left(q^{(1)}, p^{(1)} \right)$ are the new ones. This can be repeated to get explicitly the symplectic changes generated by G_4, $G_5, \ldots$ and so on, up to the required degree. Of course, a similar algorithm to Algorithm 1 can be applied coordinatewise to mechanize the computations (again, see [17] for details).

Proceeding in this way up to order $s \geq 4$, the final Hamiltonian, $\mathscr{H}^{(s-2)}$, is the sum $\mathscr{H}^{(s-2)} = Z^{(s)} + \mathscr{H}_{>s}$, where

$$Z^{(s)} = Z_2 + Z_3 + Z_4 + \cdots + Z_s$$

is the *normal form* (up to degree s), made up of resonant terms; whilst

$$\mathscr{H}_{>s} = \mathscr{H}_{s+1}^{(s-2)} + \mathscr{H}_{s+2}^{(s-2)} + \ldots$$

is the *remainder*, that holds higher order terms.

The normal form at $1{:}{-}1$ non semisimple resonant equilibrium point in a family of Hamiltonian systems has been investigated in many papers, here we quote: [33], [38], [39]. The same resonance can take place in a family of periodic orbits (see [15], [27], [28], [29], [30]), and in a family of lower dimensional invariant tori (see [7]). Whatever the algorithm to perform the transformations is, the key point of the reduction to normal form lies in the solvability of the homological equations (32) (see the quoted references for an outlook of the different approaches). In the context of the periodic Hopf bifurcation, this is tackled in [28], Proposition 4.1, which we adapt here to the special case of a 3-degree of freedom (complexified) Hamiltonian (28), depending on the *normal coordinates* $q, p \in \mathbb{C}^2$, an "action" $\mu \in \mathbb{C}$ (originally, the real parameter of the family of Hamiltonians), but not explicitly on its conjugate angle.

Remark 6. In what follows we shall denote the subspaces

$$\mathbb{E}_\sigma[\mu, q^{(\sigma-2)}, p^{(\sigma-2)}], \quad \mathbb{E}_\sigma^{\mathcal{S}}[\mu, q^{(\sigma-2)}, p^{(\sigma-2)}], \quad \mathbb{E}_{\ell MN}[\mu, q^{(\sigma-2)}, p^{(\sigma-2)}], \quad \text{and} \quad \mathbb{E}_{\ell MN}^{\mathcal{S}}[\mu, q^{(\sigma-2)}, p^{(\sigma-2)}]$$

just by $\mathbb{E}_\sigma$, $\mathbb{E}_\sigma^{\mathcal{S}}$, $\mathbb{E}_{\ell MN}$ and $\mathbb{E}_{\ell MN}^{\mathcal{S}}$ respectively, without specifying the coordinates μ, $q^{(\sigma-2)}$, $p^{(\sigma-2)}$. On the other hand, we shall also stop using the super-indices $^{(\sigma-2)}$ (or the corresponding ones) on the positions $q = (q_1, q_2)$ and momenta $p = (p_1, p_2)$. In both cases, it should be clear which coordinates are being used at each step.

Proposition 1. *Let us consider $\mathscr{H}_2$ in (29), the decomposition of $\mathbb{E}_\sigma$ into $\mathbb{E}_\sigma = \mathbb{E}_\sigma^0 \oplus \mathbb{E}_\sigma^+$, with*

$$\mathbb{E}_\sigma^0 = \bigoplus_{2\ell + 2M = \sigma} \mathbb{E}_{\ell MM}, \qquad \mathbb{E}_\sigma^+ = \bigoplus_{\substack{2\ell + M + N = \sigma \\ (M \neq N)}} \mathbb{E}_{\ell MN},$$

so that $\mathbb{E}_\sigma^0 = \{0\}$ if σ is odd. Given $\mathscr{H}_\sigma^{(\sigma-3)}$, $\sigma \geq 3$, we split it as

$$\mathscr{H}_\sigma^{(\sigma-3)} = \mathring{\mathscr{H}}_\sigma^{(\sigma-3)} + \hat{\mathscr{H}}_\sigma^{(\sigma-3)}, \qquad \mathring{\mathscr{H}}_\sigma^{(\sigma-3)} \in \mathbb{E}_\sigma^0, \qquad \hat{\mathscr{H}}_\sigma^{(\sigma-3)} \in \mathbb{E}_\sigma^+.$$

Then, we have:

(a) *There exists a unique $G_\sigma^+ \in \mathbb{E}_\sigma^+$; such that $L_{Z_2} G_\sigma^+ = \hat{\mathscr{H}}_\sigma^{(\sigma-3)}$. Moreover, $G_\sigma^+ \in \mathbb{E}_\sigma^{\mathcal{S}}$.*

(b) *If σ is even, there is a real coefficients homogeneous polynomial $\mathcal{Z}_\sigma(u,v,w)$ of standard degree $\sigma/2$, which is uniquely defined in terms of $\mathscr{H}_\sigma^{\circ(\sigma-3)}$, such that if we set*

$$Z_\sigma(\mu,q,p) := \mathcal{Z}_\sigma(\mu, q_1 p_2, \mathrm{i}(q_1 p_1 + q_2 p_2)/2), \tag{34}$$

then $Z_\sigma \in \mathbb{E}_\sigma^0 \cap \mathbb{E}_\sigma^\mathcal{S}$ and there is $G_\sigma^0 \in \mathbb{E}_\sigma^0$ verifying $L_{Z_2} G_\sigma^0 + Z_\sigma = \mathscr{H}_\sigma^{\circ(\sigma-3)}$. Moreover, G_σ^0 can be chosen so that $G_\sigma^0 \in \mathbb{E}_\sigma^\mathcal{S}$.

Therefore, if the degree σ is odd $G_\sigma := G_\sigma^+$ and $Z_\sigma := 0$ solve equation (32) in $\mathbb{E}_\sigma^\mathcal{S}$; otherwise, if σ is even so does $G_\sigma := G_\sigma^+ + G_\sigma^0$ and Z_σ given by (34).

Remark 7. Of course, one might expand the Hamiltonian (28) with respect to the (q,p) coordinates only, letting the coefficients depend on μ. Proceeding in that way, the coefficients of the normal form terms and of the generating functions –given, at each step, by the solutions of (32)– would now be rational functions of the parameter μ. Thus, the higher the degree, the more intricate the expressions. This results to be a very expensive way to compute the normal form. Hence, the approach we present here of expanding in the parameter (we recall that it is assumed to be a small quantity), seems fairly more suitable.

Remark 8. In some situations, such as when we approximate the solutions of the original Hamiltonian system using the solutions of its normal form or when we look for the "optimal" degree s up to what the normal form has to be computed to minimize the size of the remainder, we have to find explicitly the generating functions $G_3, G_4, \ldots$ At this regard, we stress that the proof of Proposition 1 we give below, not only shows the structure of the reduced Hamiltonian in this case at point, but also provides explicit formulas for its coefficients and the coefficients of the generating functions up to any required degree.

The Examples 1, 2, 3, and 4 that come up along the proof of Proposition 1 below illustrate the practical implementation of the normalization process for the particular Hamiltonian of the CP problem. Notably, the fourth order normal form $Z^{(4)}$ of the Hamiltonian (28) (and the generating functions G_3 and G_4) follow from the Examples 3, and 4. We remark that the proof of Proposition 1 is more complete and detailed than the one given in [28].

PROOF OF PROPOSITION 1. Let us consider a monomial $\alpha = \mu^\ell q^m p^n$, with $2\ell + |m|_1 + |n|_1 = \sigma$, i.e., of adapted degree $\sigma \geq 3$. The action of the operator L_{Z_2} on α gives,

$$L_{Z_2}\alpha = \left(\Omega + m_1 \frac{q_2}{q_1} - n_2 \frac{p_1}{p_2} \right) \alpha, \tag{35}$$

being $\Omega = \Omega_{|m|_1 |n|_1} := \mathrm{i}\,\omega(|m|_1 - |n|_1)$, and where it assumed that the quotient q_2/q_1 is not present when $m_1 = 0$ (the same convention applies for the quotient p_1/p_2 when $n_2 = 0$).

Remark 9 (on the values of ℓ). We note here that no linear terms in the coordinates (q,p) can appear in any of the new transformed Hamiltonians, since for any μ, the origin $(q,p) = (0,0)$ is an equilibrium point and, in the reduction process to normal form all the changes that we made are close to the identity. Therefore, $|m|_1 + |n|_1$ cannot be one at any of the successive transformed Hamiltonians along the reduction process, so the equilibrium point remains at the origin at each step. Thus, at the homogeneous polynomials

$$\mathscr{H}_\kappa^{(\sigma-2)} = \sum_{2\ell+|m|_1+|n|_1=\kappa} \mathscr{H}_{\ell\,mn}^{(\sigma-2)} \mu^\ell q^m p^n$$

of (adapted) degree $\kappa = \sigma, \sigma+1, \ldots, s$ (see (33)), the index ℓ can vary only in the range $\ell = 0, \ldots, 3\lfloor \kappa/2 \rfloor - \kappa$ ($\sigma = 3, 4, \ldots$), where $\lfloor \cdot \rfloor$ stands for the integer part.

If follows from (35) that L_{Z_2} leaves each subspace $\mathbb{E}_{\ell MN} \subseteq \mathbb{E}_\sigma$ invariant. Therefore, we can fix $\ell, M, N \in \mathbb{N}_0$ and focus on solving the projections of equations (32) onto the subspace $\mathbb{E}_{\ell MN}$; we mean, given $F \in \mathbb{E}_{\ell MN}$, we look for $G, Z \in \mathbb{E}_{\ell MN}$ such that the homological equation

$$L_{Z_2} G + Z = F \tag{36}$$

holds. It turns out that, when $\Omega \neq 0$ (i.e., when $M \neq N$) then $F \in \operatorname{Range} L_{Z_2}|_{\mathbb{E}_{\ell MN}}$ and we can set $Z = 0$ in equation above. Otherwise, when $\Omega = 0$ (i.e., when $M = N$), then resonant monomials appear generically. We analyze both cases below.

Remark 10. Prior to continuing with our analysis, let us point out that, actually, when one writes the equation (36) explicitly, the term μ^ℓ appears as a product at both sides, and can be simplified. Hence, abusing notation, this factor has been omitted in the expansions of the polynomials in $\mathbb{E}_{\ell MN}$.

The case $\Omega \neq 0$ ($M \neq N$). Let $U \in \mathbb{E}_{\ell MN}$, with ℓ, M, N, fixed, then

$$U = \sum_{\substack{|m|_1=M \\ |n|_1=N}} u_{\ell m_1 m_2 n_1 n_2} q_1^{m_1} q_2^{m_2} p_1^{n_1} p_2^{n_2} = \sum_{\substack{0 \leq m \leq M \\ 0 \leq n \leq N}} u_{\ell,m,M-m,N-n,n} q_1^m q_2^{M-m} p_1^{N-n} p_2^n,$$

(the factor μ^ℓ is omitted, as Remark 10 warns). Thus, we can set $u_{mn} := u_{\ell,m,M-m,N-n,n}$ for $0 \leq m \leq M$, $0 \leq n \leq N$; so, for every ℓ fixed, any monomial in U is specified by just a pair of indices. Now, let $u \in \mathcal{M}_{(M+1)\times(N+1),1}(\mathbb{C})$ be the array holding the coefficients u_{mn} ordered as follows: $u_{mn} \prec u_{m'n'}$ (u_{mn} precedes $u_{m'n'}$) if $m > m'$ or, when $m = m'$, if $n > n'$.

Example 1. For instance, if $M = 3$ and $N = 2$; then

$$u_{3,2} \prec u_{3,1} \prec u_{3,0} \prec u_{2,2} \prec u_{2,1} \prec u_{2,0} \prec u_{1,2} \prec u_{1,1} \prec u_{1,0} \prec u_{0,2} \prec u_{0,1} \prec u_{0,0}. \qquad \triangleright$$

Yet we can define the block-array $u^\top = (u_M \, u_{M-1} \cdots u_0) \in \mathbb{C}^{N+1} \times \mathbb{C}^{N+1} \times \cdots \times \mathbb{C}^{N+1}$, with

$$u_j^\top = (u_{j,N}, u_{j,N-1}, \ldots, u_{j,0}) \in \mathbb{C}^{N+1}$$

for $j = M, M-1, \ldots, 0$. Therefore, to find the solution of (36) we set $Z_{\ell MN} = 0$ and solve a linear system $Ag = f$; with $A \in \mathcal{M}_{(M+1)\times(N+1)}(\mathbb{C})$; $f, g \in \mathbb{C}^{(M+1)\times(N+1)}$; which, using the notation just described, can be written blockwise and looks

$$
\begin{pmatrix}
D_N \\
E_M & D_N \\
& E_{M-1} & D_N \\
& & \ddots & \ddots \\
& & & \ddots & \ddots \\
& & & & E_2 & D_N \\
& & & & & E_1 & D_N
\end{pmatrix}
\begin{pmatrix}
g_M \\
g_{M-1} \\
g_{M-2} \\
\vdots \\
\vdots \\
g_1 \\
g_0
\end{pmatrix}
=
\begin{pmatrix}
f_M \\
f_{M-1} \\
f_{M-2} \\
\vdots \\
\vdots \\
f_1 \\
f_0
\end{pmatrix}, \tag{37}
$$

where $E_j = jI_{N+1} \in \mathcal{M}_{N+1}(\mathbb{C})$, $i, j = M, M-1, \ldots, 1$; $D_N = \Omega I_{N+1} - P_N \in \mathcal{M}_{N+1}(\mathbb{C})$ with $(P_N)_{i,j} = N - i + 2$ if $i = j + 1$ for $j = 1, \ldots, N$, or $(P_N)_{i,j} = 0$ otherwise. From the band structure of A, we see that it is a lower triangular matrix with all the elements on its diagonal equal to $\Omega \neq 0$, so the linear system (37) has exactly one solution.

Remark 11 (Reality conditions). It is straightforward to show that $\bar{g}_{\ell,m,M-m,N-n,n} = (-1)^{m+n} g_{\ell,n,N-n,M-m,m}$, for $0 \le m \le M, 0 \le n \le N, 2\ell + M + N = \sigma$. Hence $G_\sigma^+ \in \mathbb{E}_\sigma^{\mathcal{S}}$.

Example 2. If, as in Example 1, we take $M = 3$, $N = 2$; then $\Omega = \mathrm{i}\,\omega(3 - 2) = \mathrm{i}\,\omega$ and

$$
P_2 = \begin{pmatrix} 0 & 0 & 0 \\ 2 & 0 & 0 \\ 0 & 1 & 0 \end{pmatrix}, \quad
D_2 = \begin{pmatrix} \mathrm{i}\,\omega & & \\ -2 & \mathrm{i}\,\omega & \\ & -1 & \mathrm{i}\,\omega \end{pmatrix}, \quad
E_j = \begin{pmatrix} j & & \\ & j & \\ & & j \end{pmatrix}, \; j = 1,2,3; \quad
A = \begin{pmatrix} D_2 & & & \\ E_3 & D_2 & & \\ & E_2 & D_2 & \\ & & E_1 & D_2 \end{pmatrix}.
$$

Therefore, for this case in point, the system (37) is written as

$$
\left(
\begin{array}{ccc|ccc|ccc|ccc}
\mathrm{i}\,\omega & & & & & & & & & & & \\
-2 & \mathrm{i}\,\omega & & & & & & & & & & \\
& -1 & \mathrm{i}\,\omega & & & & & & & & & \\
\hline
3 & 0 & 0 & \mathrm{i}\,\omega & & & & & & & & \\
0 & 3 & 0 & -2 & \mathrm{i}\,\omega & & & & & & & \\
0 & 0 & 3 & & -1 & \mathrm{i}\,\omega & & & & & & \\
\hline
& & & 2 & 0 & 0 & \mathrm{i}\,\omega & & & & & \\
& & & 0 & 2 & 0 & -2 & \mathrm{i}\,\omega & & & & \\
& & & 0 & 0 & 2 & & -1 & \mathrm{i}\,\omega & & & \\
\hline
& & & & & & 1 & 0 & 0 & \mathrm{i}\,\omega & & \\
& & & & & & 0 & 1 & 0 & -2 & \mathrm{i}\,\omega & \\
& & & & & & 0 & 0 & 1 & & -1 & \mathrm{i}\,\omega
\end{array}
\right)
\begin{pmatrix}
g_{3,2} \\ g_{3,1} \\ g_{3,0} \\ g_{2,2} \\ g_{2,1} \\ g_{2,0} \\ g_{1,2} \\ g_{1,1} \\ g_{1,0} \\ g_{0,2} \\ g_{0,1} \\ g_{0,0}
\end{pmatrix}
=
\begin{pmatrix}
f_{3,2} \\ f_{3,1} \\ f_{3,0} \\ f_{2,2} \\ f_{2,1} \\ f_{2,0} \\ f_{1,2} \\ f_{1,1} \\ f_{1,0} \\ f_{0,2} \\ f_{0,1} \\ f_{0,0}
\end{pmatrix},
$$

and it is seen at once –as we stated before for the general case– that $\det A \neq 0$, so the coefficients of the generating function are uniquely determined. $\qquad \triangleright$

Hence, we can write the component $G_\sigma^+ \in \mathbb{E}_\sigma^+$ of the generating function G_σ in the form,

$$G_\sigma^+(\mu, q, p) = \sum_{\substack{2\ell + M + N = \sigma \\ M \neq N}} G_{\ell MN} = \sum_{\substack{2\ell + M + N = \sigma \\ M \neq N}} \left(\sum_{\substack{0 \le m \le M \\ 0 \le n \le N}} g_{\ell,m,M-m,N-n,n} q_1^m q_2^{M-m} p_1^{N-n} p_2^n \right) \mu^\ell.$$

This completes the proof of the part (a) of Proposition 1.

Example 3 (Computation of G_3, $\mathscr{H}_4^{(1)}$ and G_4^+). For $s = 3$, the right hand side of (30) is given by

$$
\begin{aligned}
\mathscr{H}_3^{(0)}(\mu, q, p) = {} & \mathrm{i}\,\frac{34}{225}\,3^{5/6}\sqrt{10}\,q_1^3 - \frac{2}{25}\,3^{5/6}\sqrt{2}\,q_1^2 q_2 + \mathrm{i}\,\frac{2}{125}\,3^{5/6}\sqrt{10}\,q_1 q_2^2 - \frac{34}{1125}\,3^{5/6}\sqrt{2}\,q_2^3 - \mathrm{i}\,\frac{2}{25}\,3^{5/6}\sqrt{10}\,q_1^2 p_2 \\
& + \frac{34}{75}\,3^{5/6}\sqrt{2}\,q_1^2 p_1 - \frac{4}{25}\,3^{5/6}\sqrt{2}\,q_1 q_2 p_2 + \mathrm{i}\,\frac{4}{125}\,3^{5/6}\sqrt{10}\,q_1 q_2 p_1 - \mathrm{i}\,\frac{34}{375}\,3^{5/6}\sqrt{10}\,q_2^2 p_2 + \frac{2}{125}\,3^{5/6}\sqrt{2}\,q_2^2 p_1 \\
& - \mathrm{i}\,\frac{2}{25}\,3^{5/6}\sqrt{10}\,q_1 p_2^2 - \frac{4}{25}\,3^{5/6}\sqrt{2}\,q_1 p_1 p_2 - \mathrm{i}\,\frac{34}{375}\,3^{5/6}\sqrt{10}\,q_1 p_1^2 + \frac{34}{75}\,3^{5/6}\sqrt{2}\,q_2 p_2^2 + \mathrm{i}\,\frac{4}{125}\,3^{5/6}\sqrt{10}\,q_2 p_1 p_2 \\
& + \frac{2}{125}\,3^{5/6}\sqrt{2}\,q_2 p_1^2 + \mathrm{i}\,\frac{34}{225}\,3^{5/6}\sqrt{10}\,p_2^3 - \frac{2}{25}\,3^{5/6}\sqrt{2}\,p_1 p_2^2 + \mathrm{i}\,\frac{2}{125}\,3^{5/6}\sqrt{10}\,p_1^2 p_2 - \frac{34}{1125}\,3^{5/6}\sqrt{2}\,p_1^3.
\end{aligned}
$$

Then, setting up the homological equations (36) –for $\ell = 0$, taking $M = 3$, $N = 0$; $M = 2$, $N = 1$; $M = 1$, $N = 2$; $M = 0$, $N = 3$–, and solving the corresponding linear systems of type (37) one gets $Z_3 = 0$ and $G_3 = G_3^+ + G_3^0$, with

$$
\begin{aligned}
G_3^+(\mu, q, p) ={}& \frac{34}{225}\, 3^{5/6}\sqrt{2}\, q_1^3 + \mathrm{i}\,\frac{8}{75}\, 3^{5/6}\sqrt{10}\, q_1^2 q_2 - \frac{74}{375}\, 3^{5/6}\sqrt{2}\, q_1 q_2^2 - \mathrm{i}\,\frac{188}{5625}\, 3^{5/6}\sqrt{10}\, q_2^3 \\
& - \frac{6}{25}\, 3^{5/6}\sqrt{2}\, q_1^2 p_2 - \mathrm{i}\,\frac{16}{125}\, 3^{5/6}\sqrt{10}\, q_1^2 p_1 - \frac{24}{125}\, 3^{5/6}\sqrt{10}\, q_1 q_2 p_2 + \frac{36}{125}\, 3^{5/6}\sqrt{2}\, q_1 q_2 p_1 \\
& + \frac{38}{125}\, 3^{5/6}\sqrt{2}\, q_2^2 p_2 - \mathrm{i}\,\frac{12}{625}\, 3^{5/6}\sqrt{10}\, q_2^2 p_1 + \frac{6}{25}\, 3^{5/6}\sqrt{2}\, q_1 p_2^2 + \mathrm{i}\,\frac{24}{125}\, 3^{5/6}\sqrt{10}\, q_1 p_1 p_2 \\
& - \frac{38}{125}\, 3^{5/6}\sqrt{2}\, q_1 p_1^2 + \mathrm{i}\,\frac{16}{125}\, 3^{5/6}\sqrt{10}\, q_2 p_2^2 - \frac{36}{125}\, 3^{5/6}\sqrt{2}\, q_2 p_1 p_2 + \mathrm{i}\,\frac{12}{625}\, 3^{5/6}\sqrt{10}\, q_2 p_1^2 \\
& - \frac{34}{225}\, 3^{5/6}\sqrt{2}\, p_2^3 - \mathrm{i}\,\frac{8}{75}\, 3^{5/6}\sqrt{10}\, p_1 p_2^2 + \frac{74}{375}\, 3^{5/6}\sqrt{2}\, p_1^2 p_2 + \mathrm{i}\,\frac{188}{5625}\, 3^{5/6}\sqrt{10}\, p_1^3,
\end{aligned}
$$

and $G_3^0 = 0$. Furthermore, as

$$
\begin{aligned}
\mathscr{H}_4^{(0)}(\mu, q, p) ={}& \frac{27}{32}\, 3^{2/3}\, \mu^2 - \frac{11}{15}\, 3^{2/3}\, \mu q_1^2 - \mathrm{i}\,\frac{16}{25}\, 3^{2/3}\sqrt{5}\, \mu q_1 q_2 + \frac{56}{75}\, 3^{2/3}\, \mu q_2^2 + \frac{6}{5}\, 3^{2/3}\, \mu q_1 p_2 + \mathrm{i}\,\frac{14}{25}\, 3^{2/3}\sqrt{5}\, \mu q_1 p_1 \\
& + \mathrm{i}\,\frac{14}{25}\, 3^{2/3}\sqrt{5}\, \mu q_2 p_2 - \frac{51}{25}\, 3^{2/3}\, \mu q_2 p_1 - \frac{11}{15}\, 3^{2/3}\, \mu p_2^2 - \mathrm{i}\,\frac{16}{25}\, 3^{2/3}\sqrt{5}\, \mu p_1 p_2 + \frac{56}{75}\, 3^{2/3}\, \mu p_1^2 \\
& - \frac{203}{225}\, 3^{2/3}\, q_1^4 - \mathrm{i}\,\frac{268}{1125}\, 3^{2/3}\sqrt{5}\, q_1^3 q_2 + \frac{86}{375}\, 3^{2/3}\, q_1^2 q_2^2 + \mathrm{i}\,\frac{268}{5625}\, 3^{2/3}\sqrt{5}\, q_1 q_2^3 - \frac{203}{5625}\, 3^{2/3}\, q_2^4 \\
& + \frac{268}{225}\, 3^{2/3}\, q_1^3 p_2 + \mathrm{i}\,\frac{812}{1125}\, 3^{2/3}\sqrt{5}\, q_1^3 p_1 + \mathrm{i}\,\frac{172}{375}\, 3^{2/3}\sqrt{5}\, q_1^2 q_2 p_2 - \frac{268}{375}\, 3^{2/3}\, q_1^2 q_2 p_1 - \frac{268}{375}\, 3^{2/3}\, q_1 q_2^2 p_2 \\
& - \mathrm{i}\,\frac{172}{1875}\, 3^{2/3}\sqrt{5}\, q_1 q_2^2 p_1 - \mathrm{i}\,\frac{812}{5625}\, 3^{2/3}\sqrt{5}\, q_2^3 p_2 + \frac{268}{5625}\, 3^{2/3}\, q_2^3 p_1 - \frac{86}{75}\, 3^{2/3}\, q_1^2 p_2^2 - \mathrm{i}\,\frac{268}{375}\, 3^{2/3}\sqrt{5}\, q_1^2 p_1 p_2 \\
& + \frac{406}{375}\, 3^{2/3}\, q_1^2 p_1^2 - \mathrm{i}\,\frac{268}{375}\, 3^{2/3}\sqrt{5}\, q_1 q_2 p_2^2 + \frac{344}{375}\, 3^{2/3}\, q_1 q_2 p_1 p_2 + \mathrm{i}\,\frac{268}{1875}\, 3^{2/3}\sqrt{5}\, q_1 q_2 p_1^2 + \frac{406}{375}\, 3^{2/3}\, q_2^2 p_2^2 \\
& + \mathrm{i}\,\frac{268}{1875}\, 3^{2/3}\sqrt{5}\, q_2^2 p_1 p_2 - \frac{86}{1875}\, 3^{2/3}\, q_2^2 p_1^2 + \frac{268}{225}\, 3^{2/3}\, q_1 p_2^3 + \mathrm{i}\,\frac{172}{375}\, 3^{2/3}\sqrt{5}\, q_1 p_1 p_2^2 - \frac{268}{375}\, 3^{2/3}\, q_1 p_1^2 p_2 \\
& - \mathrm{i}\,\frac{812}{5625}\, 3^{2/3}\sqrt{5}\, q_1 p_1^3 + \mathrm{i}\,\frac{812}{1125}\, 3^{2/3}\sqrt{5}\, q_2 p_2^3 - \frac{268}{375}\, 3^{2/3}\, q_2 p_1 p_2^2 - \mathrm{i}\,\frac{172}{1875}\, 3^{2/3}\sqrt{5}\, q_2 p_1^2 p_2 + \frac{268}{5625}\, 3^{2/3}\, q_2 p_1^3 \\
& - \frac{203}{225}\, 3^{2/3}\, p_2^4 - \mathrm{i}\,\frac{268}{1125}\, 3^{2/3}\sqrt{5}\, p_1 p_2^3 + \frac{86}{375}\, 3^{2/3}\, p_1^2 p_2^2 + \mathrm{i}\,\frac{268}{5625}\, 3^{2/3}\sqrt{5}\, p_1^3 p_2 - \frac{203}{5625}\, 3^{2/3}\, p_1^4,
\end{aligned}
$$

application of Algorithm 1 yields,

$$
\begin{aligned}
\mathscr{H}_4^{(1)} &= \mathscr{H}_4^{(0)} + \frac{1}{1!}\{\mathscr{H}_3^{(0)}, G_3\} + \frac{1}{2!}\{\{Z_2, G_3\}, G_3\} \\
&= \mathscr{H}_{2,0,0}^{(1)} + \mathscr{H}_{1,2,0}^{(1)} + \mathscr{H}_{1,1,1}^{(1)} + \mathscr{H}_{1,0,2}^{(1)} + \mathscr{H}_{0,4,0}^{(1)} + \mathscr{H}_{0,3,1}^{(1)} + \mathscr{H}_{0,2,2}^{(1)} + \mathscr{H}_{0,1,3}^{(1)} + \mathscr{H}_{0,0,4}^{(1)}
\end{aligned}
$$

with $\mathscr{H}_{\ell MN}^{(1)} \in \mathbb{E}_{\ell MN}$. Explicitly,

$$
\mathscr{H}_{2,0,0}^{(1)}(\mu, q, p) = \frac{27}{32}\, 3^{2/3}\, \mu^2, \tag{38}
$$

$$
\mathscr{H}_{1,2,0}^{(1)}(\mu, q, p) = -\frac{11}{15}\, 3^{2/3}\, \mu q_1^2 - \mathrm{i}\,\frac{16}{25}\, 3^{2/3}\sqrt{5}\, \mu q_1 q_2 + \frac{56}{75}\, 3^{2/3}\, \mu q_2^2,
$$

$$
\mathscr{H}_{1,1,1}^{(1)}(\mu, q, p) = \frac{6}{5}\, 3^{2/3}\, \mu q_1 p_2 + \mathrm{i}\,\frac{14}{25}\, 3^{2/3}\sqrt{5}\, \mu q_1 p_1 + \mathrm{i}\,\frac{14}{25}\, 3^{2/3}\sqrt{5}\, \mu q_2 p_2 - \frac{51}{25}\, 3^{2/3}\, \mu q_2 p_1, \tag{39}
$$

$$
\mathscr{H}_{1,0,2}^{(1)}(\mu, q, p) = -\frac{11}{15}\, 3^{2/3}\, \mu p_2^2 - \mathrm{i}\,\frac{16}{25}\, 3^{2/3}\sqrt{5}\, \mu p_1 p_2 + \frac{56}{75}\, 3^{2/3}\, \mu p_1^2,
$$

$$
\mathscr{H}_{0,4,0}^{(1)}(\mu, q, p) = -\frac{4043}{5625}\, 3^{2/3}\, q_1^4 - \mathrm{i}\,\frac{3916}{28125}\, 3^{2/3}\sqrt{5}\, q_1^3 q_2 + \frac{1474}{3125}\, 3^{2/3}\, q_1^2 q_2^2 + \mathrm{i}\,\frac{748}{140625}\, 3^{2/3}\sqrt{5}\, q_1 q_2^3 + \frac{4453}{140625}\, 3^{2/3}\, q_2^4,
$$

$$
\begin{aligned}
\mathscr{H}_{0,3,1}^{(1)}(\mu, q, p) ={}& \frac{476}{1125}\, 3^{2/3}\, q_1^3 p_2 + \mathrm{i}\,\frac{1084}{5625}\, 3^{2/3}\sqrt{5}\, q_1^3 p_1 + \mathrm{i}\,\frac{428}{9375}\, 3^{2/3}\sqrt{5}\, q_1^2 q_2 p_2 - \frac{332}{375}\, 3^{2/3}\, q_1^2 q_2 p_1 \\
& + \frac{724}{9375}\, 3^{2/3}\, q_1 q_2^2 p_2 - \mathrm{i}\,\frac{15308}{46875}\, 3^{2/3}\sqrt{5}\, q_1 q_2^2 p_1 + \mathrm{i}\,\frac{11572}{140625}\, 3^{2/3}\sqrt{5}\, q_2^3 p_2 + \frac{23116}{14062}\, 3^{2/3}\, q_2^3 p_1,
\end{aligned}
$$

$$
\begin{aligned}
\mathscr{H}_{0,2,2}^{(1)}(\mu, q, p) ={}& \frac{14}{625}\, 3^{2/3}\, q_1^2 p_2^2 + \mathrm{i}\,\frac{12}{625}\, 3^{2/3}\sqrt{5}\, q_1^2 p_1 p_2 - \frac{638}{3125}\, 3^{2/3}\, q_1^2 p_1^2 + \mathrm{i}\,\frac{12}{625}\, 3^{2/3}\sqrt{5}\, q_1 q_2 p_2^2 + \frac{7832}{9375}\, 3^{2/3}\, q_1 q_2 p_1 p_2 \\
& + \mathrm{i}\,\frac{196}{625}\, 3^{2/3}\sqrt{5}\, q_1 q_2 p_1^2 - \frac{638}{3125}\, 3^{2/3}\, q_2^2 p_2^2 + \mathrm{i}\,\frac{196}{625}\, 3^{2/3}\sqrt{5}\, q_2^2 p_1 p_2 - \frac{4946}{15625}\, 3^{2/3}\, q_2^2 p_1^2, \tag{40}
\end{aligned}
$$

$$
\begin{aligned}
\mathscr{H}_{0,1,3}^{(1)}(\mu, q, p) ={}& \frac{476}{1125}\, 3^{2/3}\, q_1 p_2^3 + \mathrm{i}\,\frac{428}{9375}\, 3^{2/3}\sqrt{5}\, q_1 p_1 p_2^2 + \frac{724}{9375}\, 3^{2/3}\, q_1 p_1^2 p_2 + \mathrm{i}\,\frac{11572}{140625}\, 3^{2/3}\sqrt{5}\, q_1 p_1^3 \\
& + \mathrm{i}\,\frac{1084}{5625}\, 3^{2/3}\sqrt{5}\, q_2 p_2^3 - \frac{332}{375}\, 3^{2/3}\, q_2 p_1 p_2^2 - \mathrm{i}\,\frac{15308}{46875}\, 3^{2/3}\sqrt{5}\, q_2 p_1^2 p_2 + \frac{23116}{140625}\, 3^{2/3}\, q_2 p_1^3,
\end{aligned}
$$

$$
\mathscr{H}_{0,0,4}^{(1)}(\mu, q, p) = -\frac{4043}{5625}\, 3^{2/3}\, p_2^4 - \mathrm{i}\,\frac{3916}{28125}\, 3^{2/3}\sqrt{5}\, p_1 p_2^3 + \frac{1474}{3125}\, 3^{2/3}\, p_1^2 p_2^2 + \mathrm{i}\,\frac{748}{140625}\, 3^{2/3}\sqrt{5}\, p_1^3 p_2 + \frac{4453}{140625}\, 3^{2/3}\, p_1^4.
$$

Thus, as for $s = 3$, we can state the homological equations, now for $\ell = 1$, taking $M = 2$, $N = 0$; $M = 0$, $N = 2$; and for $\ell = 0$, taking $M = 4$, $N = 0$; $M = 3$, $N = 1$; $M = 1$, $N = 3$; $M = 0$, $N = 4$. As before, form the linear systems of type (37) that follow from those equations, the component G_4^+ of the generating functions are derived at once. Actually,

$$G_4^+ = G_{1,2,0}^+ + G_{1,0,2}^+ + G_{0,4,0}^+ + G_{0,3,1}^+ + G_{0,1,3}^+ + G_{0,0,4}^+,$$

with,

$$G_{1,2,0}^+ = \mathrm{i}\,\frac{11}{50}\,3^{2/3}\sqrt{5}\,\mu q_1^2 - \frac{81}{50}\,3^{2/3}\,\mu q_1 q_2 - \mathrm{i}\,\frac{71}{100}\,3^{2/3}\sqrt{5}\,\mu q_2^2,$$

$$G_{1,0,2}^+ = -\mathrm{i}\,\frac{11}{50}\,3^{2/3}\sqrt{5}\,\mu p_2^2 + \frac{81}{50}\,3^{2/3}\,\mu p_1 p_2 + \mathrm{i}\,\frac{71}{100}\,3^{2/3}\sqrt{5}\,\mu p_1^2,$$

$$G_{0,4,0}^+ = \mathrm{i}\,\frac{4043}{37500}\,3^{2/3}\sqrt{5}\,q_1^4 - \frac{3209}{7500}\,3^{2/3}\,q_1^3 q_2 - \mathrm{i}\,\frac{65823}{250000}\,3^{2/3}\sqrt{5}\,q_1^2 q_2^2 + \frac{598391}{1500000}\,3^{2/3}\,q_1 q_2^3 + \mathrm{i}\,\frac{1652677}{30000000}\,3^{2/3}\sqrt{5}\,q_2^4,$$

$$G_{0,3,1}^+ = -\mathrm{i}\,\frac{238}{1875}\,3^{2/3}\sqrt{5}\,q_1^3 p_2 + \frac{37}{375}\,3^{2/3}\,q_1^3 p_1 + \frac{1999}{3125}\,3^{2/3}\,q_1^2 q_2 p_2 + \mathrm{i}\,\frac{2539}{15625}\,3^{2/3}\sqrt{5}\,q_1^2 q_2 p_1$$

$$+\,\mathrm{i}\,\frac{1127}{3125}\,3^{2/3}\sqrt{5}\,q_1 q_2^2 p_2 - \frac{13637}{31250}\,3^{2/3}\,q_1 q_2^2 p_1 - \frac{39143}{93750}\,3^{2/3}\,q_2^3 p_2 - \mathrm{i}\,\frac{12884}{234375}\,3^{2/3}\sqrt{5}\,q_2^3 p_1,$$

$$G_{0,1,3}^+ = \mathrm{i}\,\frac{238}{1875}\,3^{2/3}\sqrt{5}\,q_1 p_2^3 - \frac{1999}{3125}\,3^{2/3}\,q_1 p_1 p_2^2 - \mathrm{i}\,\frac{1127}{3125}\,3^{2/3}\sqrt{5}\,q_1 p_1^2 p_2 + \frac{39143}{93750}\,3^{2/3}\,q_1 p_1^3$$

$$-\,\frac{37}{375}\,3^{2/3}\,q_2 p_2^3 - \mathrm{i}\,\frac{2539}{15625}\,3^{2/3}\sqrt{5}\,q_2 p_1 p_2^2 + \frac{13637}{31250}\,3^{2/3}\,q_2 p_1^2 p_2 + \mathrm{i}\,\frac{12884}{234375}\,3^{2/3}\sqrt{5}\,q_2 p_1^3,$$

$$G_{0,0,4}^+ = -\mathrm{i}\,\frac{4043}{37500}\,3^{2/3}\sqrt{5}\,p_2^4 + \frac{3209}{7500}\,3^{2/3}\,p_1 p_2^3 + \mathrm{i}\,\frac{65823}{250000}\,3^{2/3}\sqrt{5}\,p_1^2 p_2^2 - \frac{598391}{1500000}\,3^{2/3}\,p_1^3 p_2 - \mathrm{i}\,\frac{1652677}{30000000}\,3^{2/3}\sqrt{5}\,p_1^4.\,\triangleright$$

Analysis of the case $\Omega = 0$ $(M = N)$. Let $F \in \mathbb{E}_{\ell MM}$; it is readily seen that its expansion can be re-arranged in the following way

$$F = \sum_{i=0}^{M}\sum_{j=0}^{M} f_{ij}\, q_1^i q_2^{M-i} p_1^{M-j} p_2^j = \sum_{i=0}^{M}(q_1 p_2)^i \sum_{j=0}^{M-i} f_{M-j,i+j}(q_1 p_1)^{M-i-j}(q_2 p_2)^j$$

$$+ \sum_{i=1}^{M}(q_2 p_1)^i \sum_{j=0}^{M-i} f_{M-i-j,j}(q_1 p_1)^{M-i-j}(q_2 p_2)^j, \qquad (41)$$

(the same Remark 10 applies here). The polynomials,

$$\tilde{\xi}_1 = q_1 p_2, \qquad \tilde{\xi}_2 = q_2 p_1, \qquad \tilde{\xi}_3 = \frac{\mathrm{i}}{2}\,(q_1 p_1 + q_2 p_2), \qquad \tilde{\xi}_4 = \frac{1}{2}\,(q_1 p_1 - q_2 p_2). \qquad (42)$$

form a Hilbert basis of $\mathbb{C}[q,p]^{\mathbb{S}^1}$, the algebra polynomials in (q,p) that are invariant under the $\mathbb{S}^1$ action generated by the flow of the Hamiltonian vector field $X_{\tilde{\xi}_3}$ (see [12], chap. I and IV). Particularly $\mathbb{E}_{\ell MM} \subset \mathbb{C}[q,p]^{\mathbb{S}^1}$. It turns out that,

$$q_1 p_2 = \tilde{\xi}_1, \qquad q_2 p_1 = \tilde{\xi}_2, \qquad q_1 p_1 = -\mathrm{i}\,\tilde{\xi}_3 + \tilde{\xi}_4, \qquad q_2 p_2 = -\mathrm{i}\,\tilde{\xi}_3 - \tilde{\xi}_4,$$

so substitution of these products into (41) leads to

$$F = \sum_{i=0}^{M}\sum_{j=0}^{M} f_{ij}\, q_1^i q_2^{M-i} p_1^{M-j} p_2^j = \sum_{m=0}^{M}\tilde{\xi}_1^m \sum_{n=0}^{M-m}\widehat{f}_{mn}\,\tilde{\xi}_3^{M-m-n}\tilde{\xi}_4^n + \sum_{m=1}^{M}\tilde{\xi}_2^m \sum_{n=0}^{M-m}\widetilde{f}_{mn}\,\tilde{\xi}_3^{M-m-n}\tilde{\xi}_4^n \qquad (43)$$

with,

$$\widehat{f}_{mn} = (-\mathrm{i})^{M-m-n}\sum_{k=0}^{M-m} C(M-m-k,k,n)f_{M-k,m+k}, \quad \text{for } 0 \le n \le M-m,\ 0 \le m \le M, \qquad (44)$$

$$\widetilde{f}_{mn} = (-\mathrm{i})^{M-m-n}\sum_{k=0}^{M-m} C(M-m-k,k,n)f_{M-m-k,k}, \quad \text{for } 0 \le n \le M-m,\ 1 \le m \le M, \qquad (45)$$

being the coefficients

$$C(r,k,n) := \sum_{j=\max(0,n-r)}^{\min(n,k)} (-1)^j \binom{r}{n-j}\binom{k}{j}, \quad \text{for } 0 \le r,k,n \le M-m,\ 0 \le m \le M, \qquad (46)$$

where we use the notation introduced in the analysis of the previous case, now with $N = M$; i.e., as ℓ and M are assumed fixed, then $f_{ij} = f_{\ell,i,M-i,M-j,j}$, for $0 \le i \le M$, $0 \le j \le M$; $\widehat{f}_{mn} = \widehat{f}_{\ell,m,M-m,M-n,n}$, for $0 \le n \le M-m$, $0 \le m \le M$; and $\widetilde{f}_{mn} = \widetilde{f}_{\ell,m,M-m,M-n,n}$, for $0 \le n \le M-m$, $1 \le m \le M$.

14

$\left\{\tilde\xi_i,\tilde\xi_j\right\}$	$\tilde\xi_1$	$\tilde\xi_2$	$\tilde\xi_3$	$\tilde\xi_4$	$\tilde\xi_j$
$\tilde\xi_1$	0	$-2\tilde\xi_4$	0	$\tilde\xi_1$	
$\tilde\xi_2$	$2\tilde\xi_4$	0	0	$-2\tilde\xi_2$	
$\tilde\xi_3$	0	0	0	0	
$\tilde\xi_4$	$-\tilde\xi_1$	$\tilde\xi_2$	0	0	
$\tilde\xi_i$					

Table 1: Structure matrix for the Poisson bracket $\left\{\tilde\xi_i,\tilde\xi_j\right\}$, $i,j=1,2,3,4$.

Remark 12. If we hold m fixed, $0 \le m \le M$, and define

$$\widehat{f}^{(m)}_n := \widehat{f}_{mn}, \quad f^{(m)}_k := f_{M-k,m+k}, \quad \widetilde{f}^{(m)}_n := \widetilde{f}_{mn}, \quad \mathring{f}^{(m)}_k := f_{M-.m-k,k}, \quad A^{(m)}_{n,k} := C(M-m-k,k,n),$$

for $0 \le n, k \le M-m$, then equations (44), (45) can be written in matrix form as,

$$\widehat{f}^{(m)}_n = A^{(m)}_{nk} f^{(m)}_k, \qquad \widetilde{f}^{(m)}_n = A^{(m)}_{nk} \mathring{f}^{(m)}_k,$$

respectively; and it is clear that they correspond to the change of components of F as the basis changes from the canonical basis of $\mathbb{E}_{\ell MM}$ to the basis generated by $\tilde\xi_1, \tilde\xi_2, \tilde\xi_3$ and $\tilde\xi_4$ in (42).

Lemma 2. *If $F \in \mathbb{E}^{\mathcal S}_{\ell MM}$, the components $\widehat{f}_{mn}$ ($0 \le n \le M-m$, $0 \le m \le M$) and $\widetilde{f}_{mn}$ ($0 \le n \le M-m$, $1 \le m \le M$) in* (44) *and* (45) *are real.*

PROOF. It is enough to check that $\mathcal{S}(\tilde\xi_i) = \tilde\xi_i$, $i = 1,2,3,4$, i.e., that the basis (42) satisfies the $\mathcal{S}$-symmetries.

To solve the homological equations (36) in the basis generated by (42), we first see that the quadratic part of the Hamiltonian, Z_2, is given by

$$Z_2(\mu,\tilde\xi_1,\tilde\xi_2,\tilde\xi_3,\tilde\xi_4) = \frac{25}{8}\mu + \frac{2\sqrt{5}}{3}\tilde\xi_3 + \tilde\xi_2;$$

next, taking into account that, for any $u = u(\tilde\xi_1,\tilde\xi_2,\tilde\xi_3,\tilde\xi_4)$, $v = v(\tilde\xi_1,\tilde\xi_2,\tilde\xi_3,\tilde\xi_4)$, their Poisson bracket is computed using the formula

$$\{u,v\}(\tilde\xi_1,\tilde\xi_2,\tilde\xi_3,\tilde\xi_4) = \sum_{i,j=1}^{4} \frac{\partial u}{\partial \tilde\xi_i}(\tilde\xi_1,\tilde\xi_2,\tilde\xi_3,\tilde\xi_4) \left\{\tilde\xi_i,\tilde\xi_j\right\} \frac{\partial v}{\partial \tilde\xi_j}(\tilde\xi_1,\tilde\xi_2,\tilde\xi_3,\tilde\xi_4)$$
$$= \nabla u(\tilde\xi_1,\tilde\xi_2,\tilde\xi_3,\tilde\xi_4)^{\top} S \nabla v(\tilde\xi_1,\tilde\xi_2,\tilde\xi_3,\tilde\xi_4),$$

where the brackets $\left\{\tilde\xi_i,\tilde\xi_j\right\}$ are given in Table 1. Therefore S is the matrix with components $S_{ij} = \left\{\tilde\xi_i,\tilde\xi_j\right\}$, for $i,j=1,2,3,4$. Now the relations

$$L_{Z_2}\tilde\xi_1 = \left\{\tilde\xi_1, Z_2\right\} = -2\tilde\xi_4, \quad L_{Z_2}\tilde\xi_2 = \left\{\tilde\xi_2, Z_2\right\} = 0, \quad L_{Z_2}\tilde\xi_3 = \left\{\tilde\xi_3, Z_2\right\} = 0, \quad L_{Z_2}\tilde\xi_4 = \left\{\tilde\xi_4, Z_2\right\} = \tilde\xi_2,$$

follow at once. Moreover,

$$L_{Z_2}\left(\tilde\xi_1^m \tilde\xi_3^{M-m-n} \tilde\xi_4^n\right) = -2m\tilde\xi_1^{m-1}\tilde\xi_3^{M-m-n}\tilde\xi_4^{n+1} + n\tilde\xi_1^{m-1}\tilde\xi_3^{M-m-n}\tilde\xi_4^{n-1}\tilde\xi_1\tilde\xi_2$$
$$= -2m\tilde\xi_1^{m-1}\tilde\xi_3^{M-m-n}\tilde\xi_4^{n+1} - n\tilde\xi_1^{m-1}\tilde\xi_3^{M-m-n}\tilde\xi_4^{n-1}\left(\tilde\xi_3^2 + \tilde\xi_4^2\right)$$
$$= -(2m+n)\tilde\xi_1^{m-1}\tilde\xi_3^{M-m-n}\tilde\xi_4^{n+1} - n\tilde\xi_1^{m-1}\tilde\xi_3^{M-m-n+2}\tilde\xi_4^{n-1}, \tag{47}$$

for $m \ge 1$, and where we have used that

$$\tilde\xi_3^2 + \tilde\xi_4^2 = -\tilde\xi_1\tilde\xi_2. \tag{48}$$

Analogously, for $n \ge 1$,

$$L_{Z_2}\left(\tilde\xi_2^m \tilde\xi_3^{M-m-n} \tilde\xi_4^n\right) = n\tilde\xi_2^{m+1}\tilde\xi_3^{M-m-n}\tilde\xi_4^{n-1}. \tag{49}$$

So we seek for polynomials $G, Z \in \mathbb{E}_{\ell MM}$, that fulfill the homological equations (36); with

$$G = \sum_{m=1}^{M} \tilde\xi_1^m \sum_{n=0}^{M-m} \widehat{g}_{mn}\tilde\xi_3^{M-m-n}\tilde\xi_4^n + \sum_{m=0}^{M} \tilde\xi_2^m \sum_{n=0}^{M-m} \widetilde{g}_{mn}\tilde\xi_3^{M-m-n}\tilde\xi_4^n \tag{50}$$

and Z holding the resonant terms that belong to a complementary space of $\mathrm{Range}\, L_{Z_2}$.

15

Remark 13. We note that the sums in (50) are arranged differently that those in (43); this is suggested by the action of L_{Z_2} on the monomials $\tilde{\xi}_1^m \tilde{\xi}_3^{M-m-n} \tilde{\xi}_4^n$ and $\tilde{\xi}_2^m \tilde{\xi}_3^{M-m-n} \tilde{\xi}_4^n$ shown in (47) and in (49) respectively.

Hence, assuming $M \geq 3$, the homological equation (36) in the current polynomial basis, $\tilde{\xi}_1, \tilde{\xi}_2, \tilde{\xi}_3, \tilde{\xi}_4$, looks as

$$-2M\widehat{g}_{M,0}\, \tilde{\xi}_1^{M-1}\tilde{\xi}_4 - (2M-2)\widehat{g}_{M-1,0}\, \tilde{\xi}_1^{M-2}\tilde{\xi}_3\tilde{\xi}_4 - (2M-1)\widehat{g}_{M-1,1}\, \tilde{\xi}_1^{M-2}\tilde{\xi}_4^2 - \widehat{g}_{M-1,1}\, \tilde{\xi}_1^{M-2}\tilde{\xi}_3^2$$

$$- \sum_{m=0}^{M-3}\left[\widehat{g}_{m+1,1}\, \tilde{\xi}_3^{M-m} + \sum_{n=1}^{M-m-2} \{(2m+n+1)\widehat{g}_{m+1,n-1} + (n+1)\widehat{g}_{m+1,n+1}\} \times \tilde{\xi}_3^{M-m-n}\tilde{\xi}_4^n \right.$$

$$\left. + (M+m)\widehat{g}_{m+1,M-m-2}\, \tilde{\xi}_3\tilde{\xi}_4^{M-m-1} + (M+m+1)\widehat{g}_{m+1,M-m-1}\, \tilde{\xi}_4^{M-m} \right] \times \tilde{\xi}_1^m$$

$$+ \sum_{m=1}^{M} \tilde{\xi}_2^m \sum_{n=0}^{M-m} (n+1)\widetilde{g}_{m-1,n+1}\, \tilde{\xi}_3^{M-m-n}\tilde{\xi}_4^n + Z$$

$$= \widehat{f}_{M,0}\, \tilde{\xi}_1^M + \widehat{f}_{M-1,0}\, \tilde{\xi}_1^{M-1}\tilde{\xi}_3 + \widehat{f}_{M-1,1}\, \tilde{\xi}_1^{M-1}\tilde{\xi}_4 + \widehat{f}_{M-2,0}\, \tilde{\xi}_1^{M-2}\tilde{\xi}_3^2 + \widehat{f}_{M-2,1}\, \tilde{\xi}_1^{M-2}\tilde{\xi}_3\tilde{\xi}_4$$

$$+ \widehat{f}_{M-2,2}\, \tilde{\xi}_1^{M-2}\tilde{\xi}_4^2 + \sum_{m=0}^{M-3}\left[\widehat{f}_{m,0}\, \tilde{\xi}_3^{M-m} + \sum_{n=1}^{M-m-2} \widehat{f}_{mn}\, \tilde{\xi}_3^{M-m-n}\tilde{\xi}_4^n \right.$$

$$\left. + \widehat{f}_{m,M-m-1}\, \tilde{\xi}_3\tilde{\xi}_4^{M-m-1} + \widehat{f}_{m,M-m}\, \tilde{\xi}_4^{M-m} \right] \times \tilde{\xi}_1^m$$

$$+ \sum_{m=1}^{M} \tilde{\xi}_2^m \sum_{n=0}^{M-m} \widetilde{f}_{mn}\, \tilde{\xi}_3^{M-m-n}\tilde{\xi}_4^n, \tag{51}$$

so comparison of coefficients leads, on the one hand, to the linear system,

$$-2M\widehat{g}_{M,0} = \widehat{f}_{M-1,1}, \tag{52}$$

$$-(2M-2)\widehat{g}_{M-1,0} = \widehat{f}_{M-2,1}, \tag{53}$$

$$-(2M-1)\widehat{g}_{M-1,1} = \widehat{f}_{M-2,2}, \tag{54}$$

$$\left.\begin{aligned} -(2m+n+1)\widehat{g}_{m+1,n-1} - (n+1)\widehat{g}_{m+1,n+1} &= \widehat{f}_{mn}, \quad 1 \leq n \leq M-m-2, \\ -(M+m)\widehat{g}_{m+1,M-m-2} &= \widehat{f}_{m,M-m-1}, \\ -(M+m+1)\widehat{g}_{m+1,M-m-1} &= \widehat{f}_{m,M-m}, \end{aligned}\right\}, \; 0 \leq m \leq M-3 \tag{55}$$

$$(n+1)\widetilde{g}_{m-1,n+1} = \widetilde{f}_{mn}, \qquad 0 \leq n \leq M-m, \; 1 \leq m \leq M \tag{56}$$

(in fact, the last equation (56), holds also for $M=1$ and $M=2$). For $0 \leq m \leq M \geq 3$, $M \geq 3$ fixed, the linear system (55) is determinate compatible (it is a lower triangular system with no zeros at the diagonal).

Therefore, for $M \geq 3$, the components $\widehat{g}_{mn}, \widetilde{g}_{mn}$, $0 \leq n \leq M-m, 0 \leq m \leq M$, of the generating function (50) are obtained solving the equations (52)-(56), except the terms $\widetilde{g}_{m,0}$ (for $0 \leq m \leq M$) that, due to the action of L_{Z_2} (see (49)), do not appear in $L_{Z_2}G$. Consequently, they are not determined by the homological equations (they are "responsible for the non-uniqueness of G"), and can be set arbitrarily. As in [28], we fix them to 0. Furthermore, if $F \in \mathbb{E}^{\mathcal{S}}_{\ell\, MM}$, the right hand side of the system (52)-(56) is real (Lemma 2). Besides, as the choice $\widetilde{g}_{m,0} = 0$ (for $0 \leq m \leq M$) preserves the $\mathcal{S}$-symmetries, it follows that $G \in \mathbb{E}^{\mathcal{S}}_{\ell\, MM}$.

Resonant terms. For every M fixed, we see that the component $\widehat{g}_{M-1,1}$ is determined by the equation (54) and $\widehat{g}_{m+1,1}$ $(0 \leq m \leq M-3)$ appear at left hand side of the first equation of (55) for $n=2$, so these components are also determined once the system is solved. Therefore, the terms $-\widehat{g}_{M-1,1}\tilde{\xi}_1^{M-2}\tilde{\xi}_3^2$ and $-\widehat{g}_{m+1,1}\tilde{\xi}_1^m\tilde{\xi}_3^{M-m}$ (for $0 \leq m \leq M-3$) cannot be used to remove the corresponding terms $\widehat{f}_{M-2,0}\tilde{\xi}_1^{M-2}\tilde{\xi}_3^2$ and $\widehat{f}_{m,0}\tilde{\xi}_1^m\tilde{\xi}_3^{M-m}$ that are present at the right hand side of (51). Thus, all these terms –together with $\widehat{f}_{M,0}\tilde{\xi}_1^M$, $\widehat{f}_{M-1,1}\tilde{\xi}_1^{M-1}\tilde{\xi}_3^1$– must be included (the former ones, with opposite sign and their corresponding values substituted) in Z, at the left hand side of (51), so

$$Z = \sum_{m=0}^{M} \widehat{f}_{m,0}\, \tilde{\xi}_1^m\tilde{\xi}_3^{M-m} + \sum_{m=0}^{M-2} \widehat{g}_{m+1,1}\, \tilde{\xi}_1^m\tilde{\xi}_3^{M-m} = \sum_{m=0}^{M} \widehat{Z}_m\tilde{\xi}_1^m\tilde{\xi}_3^{M-m}, \tag{57}$$

where the components $\widehat{g}_{m+1,1}$ are given by the solution of equations (52)-(55). Since all the coefficients in Z are real, and $\mathcal{S}(\tilde{\xi}_i) = \tilde{\xi}_i$, $i = 1, 2, 3, 4$, we see that $Z \in \mathbb{E}^{\mathcal{S}}_{\ell\, MM}$.

On the other hand, for $M = 1$, the working space of $\mathcal{S}$-symmetric homogeneous polynomials is $\mathbb{E}^{\mathcal{S}}_{\ell,1,1}$, with $\ell = 1, \ldots 3\lfloor \sigma/2 \rfloor - \sigma$, for $\sigma = 4, 5, \ldots$ Then, according to (43) and (50),

$$F = \widehat{f}_{1,0}\, \tilde{\xi}_1 + \widetilde{f}_{1,0}\, \tilde{\xi}_2 + \widehat{f}_{0,0}\, \tilde{\xi}_3 + \widehat{f}_{0,1}\, \tilde{\xi}_4, \qquad G = \widehat{g}_{1,0}\, \tilde{\xi}_1 + \widetilde{g}_{1,0}\, \tilde{\xi}_2 + \widetilde{g}_{0,0}\, \tilde{\xi}_3 + \widetilde{g}_{0,1}\, \tilde{\xi}_4,$$

and $L_{Z_2} G = \widetilde{g}_{0,1}\, \tilde{\xi}_2 - 2\widehat{g}_{1,0}\, \tilde{\xi}_4$, so the homological equation (36) is solved taking

$$\widetilde{g}_{0,1} = \widetilde{f}_{1,0}, \qquad \widehat{g}_{1,0} = -\frac{\widehat{f}_{0,1}}{2}.$$

The coefficient $\widetilde{g}_{0,0}$ is not determined but, as we pointed out before, it can be set to 0, so we take $\widetilde{g}_{0,0} = 0$ and then

$$G = -\frac{\widehat{f}_{0,1}}{2}\, \tilde{\xi}_1 + \widetilde{f}_{1,0}\, \tilde{\xi}_4, \qquad Z = \widehat{f}_{1,0}\, \tilde{\xi}_1 + \widehat{f}_{0,0}\, \tilde{\xi}_3 \tag{58}$$

and clearly, $F, G \in \mathbb{E}^{\mathcal{S}}_{\ell,1,1}$. Finally, for $M = 2$,

$$F = \widehat{f}_{1,1}\, \tilde{\xi}_1\tilde{\xi}_4 + \widetilde{f}_{2,0}\, \tilde{\xi}_2^2 + \widetilde{f}_{1,0}\, \tilde{\xi}_2\tilde{\xi}_3 + \widetilde{f}_{1,1}\, \tilde{\xi}_2\tilde{\xi}_4 + \widehat{f}_{0,1}\, \tilde{\xi}_3\tilde{\xi}_4 + \widehat{f}_{0,2}\, \tilde{\xi}_4^2 + \widehat{f}_{2,0}\, \tilde{\xi}_1^2 + \widehat{f}_{1,0}\, \tilde{\xi}_1\tilde{\xi}_3 + \widehat{f}_{0,0}\, \tilde{\xi}_3^2,$$

and,

$$G = \widehat{g}_{1,0}\, \tilde{\xi}_1\tilde{\xi}_3 + \widehat{g}_{1,1}\, \tilde{\xi}_1\tilde{\xi}_4 + \widehat{g}_{2,0}\, \tilde{\xi}_1^2 + \widetilde{g}_{0,0}\, \tilde{\xi}_3^2 + \widetilde{g}_{0,1}\, \tilde{\xi}_3\tilde{\xi}_4 + \widetilde{g}_{0,2}\, \tilde{\xi}_4^2 + \widetilde{g}_{1,0}\, \tilde{\xi}_2\tilde{\xi}_3 + \widetilde{g}_{1,1}\, \tilde{\xi}_2\tilde{\xi}_4 + \widetilde{g}_{2,0}\, \tilde{\xi}_2^2,$$

so the homological equation (36) takes the form,

$$-4\widehat{g}_{2,0}\, \tilde{\xi}_1\tilde{\xi}_4 + \widetilde{g}_{1,1}\, \tilde{\xi}_2^2 + \widetilde{g}_{0,1}\, \tilde{\xi}_2\tilde{\xi}_3 + 2\widetilde{g}_{0,2}\, \tilde{\xi}_2\tilde{\xi}_4 - 2\widehat{g}_{1,0}\, \tilde{\xi}_3\tilde{\xi}_4 - \widehat{g}_{1,1}\, \tilde{\xi}_3^2 - 3\widehat{g}_{1,1}\, \tilde{\xi}_4^2 + Z$$
$$= \widehat{f}_{1,1}\, \tilde{\xi}_1\tilde{\xi}_4 + \widetilde{f}_{2,0}\, \tilde{\xi}_2^2 + \widetilde{f}_{1,0}\, \tilde{\xi}_2\tilde{\xi}_3 + \widetilde{f}_{1,1}\, \tilde{\xi}_2\tilde{\xi}_4 + \widehat{f}_{0,1}\, \tilde{\xi}_3\tilde{\xi}_4 + \widehat{f}_{0,2}\, \tilde{\xi}_4^2 + \widehat{f}_{2,0}\, \tilde{\xi}_1^2 + \widehat{f}_{1,0}\, \tilde{\xi}_1\tilde{\xi}_3 + \widehat{f}_{0,0}\, \tilde{\xi}_3^2 \tag{59}$$

and fixes the coefficients

$$\widehat{g}_{2,0} = -\frac{\widehat{f}_{1,1}}{4}, \qquad \widehat{g}_{1,0} = -\frac{\widehat{f}_{0,1}}{2}, \qquad \widehat{g}_{1,1} = -\frac{\widehat{f}_{0,2}}{3}, \qquad \widetilde{g}_{1,1} = \widetilde{f}_{2,0}, \qquad \widetilde{g}_{0,1} = \widetilde{f}_{1,0}, \qquad \widetilde{g}_{0,2} = \frac{\widetilde{f}_{1,1}}{2} \tag{60}$$

of G. Again there the undetermined coefficients, and yet again they are set to 0, i.e., $\widetilde{g}_{0,0} = \widetilde{g}_{1,0} = \widetilde{g}_{2,0} = 0$. This gives rise to

$$G = -\frac{\widehat{f}_{0,1}}{2}\, \tilde{\xi}_1\tilde{\xi}_3 - \frac{\widehat{f}_{0,2}}{3}\, \tilde{\xi}_1\tilde{\xi}_4 - \frac{\widehat{f}_{1,1}}{4}\, \tilde{\xi}_1^2 + \widetilde{f}_{1,0}\, \tilde{\xi}_3\tilde{\xi}_4 + \frac{\widetilde{f}_{1,1}}{2}\, \tilde{\xi}_4^2 + \widetilde{f}_{2,0}\, \tilde{\xi}_2\tilde{\xi}_4 \tag{61}$$

whereas the components $\widehat{f}_{1,0}$, $\widehat{f}_{2,0}$ cannot be removed. Neither does $\widehat{f}_{0,0}$, since in this last case $\widehat{g}_{1,1}$ is first exacted by the homological equation (59) to $\widehat{g}_{1,1} = -\widehat{f}_{0,2}/3$ (see (60)), so $-\widehat{g}_{1,1}\, \tilde{\xi}_3^2$ cannot be used to remove the term $\widehat{f}_{0,0}\, \tilde{\xi}_3^2$ on the right hand side of (59), and both them (the former with its opposite sign and its value substituted) must be present in Z. Consequently,

$$Z = \widehat{f}_{0,0}\, \tilde{\xi}_3^2 + \widehat{f}_{1,0}\, \tilde{\xi}_1\tilde{\xi}_3 + \widehat{f}_{2,0}\, \tilde{\xi}_1^2 + \widehat{g}_{1,1}\, \tilde{\xi}_3^2 = \left(\widehat{f}_{0,0} - \frac{\widehat{f}_{0,2}}{3}\right)\tilde{\xi}_3^2 + \widehat{f}_{1,0}\, \tilde{\xi}_1\tilde{\xi}_3 + \widehat{f}_{2,0}\, \tilde{\xi}_1^2. \tag{62}$$

Thus, we have shown that the normal form, Z_σ, depends only on μ, $\tilde{\xi}_1 = q_1 p_2$ and $\tilde{\xi}_3 = \frac{i}{2}(q_1 p_1 + q_2 p_2)$. More precisely that, when σ is even (and $\sigma \geq 4$) then $Z_\sigma(\mu, q, p) = \mathcal{Z}_\sigma\left(\mu, \tilde{\xi}_1, \tilde{\xi}_3\right)$, being $\mathcal{Z}_\sigma(u, v, w)$ a polynomial of *standard* degree $\sigma/2$ with *real* coefficients. Furthermore, it is clear that the normal is given by (34). This closes the proof of statement (b) of Proposition 1. $\qquad\square$

Example 4 (Computation of G_4^0 and Z_4). We use (44) and (45) to express the components of Z, G in (58), and Z, G in (61) and (62) as linear combinations of the components of $\mathscr{H}^{(1)}_{1,1,1}$ and $\mathscr{H}^{(1)}_{0,2,2}$ with respect to the standard basis of $\mathbb{E}_{\ell MM}$. These components are shown in Table 1, so

$$\mathscr{H}^{(1)}_{\ell MM} = \sum_{m,n=0}^{M} \mathscr{H}^{(1)}_{\ell,m,M-m,M-n,n}\, q_1^m q_2^{M-m} p_1^{M-n} p_2^n \tag{63}$$

corresponds to $\mathscr{H}^{(1)}_{1,1,1}$ in (39) for $\ell = 1$ and $M = 1$, whereas it matches $\mathscr{H}^{(1)}_{022}$ in (40) when $\ell = 0$ and $M = 2$. Therefore,

(i) for $M = 1$ ($\ell = 1$),

$$\widehat{f}_{0,0} = -\mathrm{i}\,(f_{1,0} + f_{0,1}) = -\mathrm{i}\left(\mathscr{H}^{(1)}_{1,1,0,1,0} + \mathscr{H}^{(1)}_{1,0,1,0,1}\right) = \frac{28}{25}\, 3^{2/3}\sqrt{5},$$

$$\widehat{f}_{0,1} = f_{1,0} - f_{0,1} = \mathscr{H}^{(1)}_{1,1,0,1,0} - \mathscr{H}^{(1)}_{1,0,1,0,1} = 0, \qquad\qquad (\mathcal{S}\text{-symmetries})$$

$$\widehat{f}_{1,0} = f_{1,1} = \mathscr{H}^{(1)}_{1,1,0,0,1} = \frac{6}{5}\, 3^{2/3},$$

$$\widetilde{f}_{1,0} = f_{0,0} = \mathscr{H}^{(1)}_{1,0,1,1,0} = -\frac{51}{25}\, 3^{2/3},$$

17

ℓ	m_1	m_2	n_1	n_2	$\mathscr{H}^{(1)}_{\ell\, m_1 m_2 n_1 n_2}$
1	1	0	0	1	$\frac{6}{5}\,3^{2/3}$
1	1	0	1	0	$\mathrm{i}\,\frac{14}{25}\,3^{2/3}\sqrt{5}$
1	0	1	0	1	$\mathrm{i}\,\frac{14}{25}\,3^{2/3}\sqrt{5}$
1	0	1	1	0	$-\frac{51}{25}\,3^{2/3}$
0	2	0	0	2	$\frac{14}{625}\,3^{2/3}$
0	2	0	1	1	$\mathrm{i}\,\frac{12}{625}\,3^{2/3}\sqrt{5}$
0	2	0	2	0	$-\frac{638}{3125}\,3^{2/3}$
0	1	1	0	2	$\mathrm{i}\,\frac{12}{625}\,3^{2/3}\sqrt{5}$
0	1	1	1	1	$\frac{7832}{9375}\,3^{2/3}$
0	1	1	2	0	$\mathrm{i}\,\frac{196}{625}\,3^{2/3}\sqrt{5}$
0	0	2	0	2	$-\frac{638}{3125}\,3^{2/3}$
0	0	2	1	1	$\mathrm{i}\,\frac{196}{625}\,3^{2/3}\sqrt{5}$
0	0	2	2	0	$-\frac{4946}{15625}\,3^{2/3}$

Table 2: Coefficients of homogeneous polynomials (of adapted degree $2\ell + 2M = 4$) $\mathscr{H}^{(1)}_{1,1,1}$ in (39) and $\mathscr{H}^{(1)}_{0,2,2}$ in (40), where $\mathscr{H}^{(1)}_{\ell M M}$ is given by the sum (63).

(ii) for $M = 2$ ($\ell = 0$),

$$\widehat{f}_{0,0} = -(f_{2,0} + f_{1,1} + f_{0,2}) = -\left(\mathscr{H}^{(1)}_{0,2,0,2,0} + \mathscr{H}^{(1)}_{0,1,1,1,1} + \mathscr{H}^{(1)}_{0,0,2,0,2} \right) = -\frac{4004}{9375}\,3^{2/3},$$

$$\widehat{f}_{1,0} = -\mathrm{i}\,(f_{2,1} + f_{1,2}) = -\mathrm{i}\left(\mathscr{H}^{(1)}_{0,2,0,1,1} + \mathscr{H}^{(1)}_{0,1,1,0,2} \right) = \frac{24}{625}\,3^{2/3}\sqrt{5},$$

$$\widehat{f}_{0,1} = -2\,\mathrm{i}\,(f_{2,0} - f_{0,2}) = -2\,\mathrm{i}\left(\mathscr{H}^{(1)}_{0,2,0,2,0} - \mathscr{H}^{(1)}_{0,0,2,0,2} \right) = 0, \qquad\qquad (\mathcal{S}\text{-symmetries})$$

$$\widehat{f}_{2,0} = f_{2,2} = \mathscr{H}^{(1)}_{0,2,0,0,2} = \frac{14}{625}\,3^{2/3},$$

$$\widehat{f}_{1,1} = f_{1,2} - f_{2,1} = \mathscr{H}^{(1)}_{0,2,0,1,1} - \mathscr{H}^{(1)}_{0,1,1,0,2} = 0, \qquad\qquad (\mathcal{S}\text{-symmetries})$$

$$\widehat{f}_{0,2} = f_{2,0} - f_{1,1} + f_{0,2} = \mathscr{H}^{(1)}_{0,2,0,2,0} - \mathscr{H}^{(1)}_{0,1,1,1,1} + \mathscr{H}^{(1)}_{0,0,2,0,2} = -\frac{2332}{1875}\,3^{2/3},$$

$$\widetilde{f}_{1,0} = -\mathrm{i}\,(f_{1,0} + f_{0,1}) = -\mathrm{i}\left(\mathscr{H}^{(1)}_{0,1,1,2,0} + \mathscr{H}^{(1)}_{0,0,2,1,1} \right) = \frac{392}{625}\,3^{2/3}\sqrt{5},$$

$$\widetilde{f}_{1,1} = f_{1,0} - f_{0,1} = \mathscr{H}^{(1)}_{0,1,1,2,0} - \mathscr{H}^{(1)}_{0,0,2,1,1} = 0, \qquad\qquad (\mathcal{S}\text{-symmetries})$$

$$\widetilde{f}_{2,0} = f_{0,0} = \mathscr{H}^{(1)}_{0,0,2,2,0} = -\frac{4946}{15625}\,3^{2/3},$$

(we have tagged the terms that cancel due to the reality conditions). Substitution of these coefficients in (58), (61) and (62)

18

yields,

$$G_{1,1,1}^0 = \mathscr{H}_{1,0,1,1,0}^{(1)} \mu \tilde{\xi}_4 = -\frac{51}{25}\, 3^{2/3} \mu \tilde{\xi}_4,$$

$$Z_{1,1,1} = \mathscr{H}_{1,1,0,0,1}^{(1)} \mu \tilde{\xi}_1 - \mathrm{i} \left(\mathscr{H}_{1,1,0,1,0}^{(1)} + \mathscr{H}_{1,0,1,0,1}^{(1)} \right) \mu \tilde{\xi}_3 = \frac{6}{5}\, 3^{2/3} \mu \tilde{\xi}_1 + \frac{28}{25}\, 3^{2/3} \sqrt{5}\, \mu \tilde{\xi}_3,$$

$$G_{0,2,2}^0 = -\frac{1}{3} \left(\mathscr{H}_{0,2,0,2,0}^{(1)} - \mathscr{H}_{0,1,1,1,1}^{(1)} + \mathscr{H}_{0,0,0,2,0,2}^{(1)} \right) \tilde{\xi}_1 \tilde{\xi}_4 - \mathrm{i} \left(\mathscr{H}_{0,1,1,2,0}^{(1)} + \mathscr{H}_{0,0,2,1,1}^{(1)} \right) \tilde{\xi}_3 \tilde{\xi}_4 + \mathscr{H}_{0,0,2,2,0}^{(1)} \tilde{\xi}_2 \tilde{\xi}_4$$

$$= \frac{2332}{5625}\, 3^{2/3} \tilde{\xi}_1 \tilde{\xi}_4 + \frac{392}{625}\, 3^{2/3} \sqrt{5}\, \tilde{\xi}_3 \tilde{\xi}_4 - \frac{4946}{15625}\, 3^{2/3} \tilde{\xi}_2 \tilde{\xi}_4,$$

$$Z_{0,2,2} = -\left(\frac{4}{3} \mathscr{H}_{0,2,0,2,0}^{(1)} + \frac{2}{3} \mathscr{H}_{0,1,1,1,1}^{(1)} + \frac{4}{3} \mathscr{H}_{0,0,2,0,2}^{(1)} \right) \tilde{\xi}_3^2 - \mathrm{i} \left(\mathscr{H}_{0,2,0,1,1}^{(1)} + \mathscr{H}_{0,1,1,0,2}^{(1)} \right) \tilde{\xi}_1 \tilde{\xi}_3 + \mathscr{H}_{0,2,0,0,2}^{(1)} \tilde{\xi}_1^2$$

$$= -\frac{352}{28125}\, 3^{2/3} \tilde{\xi}_3^2 + \frac{24}{625}\, 3^{2/3} \sqrt{5}\, \tilde{\xi}_1 \tilde{\xi}_3 + \frac{14}{625}\, 3^{2/3} \tilde{\xi}_1^2$$

where $\tilde{\xi}_i$, $i = 1, 2, 3, 4$ must be replaced by their definition in terms of (q, p) in (42). Hence, $G_4^0 = G_{1,1,1}^0 + G_{0,2,2}^0 \in \mathbb{E}_4^0$ and the complete generating function at degree 4, G_4, is the sum $G_4 = G_4^+ + G_4^0$ (we recall that $G_4^+ \in \mathbb{E}_4^+$ was found in Example 3). Besides, the (complex) normal form up to (adapted) degree 4 results to be

$$Z^{(4)} = Z_2 + Z_{2,0,0} + Z_{1,1,1} + Z_{0,2,2} = \frac{25}{8} \mu + \frac{27}{32} 3^{2/3} \mu^2 + \frac{2}{3} \sqrt{5}\, \tilde{\xi}_3 + \tilde{\xi}_2 + \frac{6}{5}\, 3^{2/3} \mu \tilde{\xi}_1 + \frac{28}{25}\, 3^{2/3} \sqrt{5}\, \mu \tilde{\xi}_3$$

$$- \frac{352}{28125}\, 3^{2/3} \tilde{\xi}_3^2 + \frac{24}{625}\, 3^{2/3} \sqrt{5}\, \tilde{\xi}_1 \tilde{\xi}_3 + \frac{14}{625}\, 3^{2/3} \tilde{\xi}_1^2, \tag{64}$$

being $Z_{2,0,0} = \mathscr{H}_{2,0,0}^{(1)} = \frac{27}{32} 3^{2/3} \mu^2$. This corresponds to the trivial case $M = 0$, see (38). $\quad \triangleright$

The normal form transformation. Now, let $\mathcal{V}$ be the complexification (26) and $\mathcal{U}$ the normalizing transformation of the quadratic part of the Hamiltonian stated in Lemma 1. Proceeding as in [28] (see Proposition 7.1 there), it can be shown that, for any integer $s \geq 3$ fixed, and any $\kappa_* > 1$ given, there exists $R_s > 0$ such that the symplectic transformation

$$\widetilde{\mathcal{T}} := \mathcal{T}_{t=1}^{G_3 \circ \mathcal{U}^{-1} \circ \mathcal{V}^{-1}} \circ \mathcal{T}_{t=1}^{G_4 \circ \mathcal{U}^{-1} \circ \mathcal{V}^{-1}} \circ \cdots \circ \mathcal{T}_{t=1}^{G_s \circ \mathcal{U}^{-1} \circ \mathcal{V}^{-1}}, \tag{65}$$

is a real analytic diffeomorphism defined in the polydisk $\mathscr{D}_{R_s}$, with $\widetilde{\mathcal{T}}(\mathscr{D}_R) \subseteq \mathscr{D}_{\kappa_* R}$, $0 < R < R_s$. Thus, Proposition 2 below follows then from these last considerations and from Proposition 1.

Proposition 2 (Sokol′skiĭ's normal form). *Consider the 2D of freedom real analytic Hamiltonian $\mathcal{H}$ in (22), depending on a parameter $\mu \in \mathbb{R}$, which has no linear terms in (x, y), so the origin O: $(x, y) = (0, 0)$ is an equilibrium point for every μ. Assume that, for some $\mu_* < 0$, $\mu^* > 0$, its quadratic part, $\mathcal{H}_2$, is a center for $\mu_* < \mu < 0$, has a non semi-simple 1:−1 resonance for $\mu = 0$ (i.e., its characteristic exponents are pure imaginary with algebraic multiplicity two and geometric multiplicity one), and a complex-saddle for $0 < \mu < \mu^*$. Then, given $s \in \mathbb{N}$, $s \geq 4$ even, there exists μ_0, $0 < \mu_0 \leq \min\{|\mu_*|, \mu^*\}$, such that: (i) for every μ, $|\mu| < \mu_0$, the symplectic transformation (65), $(\tilde{x}, \tilde{y}) \mapsto (x, y) = \widetilde{\mathcal{T}}(\mu, \tilde{x}, \tilde{y})$, is a real analytic diffeomorphism defined in a neighborhood of $\widetilde{O}$: $(\tilde{x}, \tilde{y}) = (0, 0)$, and (ii) the transformed Hamiltonian*

$$\widetilde{\mathcal{H}}^{(s-2)}(\mu, \tilde{x}, \tilde{y}) = \mathcal{H}\left(\mu, \widetilde{\mathcal{T}}(\mu, \tilde{x}, \tilde{y}) \right)$$

$$= \tilde{\alpha}\mu + \frac{\epsilon}{2}\left(\tilde{y}_1^2 + \tilde{y}_2^2 \right) + \varpi(\tilde{y}_1 \tilde{x}_2 - \tilde{y}_2 \tilde{x}_1) + \sum_{\kappa=2}^{s/2} \sum_{\ell+i+j=\kappa} \widetilde{Z}_{\ell\,ij}^{(2\kappa)} \mu^\ell \left(\tilde{y}_1 \tilde{x}_2 - \tilde{y}_2 \tilde{x}_1 \right)^i \left(\tilde{x}_1^2 + \tilde{x}_2^2 \right)^j + \widetilde{\mathcal{H}}_{>s}(\mu, \tilde{x}, \tilde{y}), \tag{66}$$

is also real analytic in that neighborhood. The Hamiltonian (66) is the sum, $\widetilde{\mathcal{H}}^{(s-2)} = \widetilde{Z}_2 + \widetilde{Z}_4 + \cdots + \widetilde{Z}_s + \widetilde{\mathcal{H}}_{>s}$, of

(1) an integrable part, the normal form, $\widetilde{Z}^{(s)} = \widetilde{Z}_2 + \widetilde{Z}_4 + \widetilde{Z}_6 + \cdots + \widetilde{Z}_s$, with a quadratic (with respect to the adapted degree) term given by

$$\widetilde{Z}_2(\mu, x, y) = \tilde{\alpha}\mu + \frac{\epsilon}{2}\left(\tilde{y}_1^2 + \tilde{y}_2^2 \right) + \varpi(\tilde{y}_1 \tilde{x}_2 - \tilde{y}_2 \tilde{x}_1),$$

being $\epsilon = \mathrm{sign}(\Delta)$ (with Δ defined in Lemma 1), and higher order terms $\widetilde{Z}_4, \widetilde{Z}_6, \ldots, \widetilde{Z}_s$, that are polynomials in μ, $\tilde{y}_1 \tilde{x}_2 - \tilde{y}_2 \tilde{x}_1$, $\tilde{x}_1^2 + \tilde{x}_2^2$ of (ordinary) degree $k = 2, 3, \ldots, s/2$ –so homogeneous polynomials of even (adapted) degree $\sigma = 4, 6, \ldots, s$ in μ, $\tilde{x}$, $\tilde{y}$–. We write,

$$\widetilde{Z}_\sigma(\mu, \tilde{x}, \tilde{y}) = \sum_{\ell+i+j=\sigma/2} \widetilde{Z}_{\ell\,ij}^{(\sigma)} \mu^\ell \left(\tilde{y}_1 \tilde{x}_2 - \tilde{y}_2 \tilde{x}_1 \right)^i \left(\tilde{x}_1^2 + \tilde{x}_2^2 \right)^j,$$

(2) and the non normalized part, the remainder, $\widetilde{\mathcal{H}}_{>s}$, that begins with terms of degree $> s$.

Remark 14. We note that the normal form in the above proposition is slightly different from the one that appears in [36], [37], but coincides with that in [24], [33] and [39].

4. Stability of the Rydberg's electron at the Hamiltonian Hopf bifurcation

Here, we discuss the stability of the equilibrium O: $(x, y) = (0, 0)$ of the Hamiltonian (22) –and hence, of the equilibrium L_2: $(x, y, p_x, p_y) = (\delta, 0, 0, \delta)$, with $\delta = \delta(\mu)$ given in (20), of the Hamiltonian (2) corresponding to the CP problem, the Rydberg's atom–. Next, we claim in Theorem 1) that, at the equilibrium $\widetilde{O}$ of Hamiltonian (66) (correspondingly, at the equilibrium L_2 of Hamiltonian (2)), it takes place a supercritical Hamiltonian Hopf bifurcation as μ (K) moves from $\mu < 0$ $(K < K_{crit})$ to $\mu > 0$ $(K > K_{crit})$, crossing the critical value $\mu = 0$ $(K = K_{crit})$. Finally, we describe the quasiperiodic bifurcation phenomena that take place around both, the Liapunov elliptic periodic orbits (for $\mu < 0$) and the bifurcated elliptic periodic orbits (for $\mu \geq 0$). These items are summarized in Proposition 3.

The computations carried out in Examples 3 and 4 yield, after changing back to real coordinates using the inverse of the complexification (26), that is,

$$q_1 = \frac{\tilde{x}_1 - \mathrm{i}\,\tilde{x}_2}{\sqrt{2}}, \qquad q_2 = \frac{\tilde{y}_1 - \mathrm{i}\,\tilde{y}_2}{\sqrt{2}}, \qquad p_1 = \frac{\tilde{y}_1 + \mathrm{i}\,\tilde{y}_2}{\sqrt{2}}, \qquad p_2 = -\frac{\tilde{x}_1 + \mathrm{i}\,\tilde{x}_2}{\sqrt{2}}, \qquad (67)$$

to the reduced *r*eal analytic Hamiltonian $\widetilde{\mathcal{H}}^{(2)}(\mu, \tilde{x}, \tilde{y}) = \widetilde{Z}^{(4)}(\mu, \tilde{x}, \tilde{y}) + \widetilde{\mathcal{H}}_{>4}(\mu, \tilde{x}, \tilde{y})$, where the fourth-degree normal form, $\widetilde{Z}^{(4)}$, looks as

$$\widetilde{Z}^{(4)}(\mu, \tilde{x}, \tilde{y}) = \tilde{\alpha}\mu + \tilde{\beta}\mu^2 + \frac{1}{2}\left(\tilde{y}_1^2 + \tilde{y}_2^2\right) + \omega(\mu)\left(\tilde{y}_1\tilde{x}_2 - \tilde{y}_2\tilde{x}_1\right) - \frac{\varepsilon(\mu)}{2}\left(\tilde{x}_1^2 + \tilde{x}_2^2\right)$$
$$+ A\left(\tilde{x}_1^2 + \tilde{x}_2^2\right)^2 + B\left(\tilde{x}_1^2 + \tilde{x}_2^2\right)\left(\tilde{y}_1\tilde{x}_2 - \tilde{y}_2\tilde{x}_1\right) + C\left(\tilde{y}_1\tilde{x}_2 - \tilde{y}_2\tilde{x}_1\right)^2, \qquad (68)$$

with coefficients,

$$\tilde{\alpha} = \frac{25}{8}, \qquad \tilde{\beta} = \frac{27}{32}\,3^{2/3}, \qquad \tilde{\gamma} = \frac{14}{25}\,3^{2/3}\,\sqrt{5},$$
$$\varpi = \frac{\sqrt{5}}{3}, \qquad \omega(\mu) = \varpi + \tilde{\gamma}\mu, \qquad \varepsilon(\mu) = \frac{6}{5}\,3^{2/3}\mu,$$
$$A = \frac{7}{1250}\,3^{2/3}, \qquad B = -\frac{6}{625}\,3^{2/3}\,\sqrt{5}, \qquad C = -\frac{88}{28125}\,3^{2/3}. \qquad (69)$$

and the corresponding Hamiltonian system is

$$\dot{\tilde{x}} = \partial_{\tilde{y}}\widetilde{Z}^{(4)}(\mu, \tilde{x}, \tilde{y}), \qquad \dot{\tilde{y}} = -\partial_{\tilde{x}}\widetilde{Z}^{(4)}(\mu, \tilde{x}, \tilde{y}). \qquad (70)$$

Regarding the linear stability of the origin, it is checked at once that the characteristic exponents (the eigenvalues of the Jacobian matrix of system (70)) are

$$\alpha_\pm = \pm\left(\mathrm{i}\,\varpi + \sqrt{\varepsilon(\mu)}\right) + \mathcal{O}(\mu), \qquad \beta_\pm = \pm\left(\mathrm{i}\,\varpi - \sqrt{\varepsilon(\mu)}\right) + \mathcal{O}(\mu). \qquad (71)$$

Hence, as it was already mentioned in Section 3.2, for $\mu < 0$ the equilibrium $\widetilde{O}$: $(\tilde{x}, \tilde{y}) = (0, 0)$ of the Hamiltonian (66) is a center, so its characteristic exponents are pure imaginary; for $\mu = 0$ the characteristic exponents collide on the imaginary axis and leave off, pairwise, the imaginary axis to the complex plane for $\mu > 0$. Therefore, the stability of the point $\widetilde{O}$ changes from a center to a complex saddle through a degenerate (in fact, a non semisimple) center.

(Nonlinear) Stability of the equilibrium. The stability of the equilibrium $\widetilde{O}$ is determined by the signs of the parameter μ, the coefficient A and the fourth-degree normal form (68) –we recall, see (69), that in the current case, $A = 7 \times 3^{2/3}/1250 > 0$–. The discussion of all possible cases can be found, for example, in [22]. Thus, as pointed out there, for $A > 0$ and $\mu < 0$ the characteristic exponents of $\widetilde{O}$ are pure imaginary, no low order resonances are present, and the conditions of of Arnold theorem (see [2], chap. 5) are met, so the equilibrium $\widetilde{O}$ is stable. For $A > 0$ and $\mu > 0$, $\widetilde{O}$ is a complex saddle and, clearly, it is unstable. For $\mu = 0$, $\widetilde{O}$ is still elliptic but a 1:$-$1 non semisimple resonance shows up, and its stability cannot be determined so straightforward. This issue has had a historically relevant motivation in the field of Celestial Mechanics: the concern about the Liapunov stability of Lagrange triangular points L_4, L_5 of the Restricted Circular Three Body Problem for the Routh critical mass ratio.

The first results in this direction were achieved in [36], proving formal stability of the equilibrium $\widetilde{O}$ for $A > 0$ (and its instability for $A < 0$). Later, the same author tackled the Liapunov stability for $A > 0$ in [37] (see the comments in [22] plus the observations and references at the end of sec. 6 of chap. 13 in [24]). More recent proofs are found in [3] –where the author uses the Arnold-Neishtadt KAM theorem, suitable for systems with *proper degeneracy*, when the unperturbed Hamiltonian depends on some, but not on all the actions and the perturbation removes the degeneracy (see [2], chap. 5)–, [22], and [25].

Bifurcation of periodic orbits. The presence of two families of elliptic periodic orbits, around the origin, for $\mu < 0$ follows from the Liapunov center theorem. Moreover, for $\mu = 0$, the two families still persist and hold the equilibrium point $\widetilde{O}$
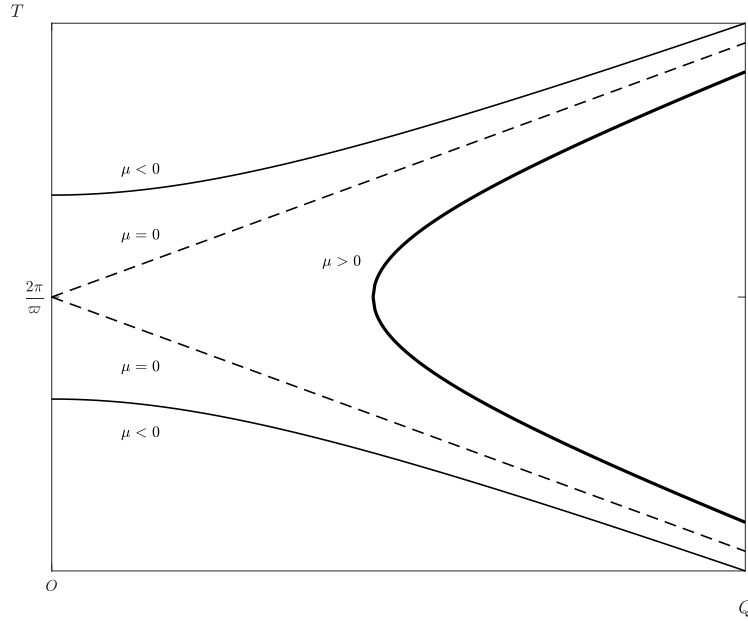
Figure 1: The bifurcated families of periodic orbits. In the horizontal axis is represented the amplitude Q of the orbit and in the vertical axis the period T. Continuous line corresponds to the Liapunov families for $\mu < 0$. The dashed line represent the two families for $\mu = 0$, and the detached family for $\mu > 0$ is plotted in thicker line.

while, for $\mu > 0$ the two families become one unique family of elliptic periodic orbits that detaches from the origin when $A > 0$ (when $A < 0$ the family no longer exists for $\mu > 0$). This last assertion follows from the Theorem 1 below (versioned from [23] and [24]). Figure 1 (see [24], chap. 11) shows the evolution of the families of periodic orbits with respect to the parameter μ in (Q, T) variables, being $Q = \sqrt{\widetilde{x}_1^2 + \widetilde{x}_2^2}$ the amplitude of the periodic orbit, which is constant in these variables, and T the period.

Theorem 1. *If $A > 0$ then there exists a neighborhood $\mathcal{N}$ of $\widetilde{O}$, a $\mu_0 > 0$, an $h_0 > 0$, and a two parameter family of periodic solutions of the Hamiltonian* (66), *denoted by $\phi(t, \mu, h)$, which lie in $\mathcal{N}$ for all $|\mu| < \mu_0$, $|h| < h_0$, $h \neq 0$ when $\mu \leq 0$. The parameter h may be taken as the value of the Hamiltonian. The function $\phi(t, \mu, h)$ is real analytic in all its arguments in its domain of definition. For all values of μ under consideration the periodic solution $\phi(t, \mu, h)$ is elliptic. For $\tilde{\mu}$ fixed and $-\mu_0 \leq \tilde{\mu} \leq 0$, $\phi(t, \tilde{\mu}, h) \to 0$ as $h \to 0^{\pm}$ and the frequency tends to $\varpi \pm \sqrt{\varepsilon(\tilde{\mu})} + \mathcal{O}(\tilde{\mu})$. For $\tilde{\mu}$ fixed and $0 < \tilde{\mu} \leq \mu_0$, the one parameter family of periodic solutions $\phi(t, \tilde{\mu}, h)$ does not contain the equilibrium $\widetilde{O}$.*

The case $A < 0$ is also discussed in the quoted references. For a thorough study of the Hamiltonian Hopf Bifurcation the reader is pointed to [39].

(Quasi) periodic bifurcation. In the literature (see [7]), the bifurcating phenomena described in Theorem 1 are referred to as the *supercritical bifurcation*. Thus, the system defined by Hamiltonian (66) undergoes a supercritical Hopf bifurcation at the equilibrium $\widetilde{O}$, and, consequently, so does the system defined by the initial Hamiltonian (2) at L_2. Thus, all the families of periodic orbits that evolve and detach are elliptic and it is known that, when the elliptic directions are present in the monodromy of a periodic orbit then, generically, a Cantor family of quasi-periodic solutions appear "wrapping" that periodic orbit. One way to see this is singling out an elliptic periodic orbit and take normal form around it (see [10], [11]), then the unfolding of 2D Lagrangian invariant tori follows as a particular case from the results exposed in [7], [18] and [20].

As more than two degrees of freedom are considered, families of elliptic lower dimensional reducible tori (typically KAM tori) can undergo collisions of characteristic multipliers on the unit circle. Under suitable conditions of non resonance and non degeneracy, it gives rise to the unfolding of families of tori of higher dimension. For an account of these phenomena, known globally as quasiperiodic Hopf bifurcation, see [7].

The next proposition follows from the normal form (68), that is gleaned form the computations in the Examples 3 and 4, the fact that the computed value of the coefficient A is positive (see (69)), and then from the application of the inverse change (67), the Theorem 1, and the results in [10], [11], [18], [22], [37]. It describes the local behavior of the trajectories traced by the Rydberg's electron in a neighborhood in the phase space (x, y, p_x, p_y) of the equilibrium point L_2, for values of the polarization parameter, K, close to K_{crit}.

Proposition 3. *The equilibrium point L_2 of Hamiltonian* (2) *is stable for $K \leq K_{crit}$ and unstable for $K > K_{crit}$. For $K < K_{crit}$ there exist two Liapunov families of elliptic periodic orbits that contain the equilibrium point. Both families still persist for $K = K_{crit}$. For $K > K_{crit}$ the two families become one unique family of elliptic periodic orbits that no longer*

21

holds the equilibrium. Moreover, if for some K close to K_{crit} one singles out an elliptic periodic orbit, then the excitations in the elliptic directions yield the unfolding of a Cantor family of Lagrangian 2D-tori having that periodic orbit as its fiber.

This justifies that the normal form $\widetilde{Z}^{(s)}$ can be used to approximate the dynamics of the Hamiltonian (66) close to the equilibrium $\widetilde{O}$, and so, to explore the local dynamics of Hamiltonian (2) in a neighborhood of L_2.

5. Dynamics of the Hamiltonian normal form

In this section we describe in detail the dynamics close to the Hopf bifurcation and the bifurcated invariant objects involved when μ is close to 0 in Hamiltonian (66), that is, when K is near K_{crit} in the original Hamiltonian (2). For this purpose it is useful to consider the polar coordinates Q, θ and their canonically-conjugated momentum and action P and J (see [15]),

$$\tilde{x}_1 = Q\cos\theta, \qquad\qquad \tilde{y}_1 = P\cos\theta - \frac{J}{Q}\sin\theta,$$

$$\tilde{x}_2 = -Q\sin\theta, \qquad\qquad \tilde{y}_2 = -P\sin\theta - \frac{J}{Q}\cos\theta.$$

In the new symplectic coordinates (θ, Q, J, P), the normal form (68) becomes an (integrable) Hamiltonian, Γ, with *real* coefficients

$$\Gamma(\mu, Q, J, P) = \Gamma_0(\mu) + \omega(\mu)J + CJ^2 + \frac{P^2}{2} + \frac{J^2}{2Q^2} + \left(BJ - \frac{\varepsilon(\mu)}{2}\right)Q^2 + AQ^4, \tag{72}$$

with

$$\Gamma_0(\mu) = \tilde{\alpha}\mu + \tilde{\beta}\mu^2,$$

and the coefficients $\tilde{\alpha}$, $\tilde{\beta}$, $\omega(\mu)$, $\varepsilon(\mu)$, A, B, and C those in (69). As $\Gamma(\mu, Q, J, P)$ does not depend explicitly on the angle θ, J is a first integral of (72), so $\Gamma(\mu, Q, J, P)$ can be regarded as a 1-degree of freedom Hamiltonian depending on the coordinates (Q, P), whereas J (and μ) will be thought of as parameters. Thus, the difference $\Gamma - \Gamma_0(\mu)$ is a *natural* Hamiltonian, made up of the sum of kinetic plus potential energy, i.e., $\Gamma - \Gamma_0(\mu) = P^2/2 + V(\mu, Q, J)/2$, being

$$V(\mu, Q, J) := 2\omega(\mu)J + 2CJ^2 + \frac{J^2}{Q^2} + (2BJ - \varepsilon(\mu))Q^2 + 2AQ^4.$$

To obtain the phase portraits for different sets of parameters, an easy way to proceed is to obtain the relation

$$P = \pm\sqrt{E - V(\mu, Q, J)}, \tag{73}$$

with $E = 2(\Gamma - \Gamma_0(\mu))$ and we simply consider the potential curves $(Q, V(\mu, Q, J))$ for a given value of μ. We plot in Figures 2 and 3 left, the potential curves for $\mu = -0.001 < 0$ (similar for $\mu = 0$) and $\mu = 0.001 > 0$ and taking different values of J.

We recall that, for any value of μ fixed, we have an equilibrium point which is the origin $-L_2$ in original variables– for $J = 0$ and $E = 0$, i.e. $\Gamma = \Gamma_0(\mu)$. Now, let us focus on each of the three cases $\mu < 0$, $\mu = 0$ and $\mu > 0$ and describe the dynamics in (Q, P) variables, when varying E.

- If $\mu < 0$ is fixed and small, the origin is a center×center equilibrium point with characteristic exponents $\pm i\,\omega_1$ and $\pm i\,\omega_2$ (depending on μ).

  - For $E = 0$, we have just the equilibrium point and 2D invariant tori –varying $J < 0$–.

  - For a fixed $E > 0$ ($E < 0$), we have a stable periodic orbit –associated with the minimum point of the potential $V(\mu, Q, J)$ for a suitable value of J –surrounded by 2D invariant tori (corresponding to different values of J). In the phase portrait in (Q, P) variables, they can bee seen respectively as a fixed point (on the Q axis) surrounded by closed curves. See Figure 2.

  - Varying $E > 0$ (similarly $E < 0$), we obtain a family of periodic orbits –the minimum points of $V(\mu, Q, J)$ when varying $J > 0$ ($J < 0$)– which are stable. So we obtain two families of periodic orbits, parametrized by the energy, that are born at the equilibrium point. This is in accordance with the Liapunov center Theorem.

- If $\mu = 0$, the origin is a degenerated center×center equilibrium point with characteristic exponents $\pm i\,\omega_1 = \pm i\,\omega_2 = \pm i\,\omega$. Then the two families of periodic orbits, parametrized by the energy E, become one family in the sense that when the energy E tends to 0, the characteristic multipliers of the periodic orbit tend to the same value $2\pi/\omega$. As in the previous case, for a fixed $E > 0$ ($E < 0$), we have a periodic stable orbit surrounded by 2d invariant tori. See Figure 2 (the qualitative plot for $(Q, V(\mu, Q, J))$ is the same for both $\mu > 0$ and $\mu = 0$).

- If $\mu > 0$, the origin is a complex saddle equilibrium point with characteristic exponents $\pm a_1 \pm i\,b_1$. The typical behavior for a direct Hopf bifurcation can be shown here.

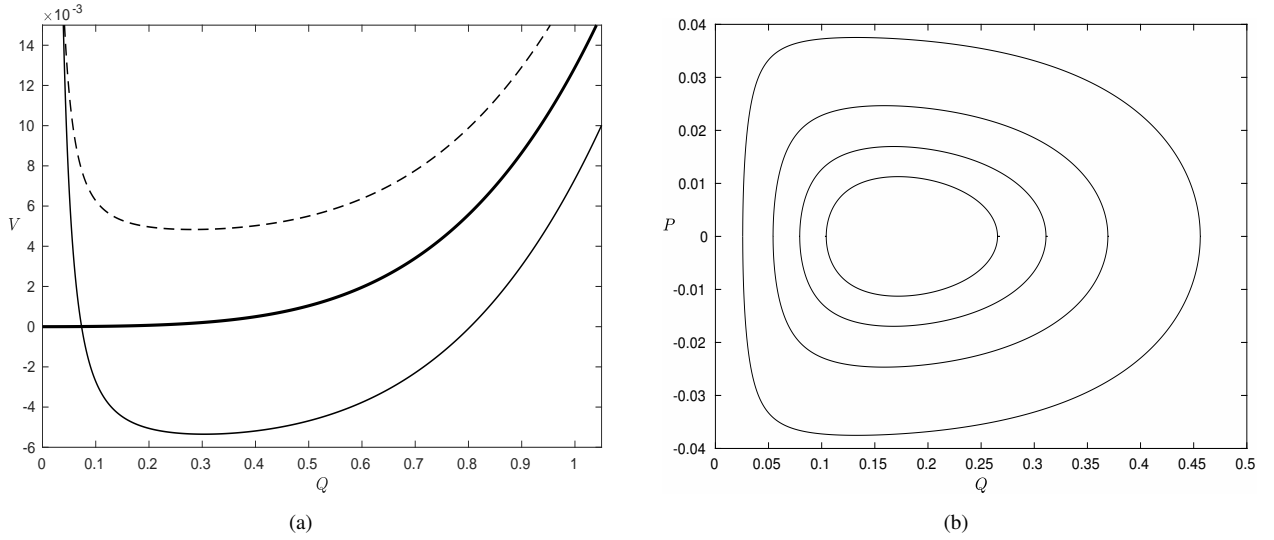Figure 2: $\mu = -0.001 < 0$. Left. Potential curves $(Q, V(\mu, Q, J))$, $J = 0$ (thick line), $J > 0$ (dashed line), $J < 0$ (continuous line). Right. (Q, P) variables and $E = 0.003$. From outer to inner curves, $J = 0.001, 0.0015, 0.0017, 0.0018$.

- A main difference with respect to the two previous cases $\mu \geq 0$, is that, for $E = 0$, there exist 2D invariant unstable and stable manifolds associated with the equilibrium point, $W^u(0)$ and $W^s(0)$, which are coincident (they will not be so in original coordinates, of course). Their parametrization is obtained from the level sets $E = 0$ and $J = 0$ and (73),

$$W^{u,s}(\widetilde{O}) = \left\{ (\theta, Q, J, P) = \left(\theta, Q, 0, \pm\sqrt{-V(\mu, Q, 0)} \right), \theta \in \mathbb{T}^1, 0 < Q \leq \sqrt{\varepsilon(\mu)/(2A)} \right\},$$

where the plus sign describes the unstable (outgoing) manifold whereas the minus sign describes the stable (incoming) one (see Figure 3 middle). Of course, more precise parametrizations can be derived taking normal form up to a convenient high degree. See [27] for a more detailed account on parametrizations of invariant objects in a similar context.

- As expected in a supercritical Hopf bifurcation the family of periodic orbits that bifurcates is detached from the origin (the equilibrium point). This can be easily seen from the potential curves $(Q, V(\mu, Q, J))$ for $E = 0$, where the periodic orbit (a minimum of the potential curve for a suitable J value) has a $Q > 0$ value (see Figure 3 left). We can follow this family of periodic orbits varying the energy E.

- These bifurcated periodic orbits that appear on the complex unstable side are stable, so they are surrounded by 2D invariant tori.

- For $E = 0$, we can distinguish between two *kinds* of 2D invariant tori: the *internal* ones that are born around the bifurcated periodic orbit and the *external* KAM tori that already existed for $\mu < 0$ (see Figure 3 middle).

A final important remark is that we have described the dynamics for a fixed value of $\mu > 0$ and $\mu < 0$ of Γ in (72) which is an integrable Hamiltonian. Of course this normal form Hamiltonian is just an approximation of the original one, which is non integrable. So the "integrable" part of the dynamics described so far is valid only as an approximation of the real dynamics of the original Hamiltonian for a *local* neighborhood both of the equilibrium point (the origin in (Q, P) variables and L_2 in original ones) and values of μ close to 0 (for Hamiltonian (72)), that is, values of K near K_{crit}.

The next step is to describe the dynamics of the original Hamiltonian and the consequences of the Hopf bifurcation. Our approach is to consider not only a neighborhood of the equilibrium point but a large region of the phase space configuration. We will take values of K in an interval (not necessarily small) containing K_{crit}. We will also show that the periodic stable orbits and the invariant manifolds (of L_2 and of the Liapunov periodic orbits) are invariant objects that become relevant for the dynamics.

Before focusing on the original Hamiltonian, and in order to have a self contained paper, we include a short Section devoted to the numerical methodology used to compute such relevant invariant objects.

6. Numerical computation of the invariant objects involved

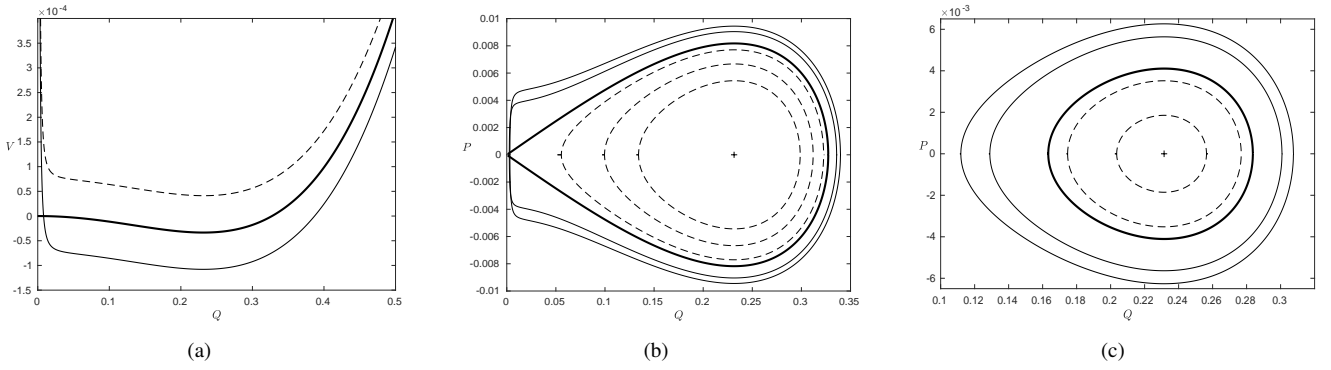We will be focused on Poincaré section plots (PSP), equilibrium points, periodic orbits and their manifolds.

Figure 3: $\mu = 0.001 > 0$. Left. $(Q, V(\mu, Q, J))$ for three values of J: $J = 0.0001$ (dashed line), $J = 0$ (thick line), $J = -0.0001$ (continuous line). Middle. (Q, P) coordinates at the level set $E = 0$. The 2D Lagrangian tori with $J < 0$ are drawn in continuous line. For $J = 0$, the thick line represents the pinched torus, i.e., the union of the equilibrium point with its stable and unstable manifolds (note that these manifold coincide, for the normal form is integrable) and, in continuous line, the 2D Lagrangian tori around the detached bifurcated elliptic periodic orbit with $J > 0$). Right. Same line width code for $E = -0.00005$.

6.1. Poincaré section plots (PSP)

For a given K and $H = h$, being H the original Hamiltonian (2), we consider the original system of ODE (3) and the Poincaré section $\Sigma : x' = p_x + y = 0$. We will call the Poincaré section plot (PSP) the plot obtained with the intersection of a given solution –or many solutions– (in this level of energy h and integrated for a range of time) with Σ such that $y' = p_y - x < 0$. Actually the PSP will the plot with the (x,y) projection of such intersection points.

6.2. Equilibrium points and 2D associated manifolds

Once K is given, in order to find the equilibrium points, we simply solve the polynomial equation of third degree (11). So L_i is obtained with coordinates $(x_{L_i}, 0, 0, x_{L_i})$, for $i = 1, 2$.

Next, for $K > K_{crit}$, in order to compute the 2D unstable/stable manifold of L_2, $W^{u/s}(L_2)$, we will take a set of initial conditions on it. For each initial condition we will compute the corresponding orbit integrating the system of ODE –forward in time for $W^u(L_2)$ and backwards in time for $W^s(L_2)$– and checking that the Hamiltonian value $h(L_2)$ remains constant along the integration for all the range of time considered.

To find such a set of initial conditions we can proceed following two different approaches:

(i) Either we take the set of initial conditions from the fourth order normal form, that is, for $\mu > 0$ small given, we consider (Q, P, θ, J) with (Q, P) in a neighborhood of the origin and satisfying (73), $\theta \in [0, 2\pi]$, $\mu > 0$ small and $J = 0$ (see Figure 3), we apply the normalizing change of variables that reduces the Hamiltonian (2) to the form (66) –see Remark 5–, we obtain a value of K and an approximation of the initial conditions in the original variables (x, y, p_x, p_y) of Hamiltonian (2).

(ii) Or we take a set of initial conditions, using directly the original variables, on the linear approximation of the manifold, that is on its tangent plane. More precisely: we consider the Jacobian matrix of system of ODE (3), its eigenvalues $\lambda_{1,2} = a_1 \pm i b_1$, $\lambda_{3,4} = -a_1 \pm i b_1$ with $a > 0$. Let us denote $\boldsymbol{u}_1 \pm i \boldsymbol{u}_2$ and $\boldsymbol{u}_3 \pm i \boldsymbol{u}_4$ the associated eigenvectors.

To compute the unstable manifold $W^u(L_2)$, we take the orthonormal basis $\boldsymbol{v}_1$, $\boldsymbol{v}_2$ (obtained from $\boldsymbol{u}_1$, $\boldsymbol{u}_2$ and generating the same plane through L_2) and a circle (centered at L_2 and radius $\xi > 0$ small, typically $\xi = 1.d - 6$) of initial conditions given by

$$L_2 + \xi(\cos s \boldsymbol{v}_1 + \sin s \boldsymbol{v}_2), \qquad s \in [0, 2\pi]. \tag{74}$$

For the computation of the stable manifold $W^s(L_2)$, we proceed similarly taking into account $\boldsymbol{u}_3$ and $\boldsymbol{u}_4$.

We have implemented both methods achieving the same results. Of course, the first approach can be applied only for values of K very close to K_{crit} (i.e. $\mu > 0$ small), whereas the second one works for any K.

6.3. Periodic orbits, stability and 2D associated manifolds

To compute families of periodic orbits (PO), a standard methodology consists in solving the nonlinear system of equations (using a predictor-corrector method)

$$
\begin{aligned}
H(z) - h &= 0, \\
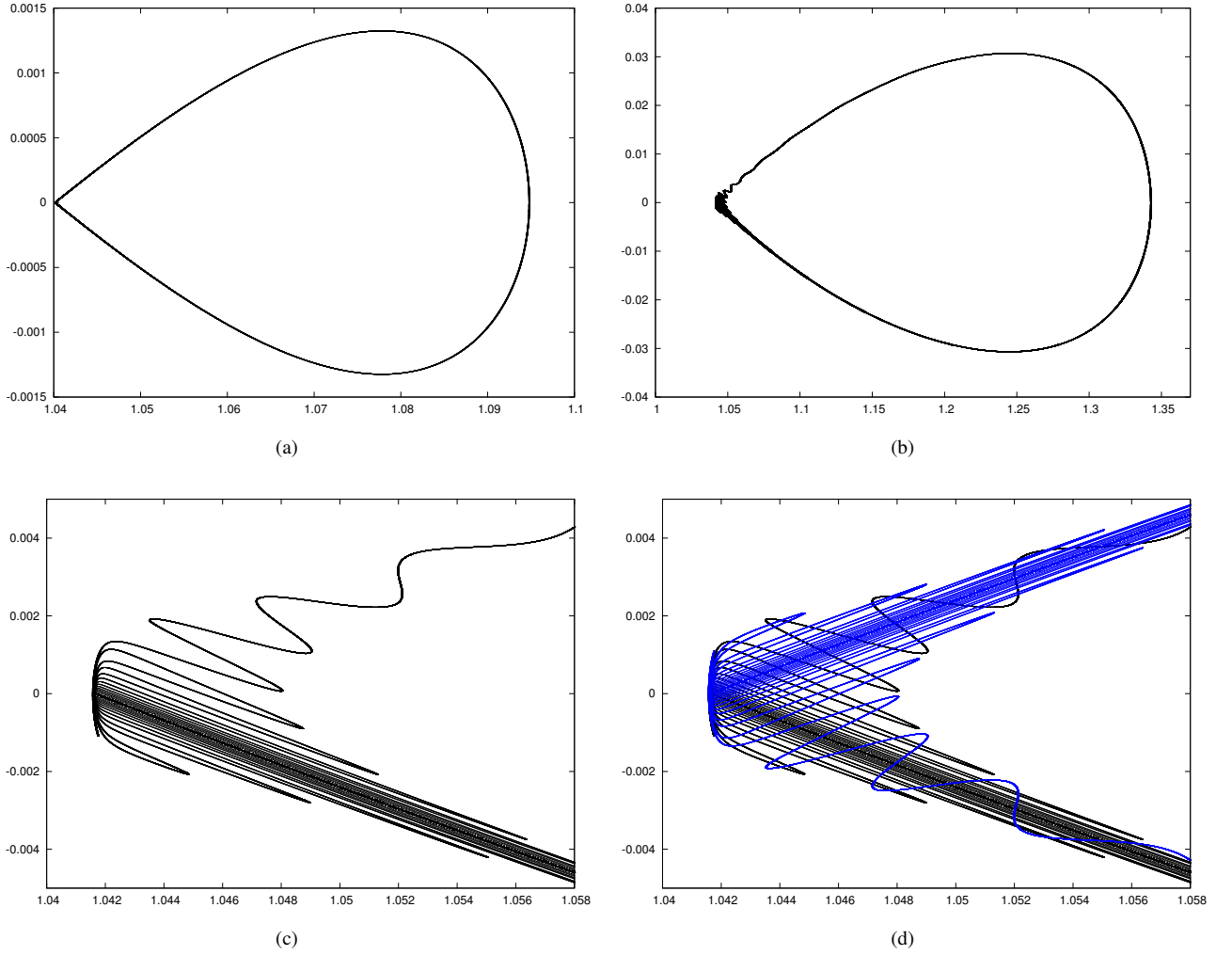g(z) &= 0, \\
\Phi_T(z) - z &= 0,
\end{aligned}
\tag{75}
$$

Figure 4: (x, y) projection of the PSP for $W^u(L_2)$, $W^s(L_2)$. Top. Left. $K = 0.1157$. Right. $K = 0.12$, just $W^u(L_2)$. Bottom. Left. A zoom close to L_2. Right. A zoom with both $W^u(L_2)$ and $W^s(L_2)$.

where $\Phi_t(z)$ is the t-time flow of the ODE system (3), z is an initial condition of the PO, T is its period ($\Phi_T(z) = z$) and $g(z) = 0$ is a suitable Poincaré section (a hypersurface in $\mathbb{R}^4$).

To do so we need a seed for the (approximation of the) initial condition of a PO. Once we have one PO we proceed with the continuation of a family.

Since we will focus mainly on the bifurcated periodic orbits with $H = h(L_2)$ (it is the value of h where the manifolds $W^{u,s}(L_2)$ exist), varying $K > K_{crit}$, to get a seed for an initial condition of a PO, we can proceed again in two different ways:

(i) Either we take the initial conditions from the fourth order normal form, that is, for $\mu > 0$ small given, we consider (Q, P, θ_2, J) with $P = 0$, $E = 0$ in (73), $\theta = 0$, and (Q, J) is a minimum of $V(\mu, \theta, J)$ i.e., a solution of the system

$$V(\mu, Q, J) = 0, \qquad \frac{\partial V}{\partial Q}(\mu, Q, J) = 0$$

(see Figure 3), we apply the composition of the successive changes of coordinates that lead to the normal form (as above), we obtain a value of K and the corresponding (approximation of the) initial conditions on the original variables (x, y, p_x, p_y) of the PO.

(ii) Or, we fix $K > K_{crit}$ and $H = h(L_2)$. We consider a set of different initial conditions of type $(x, 0, 0, p_y)$, with $y' = p_y - x < 0$, varying x (y' is obtained from the Hamiltonian) in a suitable interval; for each initial condition we integrate the original system (3) and obtain the corresponding solution for a big enough range of time, and we save just the points belonging to the Poincaré section plot (PSP). In the PSP obtained (see for example Figure 6 middle left), we zoom the area around the bifurcated stable PO (surrounded by invariant curves) and we have an approximation of x (and p_y) of the initial condition of the required PO.

25

We have implemented both strategies to get a seed and both have become satisfactory –again the first one only valid for K very close (and bigger than) to K_{crit}–. We have implemented Newton's method for the correction to solve system (75) to refine the seed and obtain the bifurcated PO for $H = h(L_2)$ when varying $K > K_{crit}$ (see next Section). The absolute tolerance to stop Newton iterates in the solution has been typically 10^{-11}.

Given a PO, in order to determine its (linear) stability, we have integrated both the system of ODE (3) together with its first variational equations to obtain the monodromy matrix M after a period. We recall that the value of the stability parameter $k = \operatorname{Tr} M - 2$ decides the stability character of a PO: it is stable (elliptic) if $|k| < 2$, and unstable (hyperbolic) if $k \in \mathbb{R} \setminus [-2, 2]$ (see for example [8] for details).

As will be shown in the next Section, the 2D invariant manifolds of the Liapunov orbits around L_1, ol_1, will also play a role on the description of the global dynamics. Such orbits (for the values of K and h considered) are unstable (the monodromy matrix has as eigenvalues $1, 1, \lambda > 1$ and $1/\lambda < 1$, i. e. $k \in \mathbb{R} \setminus [-2, 2]$). In order to generate the unstable manifold $W^u(ol_1)$ such that z_0 is an initial condition of the ol_1 and $\boldsymbol{v}_0$ is a unitary eigenvector associated with $\lambda > 1$, we consider a set of initial conditions on the linear approximation of the manifold given by

$$\varphi(\theta) + \xi \boldsymbol{v}(\theta), \qquad \theta \in [0, 2\pi],$$

where $\xi > 0$ or < 0 to obtain the two branches that compose the manifold, small (typically $|\xi| = 10^{-6}$) and

$$\varphi(\theta) = \Phi_{\frac{\theta}{2\pi}T}(z_0), \qquad \boldsymbol{v}(\theta) = \lambda^{\theta/2\pi} D\Phi_{\frac{\theta}{2\pi}T}(z_0)\boldsymbol{v}_0$$

are a parametrization of the PO and the eigenvector of the associated monodromy matrix corresponding to the point $\varphi(\theta)$ respectively (see [4]). For each initial condition, we obtain the corresponding solution integrating forward in time system (3) and checking that the Hamiltonian remains constant along the integration. We proceed similarly to obtain the stable manifold $W^s(ol_1)$ taking into account $\lambda < 1$ and integrating backwards in time.

7. Description of the dynamics of the original system

The purpose of this Section is to describe the Hopf bifurcation effect on the dynamics of the original non-integrable Hamiltonian system for which the fourth order integrable normal form taken into account is just an approximation (and of course valid just in a tiny neighborhood of the equilibrium point L_2 and a small interval around K_{crit}). So, in the previous Sections, we considered the dynamics of the electron from a very local point of view. Now, numerical simulations applied to the original system allow to describe the dynamics in large regions in the (x, y) plane and any value of K. We will distinguish two cases: $K > K_{crit}$ and $K < K_{crit}$ (recall that $K_{crit} = 3^{-4/3}/2 \approx 0.11556021$).

Case 1. $K > K_{crit}$. We fix the energy value $h = h(L_2)$ and we discuss different aspects of the dynamics when varying K, that can be graphically illustrated through the Poincaré section plots (PSP).

- *Invariant manifolds of L_2.* When K is very close to K_{crit}, the stable and unstable 2D manifolds, $W^u(L_2)$ and $W^s(L_2)$, are almost coincident (they do coincide for the integrable normal form, but they do not for the original non integrable Hamiltonian giving rise to the splitting of separatrices). See Figure 4 top left, where the PSP of the manifolds are plotted for $K = 0.1157$ very close to K_{crit}. As far as K increases, the typical homoclinic tangle is more visible, see Figure 4, and for bigger K, the manifolds become very intricate, see Figure 6 top left. We also remark that for K near K_{crit}, the *size* of the manifolds is small, i.e. the orbits on the manifolds visit a small region in the (x, y) plane. See the PSP of the manifolds in Figure 5 middle where the manifolds are confined by external 2D tori (invariant curves on the PSP). Whereas when K increases, the size of the manifolds becomes larger and there are some orbits on the manifolds that go tremendously far away from L_2 or even escape. Such orbits provide a mechanism for ionization of the electron. See Figure 6 middle left.

- *Existence of bifurcated periodic orbits and tori.* As foreseen by the NF description, for a given K bigger and close to K_{crit}, there exists a detached family of periodic orbits when varying h, in a neighborhood of $h(L_2)$, which are stable (for h near $h(L_2)$). For the particular fixed value of $h(L_2)$, the corresponding bifurcated periodic orbit will be surrounded by invariant 2D tori, which will be *located inside* the region enclosed by the invariant manifolds of L_2, if K is very close to K_{crit}, see Figure 5 middle left for $K = 0.1157$ where the detached periodic orbit (a fixed point on the PSP) and the surrounding 2D tori (invariant curves) are shown. We remark, on the one hand, that the continuous family of tori inside the coinciding manifolds (Figure 3) obtained from the NF now becomes a Cantor family of tori (for the original Hamiltonian system) as far as K is very close to K_{crit}. On the other hand, the destruction of many such tori is also visible when K increases and the existence of chaos is much more apparent, although the stable periodic orbit persists, see Figure 6 top for $K = 0.13$.
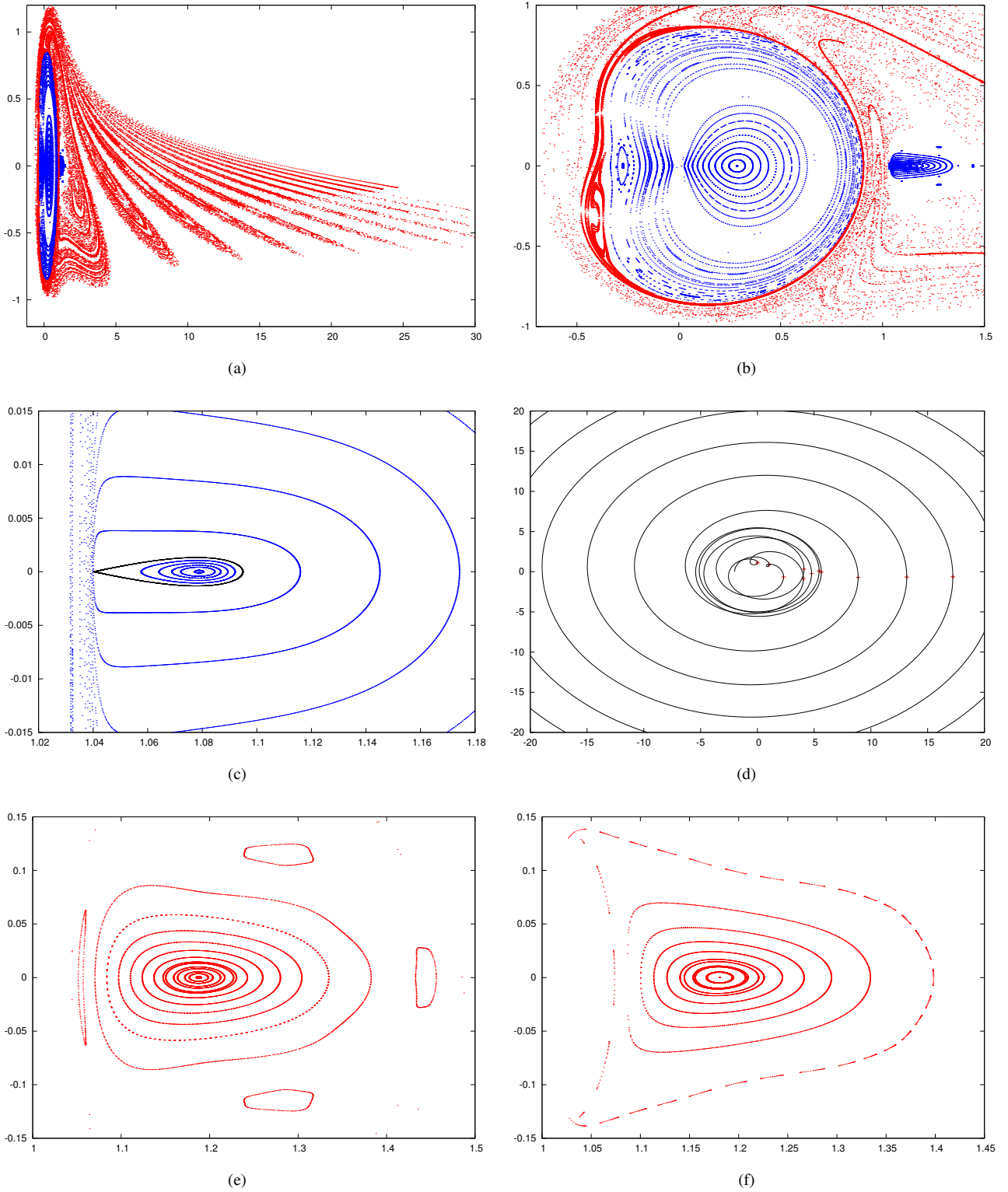
Figure 5: $K = 0.1157$. (x, y) projection of the PSP. Top and middle correspond to $h = h(L_2)$. Top. Left. Global plot. Right. Zoom. The red points correspond to $W^u(ol_1)$; two confined regions (in blue) are clearly distinguished: the one close to the origin and the one due to the bifurcated stable periodic orbit. Middle. Left. We show the KAM invariant curves (in blue) enclosing $W^u(L_2)$ and $W^s(L_2)$ (in black), and also the bifurcated stable periodic orbit and the corresponding invariant curves surrounding it (in blue). Right. Fast escape orbit ((x,y) projection,in black) and the corresponding points on the PSP overlapped (in red). Bottom: 2D KAM tori around the bifurcated stable periodic orbit for $h > h(L_2)$ (left) and $h < h(L_2)$ (right).

- *Confinement due to the invariant manifolds.* Although the appearance of the splitting phenomenon (not present for the NF Hamiltonian) for any $K > K_{crit}$, the manifolds somewhat enclose a confinement region, more visible as far as K is close to K_{crit}. See Figure 5 middle. Therefore there exist points inside this region giving rise to confined solutions, the confinement size determined by the size of the manifolds. We want to mention the remarkable different sizes of confinement regions comparing those (smaller) delimited by the invariant manifolds of L_2 and those (bigger) delimited by the 2D KAM *external* tori. See Figure 5 middle left for $K = 0.1157$. When K increases, the external tori disappear and there is a dramatic change in the intricate shape of the manifolds of L_2, see Figure 6 top and middle for $K = 0.13$.

- *Confinement due to the bifurcated elliptic periodic orbits.* As already mentioned, when K increases, the manifolds of L_2 are very complicated and the visited region (in (x, y)) is very big. However, as far as the bifurcated periodic orbit is stable, there will be still a small region of confinement for all time, due to the existence of surrounding 2D tori. So an important effect of the Hopf bifurcated orbit is to delimit, among a chaotic sea, a region where the electron will remain confined for ever. We show this behavior on the PSP of Figure 6 (b) top right for $K = 0.13$.

- *Stability of the bifurcated periodic orbits.* We have computed the family of bifurcated periodic orbits when varying K. In Figure 7 we plot two curves on the (K, x) plane: for each K, the x value of the equilibrium point L_2 and the x value of the initial condition (such that $y = x' = 0$, $y' < 0$) of the bifurcated periodic orbit for that K (and $h = h(L_2)$). We can see how the family of periodic orbits is detached from the equilibrium point as far as K increases from K_{crit}. The amplitude of the periodic orbits grows with K and we have followed the family until the orbit passes, for some time, very close to the origin, so a regularization of the system of ODE should be required, see Figure 7 right. Concerning their linear stability, there is also a change of stability: the elliptic orbits for K close to K_{crit} become unstable for bigger values of K. We plot in blue the stable periodic orbits and in red the unstable ones in Figure 7 left.

- *Homoclinic orbits. Erratic orbits.* Due to the transversal intersections between $W^u(L_2)$ and $W^s(L_2)$, see for example Figure 4 bottom right, there exist infinitely many homoclinic orbits to L_2 and, as a consequence, it is well known that the variety of behaviors for the dynamics is very rich (symbolic dynamics may be applied). Nevertheless, for values of K near K_{crit}, since the external KAM tori *confine* the invariant manifolds, the latter do not play any role in escape (ionization of the electron). See Figure 5 middle left. But, for bigger values of K, the KAM tori are destroyed and there is a second effect which is the *growth* of the manifolds, see Figure 6 middle left. Therefore, from the behavior of $W^u(L_2)$ and $W^s(L_2)$, there will coexist confined motion, some escaping orbits and some erratic "to and fro" orbits, that is, orbits that make several excursions, close to and far from L_2 (reaching different large distances), in an erratic way. Such orbits –also called multi-bump orbits– may remain confined or finally escape. In the latter case, the electron experiments a slow ionization. In Figure 8, some orbits on $W^u(L_2)$ are plotted to show such different behaviors. See also [26] for a specific study of the to and fro motion for successive excursions of the electron close to the nucleus.

- *Global picture.* As a summary and taking into account the different invariant objects involved, we describe the dynamics of the PSP from a global point of view. We should distinguish four different regions:

  - A region near the origin. A first global property to remark, and independent of the Hopf bifurcation phenomenon, is the existence of the retrograde periodic stable orbit close to the origin; this orbit together with the invariant surrounding 2d tori confine a clear region for the electron. See Figures 5 and 6. This was already observed in [5] for very small values of $K < K_{crit}$.

  - The invariant manifolds of ol_1. Regardless the value of K, for $h = h(L_2)$, there is the unstable periodic orbit around L_1, ol_1, and their invariant manifolds which play a clear role on the dynamics. As exhibited in [5] these manifolds visit a small (x, y) region for $0 < K < K_{crit}$ small, but we have just shown that they become more complex (and their homoclinic tangles as well) as K grows visiting large regions in the (x, y) plane, see Figures 5 top and 6 middle and bottom.

  - The region influenced by the Hopf bifurcation. When K is bigger and close to K_{crit}, and for $h = h(L_2)$, the dynamics of the Hopf bifurcation is very local in the sense that $W^u(L_2)$, $W^s(L_2)$, the bifurcated stable periodic orbit and the surrounding invariant 2D tori are confined by the external KAM tori, so they do not play a significant role in the dynamics. See Figure 5 middle for $K = 0.1157$. Nevertheless, as far as K increases, these KAM tori disappear and both manifolds –those of ol_1 and those of L_2– are mixed, giving rise to many different kinds of orbits and chaos. Relevant to say (and as mentioned above) is that, among this chaos, the stable bifurcated periodic orbit and associated 2D tori, confine a clear region among this chaotic sea. See Figure 6 top for $K = 0.13$. However, for bigger values of K such that the periodic bifurcated orbit is unstable, we obtain the same kind of PSP but there is no confinement around the periodic orbit at all.

– *Fast escaping orbits*. Finally and concerning the *white* region of the PSP (roughly speaking), if we take initial conditions in such regions we obtain fast escaping orbits, with a typical spiral behavior. See Figures 5 middle right and 6 bottom right, where we consider $K = 0.1157$ and $K = 0.13$ and plot two escaping spiraling orbits and the corresponding PSP overlapped.

Let us finally remark that for h close to and different from $h(L_2)$, the PSP are similar to the PSP for $h = h(L_2)$ except that the neither the equilibrium point nor the invariant manifolds exist. We show in Figure 5 a neighborhood of the bifurcated stable periodic orbit and the 2D tori that persist for $K = 0.1157$.

Case 2. $K < K_{crit}$. This case was already studied in [5] but, for completeness, we just consider $K = 0.115$ very close to K_{crit} and h near $h(L_2)$. As in Case 1, there is the *big* stable region close to the origin due to the retrograde o_r orbit and the intricate invariant manifolds associated with the periodic orbit ol_1 that cover a big chaotic region in the (x, y) plane. For $h = h(L_2)$, we have the equilibrium point L_2 which is stable, whereas for increasing/decreasing h we obtain the corresponding family of stable Liapunov periodic orbits surrounded by 2D tori. This is clearly shown in Figure 9. Of course, this dynamics is in accordance with the theoretical results obtained in Sections 4 and 5.

8. Conclusions

In the current work we have explored the CP problem for values of the energy close to $h(L_2)$ and varying K in an interval containing K_{crit}. We have distinguished two different parts: the analytical study and the numerical one.

Concerning the analytical part, since a main goal was to analyze the Hopf bifurcation appearing close to the equilibrium point L_2, a first remarkable step done was the computation of the normal form (NF) starting from the *given* Hamiltonian of the CP problem (not an academic theoretical Hamiltonian with a *suitable* expression useful to carry out the normal form, as is typically done in papers that study the Hamiltonian Hopf bifurcation). Moreover, the steps for the computation of the resonant normal form, up to any given order, have been explained in a constructive manner. The results of the analysis of the NF are summarized in Proposition 3, which enables us to describe the Hopf bifurcation and the local behavior of the dynamics in a neighborhood of the equilibrium L_2 for the original Hamiltonian.

From the numerical point of view, we have described the dynamics of the electron, focusing on the Hopf bifurcation when $h = h(L_2)$. Our conclusions, drawn from the obtained Poincaré section plots (PSP), are the following: For values of K very close to K_{crit}, the unstable/stable manifolds of the complex saddle point L_2, $W^{u,s}(L_2)$, do not essentially play any role, since they *cover* a very tiny region in the plane (x, y) and are surrounded by 2D invariant tori that act as a barrier of motion. However for bigger values of K, the tiny and local effect becomes dramatic: the 2d surrounding tori disappear and now $W^{u,s}(L_2)$ are very intricate and fill a very big region of the plane (x, y). Actually, all kinds of orbits, to and fro, erratic, fast and slow ionizing orbits, are observed belonging to these manifolds. However, the bifurcating stable orbits are robust since even for bigger values of K, there is a small region of 2D tori around the bifurcated elliptic periodic orbits that persist. Clearly shown on the PSP, the electron would remain for ever confined there, in the middle of a huge chaotic area.

Finally, in order to describe possible global behaviors of the electron for h close to $h(L_2)$, from the obtained PSP, we can conclude that, for any value of K ranging from (bigger than) 0 to $K > K_{crit}$, the dynamics is mainly organized by: (i) the stable retrograde periodic orbit (around the proton) surrounded by 2D tori which compose a robust region of confinement; and (ii) the unstable/stable manifolds of the Liapunov periodic orbit ol_1, $W^{u,s}(ol_1)$, that exist for $h > h(L_1)$, and whose intricate homoclinic tangle, gives rise to all kind of orbits, including multi-bump, erratic and escaping orbits (and therefore these manifolds provide a mechanism for ionization). It is worth mentioning that, for $K > K_{crit}$, and $h = h(L_2)$, the manifolds of L_2, $W^{u,s}(L_2)$ also play a role and the both intricate $W^{u,s}(L_2)$, and $W^{u,s}(ol_1)$ get mixed altogether filling a bigger chaotic region in the (x, y) plane.

References

[1] G. B. Arfken, H. J. Weber, Mathematical Methods for Physicists, sixth ed., Elsevier Academic Press, San Diego, Cal., 2005.

[2] V. I. Arnol′ d, V. V. Kozlov, A. I. Neĭshtadt, Dynamical systems. III, vol. 3 of Encyclopaedia of Mathematical Sciences, Springer-Verlag, Berlin, 1988, translated from the Russian by A. Iacob.
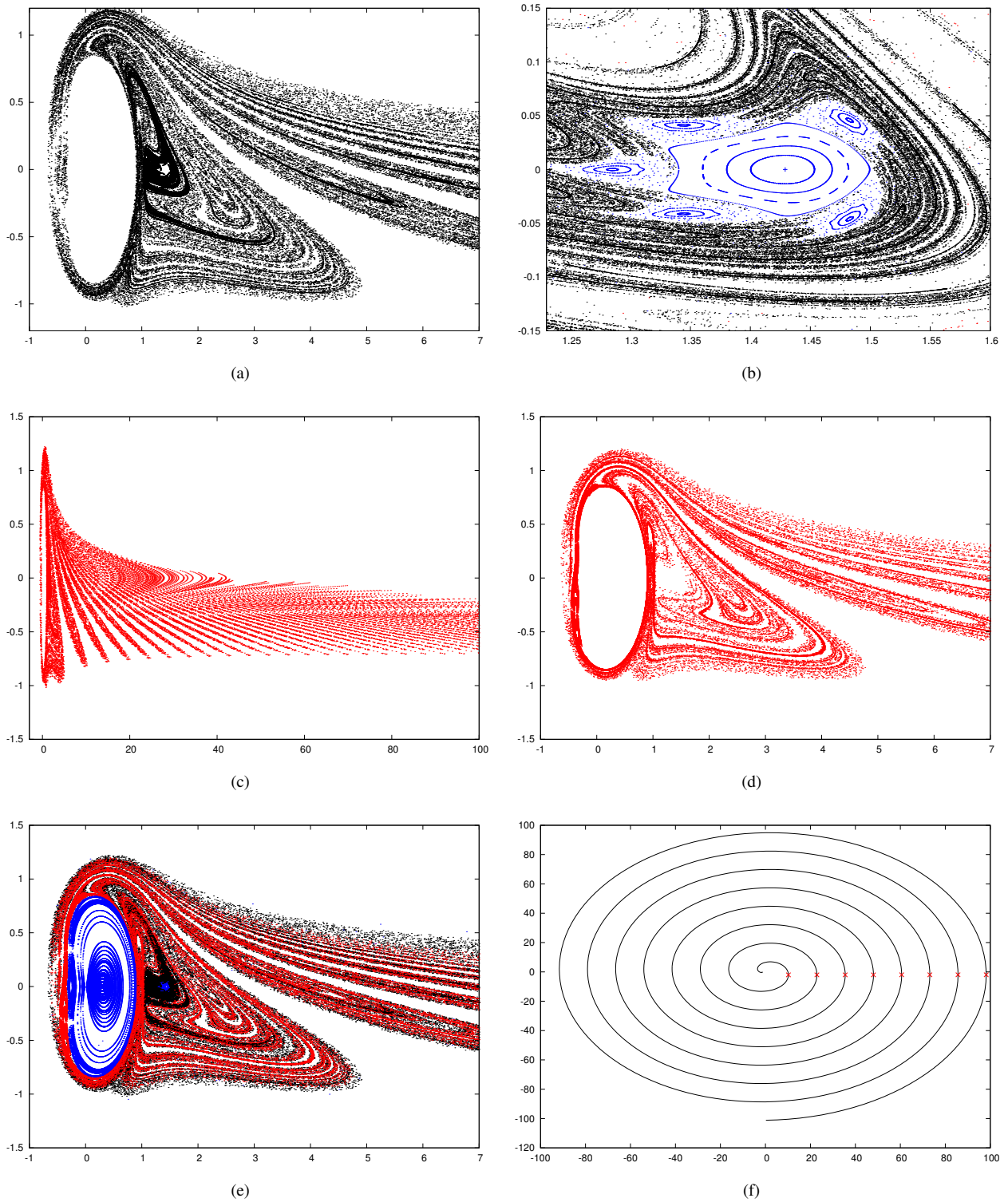
Figure 6: $K = 0.13$, $h = h(L_2)$. (x, y) projection of the PSP. Top. Left. For $W^u(L_2)$. Right. Zoom, where the bifurcated stable fixed point and invariant curves are shown. Middle. Left. A larger window, orbits on $W^u(L_2)$ can go rather far away and even escape. Right. For $W^u(ol_1)$. Bottom. Left. PSP taking into account the motion around the origin, $W^u(L_2)$ and $W^u(ol_1)$. Right. Fast escape orbit ((x, y) projection, in black) and the corresponding points on the PSP overlapped (in red).

[3] B. Bardin, On motions near the Lagrange equilibrium point L_4 in the case of Routh's critical mass ratio, Celestial Mech. Dynam. Astronom. 82 (2) (2002) 163–177, the restless universe (Blair Atholl, 2000).

[4] E. Barrabés, J. Mondelo, M. Ollé, Numerical continuation of families of homoclinic connections of periodic orbits in the RTBP, Nonlinearity 22 (12) (2009) 2901–2918.

[5] E. Barrabés, M. Ollé, F. Borondo, D. Farrelly, J. M. Mondelo, Phase space structure of the hydrogen atom in a circularly polarized microwave field, Physica D: Nonlinear Phenomena 241 (4) (2012) 333–349.
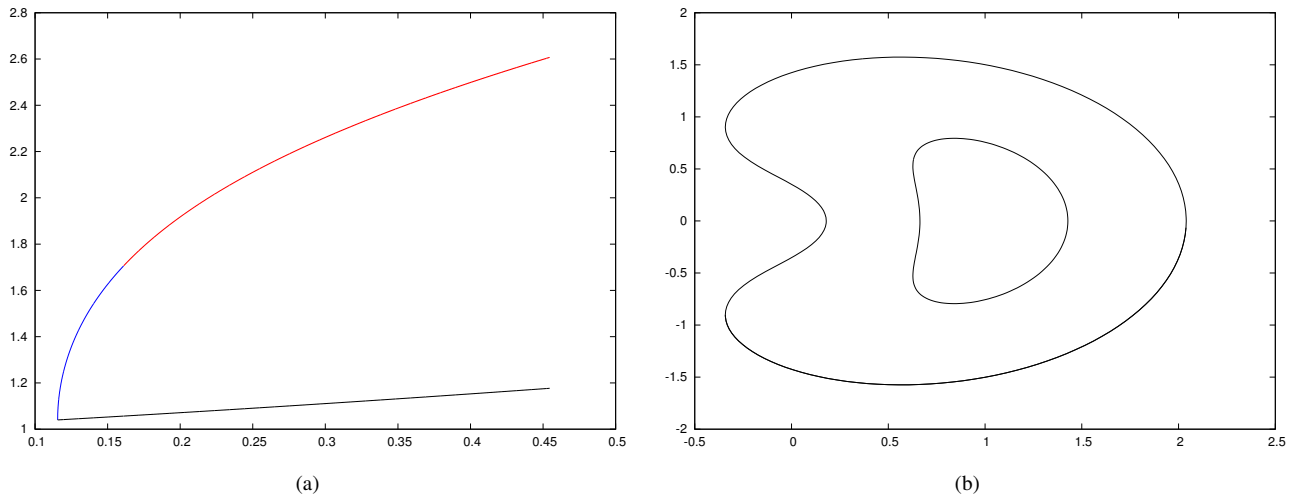
(a)

(b)

Figure 7: $h = h(L_2)$. Left. Two curves on the (K, x) plane: for each K, the (lower) x value of the equilibrium point L_2 and the (bigger) x value of the initial condition of the bifurcated periodic orbit. The blue (red) points correspond to stable (unstable) periodic orbits. Right. Plane (x, y). Bifurcated periodic orbits for $K = 0.13$ and $K = 0.23$
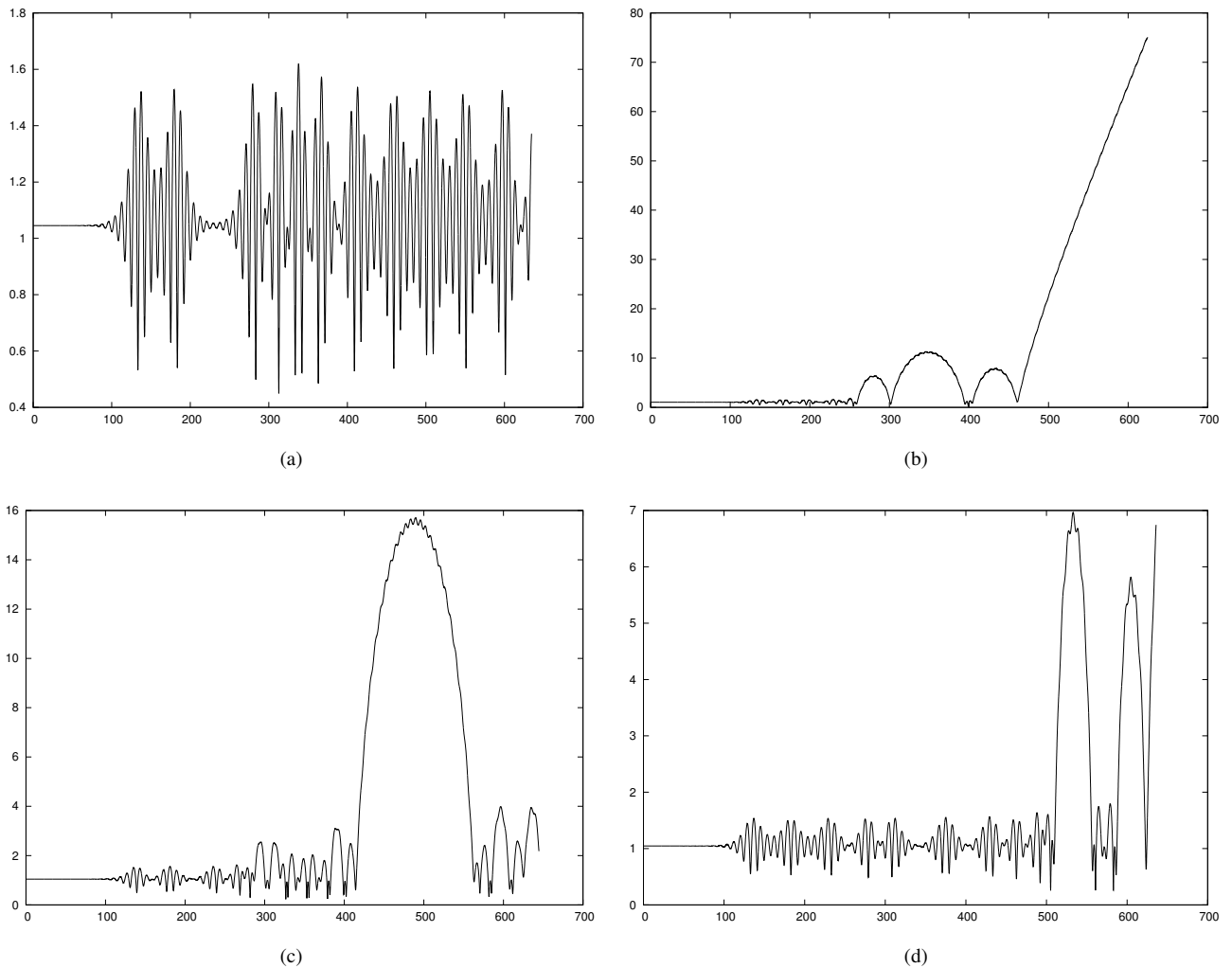

(a)

(b)

(c)

(d)

Figure 8: $K = 0.13$. (x,y) projection of some orbits in $W^u(L_2)$. Top. Left. Confined orbit. Right. Slow ionizing orbit. Bottom: two different erratic orbits with several passages, (left) close to and (right) far from L_2.

[6] T. J. Bridges, J. E. Furter, Singularity theory and equivariant symplectic maps, vol. 1558 of Lecture Notes in Mathematics, Springer-Verlag, Berlin, 1993.

[7] H. W. Broer, H. Hanßmann, J. Hoo, The quasi-periodic Hamiltonian Hopf bifurcation, Nonlinearity 20 (2) (2007) 417–460.
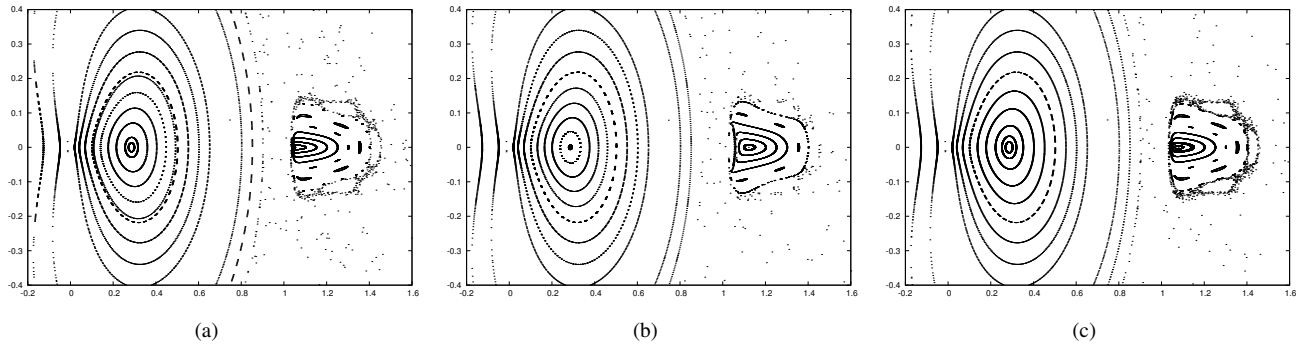
31

Figure 9: $K = 0.115 < K_{crit}$. PSP: the *big* stable region close to the origin is clearly seen. We remark the stable equilibrium point for $h = h(L_2)$ (left) and the Liapunov stable periodic orbit for $h < h(L_2)$ (middle) and the one for $h > h(L_2)$ (right).

[8] R. Broucke, Stability of periodic orbits in the Elliptic, Restricted Three-body Problem, AIAA J. 7 (6) (1969) 1003–1009.

[9] A. F. Brunello, T. Uzer, D. David Farrelly, Hydrogen atom in circularly polarized microwaves: Chaotic ionization via core scattering, Phys. Rev. 55 (5) (1997) 3730–3745.

[10] A. Bruno, Instability in Hamilton's system and the distribution of asteroids, Mat. Sb. (N.S.) 83 (125) (1970) 273–312.

[11] A. Bruno, Normalization of a Hamiltonian system near an invariant cycle or torus, Uspekhi Mat. Nauk 44 (2(266)) (1989) 49–78.

[12] R. H. Cushman, L. M. Bates, Global aspects of classical integrable systems, Birkhäuser Verlag, Basel, 1997.

[13] A. Giorgilli, A. Delshams, E. Fontich, L. Galgani, C. Simó, Effective stability for a Hamiltonian system near an elliptic equilibrium point, with an application to the restricted three-body problem, J. Differential Equations 77 (1) (1989) 167–198.

[14] L. Guirao, M. López, J. Vera, $\mathcal{C}^1$ non integrability of a hydrogen atom in a circularly polarized microwave field., Cent. Eur. J. Phys 10 (4) (2012) 742–748.

[15] D. C. Heggie, Bifurcation at complex instability, Celestial Mech. 35 (4) (1985) 357–382.

[16] C. Jaffé, D. Farrelly, T. Uzer, Transition state theory without time-reversal symmetry: Chaotic ionization of the hydrogen atom, Phys. Rev. Lett. 84 (4) (2000) 610–613.

[17] A. Jorba, A methodology for the numerical computation of normal forms, centre manifolds and first integrals of Hamiltonian systems, Experiment. Math. 8 (2) (1999) 155–195.

[18] A. Jorba, J. Villanueva, On the normal behaviour of partially elliptic lower-dimensional tori of Hamiltonian systems, Nonlinearity 10 (4) (1997) 783–822.

[19] À. Jorba, M. Zou, A software package for the numerical integration of ODEs by means of high-order Taylor methods, Experiment. Math. 14 (1) (2005) 99–117.

[20] A. Lahiri, M. Roy, The hamiltonian hopf bifurcation: an elementary perturbative approach, Int. J. Non-Linear Mech. 36 (2001) 787–802.

[21] A. J. Laub, K. Meyer, Canonical forms for symplectic and Hamiltonian matrices, Celestial Mech. 9 (1974) 213–238.

[22] L. Lerman, A. Markova, On stability at the Hamiltonian Hopf bifurcation, Regul. Chaotic Dyn. 14 (1) (2009) 148–162.

[23] K. Meyer, D. Schmidt, Periodic orbits near L_4 for mass ratios near the critical mass ratio of Routh, Celestial Mech. 4 (1971) 99–109.

[24] K. R. Meyer, G. R. Hall, D. Offin, Introduction to Hamiltonian Dynamical Systems and the N-Body Problem, vol. 90 of Applied Mathematical Sciences, 2nd ed., Springer, New York, 2009.

[25] K. R. Meyer, J. F. Palacián, P. Yanguas, Stability of a Hamiltonian system in a limiting case, Regul. Chaotic Dyn. 17 (1) (2012) 24–35.

[26] M. Ollé, To and fro motion for the hydrogen atom in a circularly polarized microwave field, Commun Nonlinear Sci Numer Simulat 54 (2017) 286–301.

[27] M. Ollé, J. Pacha, J. Villanueva, Dynamics close to a non semi-simple $1 : -1$ resonant periodic orbit, Discrete Contin. Dyn. Syst. Ser. B 5 (3) (2005) 799–816.

[28] M. Ollé, J. R. Pacha, J. Villanueva, Quantitative estimates on the normal form around a non-semi-simple $1 : -1$ resonant periodic orbit, Nonlinearity 18 (3) (2005) 1141–1172.

[29] M. Ollé, J. R. Pacha, J. Villanueva, Kolmogorov-Arnold-Moser aspects of the periodic Hamiltonian Hopf bifurcation, Nonlinearity 21 (8) (2008) 1759–1811.

[30] J. R. Pacha, On the Quasi-Periodic Hamiltonian Andronov-Hopf Bifurcation, Ph.D. thesis, Facultat de Matemàtiques, Universitat Politècnica de Catalunya (October 2002).

[31] D. L. Richardson, Analytic construction of periodic orbits about the collinear points, Celestial Mech. 22 (3) (1980) 241–253.

[32] D. L. Richardson, A note on a Lagrangian formulation for motion about the collinear points, Celestial Mech. 22 (3) (1980) 231–236.

[33] D. Schmidt, Versal normal form of the Hamiltonian function of the restricted problem of three bodies near L_4, J. Comput. Appl. Math. 52 (1-3) (1994) 155–176, oscillations in nonlinear systems: applications and numerical aspects.

[34] C. Siegel, J. Moser, Lectures on celestial mechanics, Classics in Mathematics, Springer-Verlag, Berlin, 1995, translated from the German by C.I. Kalme, Reprint of the 1971 translation.

[35] C. Simó, Estabuilitat de sistemes hamiltonians, Mem. Real. Acad. Ciencias y Artes Barcelona. 48 (7).

[36] A. Sokol′skiĭ, On the stability of an autonomous Hamiltonian system with two degrees of freedom in the case of equal frequencies, Prikl. Mat. Meh. 38 (1974) 791–799.

[37] A. G. Sokol′skiĭ, Proof of the stability of Lagrangian solutions for a critical mass ratio, Pis′ma Astron. Zh. 4 (1978) 184–152.

[38] J.-C. van der Meer, Nonsemisimple $1 : 1$ resonance at an equilibrium, Celestial Mech. 27 (2) (1982) 131–149.

[39] J.-C. van der Meer, The Hamiltonian Hopf bifurcation, vol. 1160 of Lecture Notes in Mathematics, Springer-Verlag, Berlin, 1985.

[40] J. Williamson, On the Algebraic Problem Concerning the Normal Forms of Linear Dynamical Systems, Amer. J. Math. 58 (1) (1936) 141–163.

[41] J. Williamson, On the Normal Forms of Linear Canonical Transformations in Dynamics, Amer. J. Math. 59 (3) (1937) 599–617.

[42] J. Williamson, The exponential representation of canonical matrices, Amer. J. Math. 61 (1939) 897–911.